

Multi-hump Collapsing Solutions in the Nonlinear Schrödinger Problem: Existence, Stability and Dynamics

S. Jon Chapman

*Mathematical Institute, University of Oxford,
AWB, ROQ, Woodstock Road, Oxford OX2 6GG*

M. Kavousanakis

School of Chemical Engineering, National Technical University of Athens, 15780, Athens, Greece

E.G. Charalampidis

*Department of Mathematics and Statistics, and Computational Science Research Center,
San Diego State University, San Diego, CA 92182-7720, USA*

I.G. Kevrekidis

*Department of Chemical and Biomolecular Engineering &
Department of Applied Mathematics and Statistics,
Johns Hopkins University, Baltimore, MD 21218, USA*

P.G. Kevrekidis

*Department of Mathematics and Statistics, University of Massachusetts, Amherst MA 01003-4515, USA and
Department of Physics, University of Massachusetts, Amherst MA 01003, USA*

(Dated: April 15, 2025)

In the present work we examine multi-hump solutions of the nonlinear Schrödinger equation in the blowup regime of the one-dimensional model with power law nonlinearity, bearing a suitable exponent of $\sigma > 2$. We find that families of such solutions exist for arbitrary pulse numbers, with all of them bifurcating from the critical case of $\sigma = 2$. Remarkably, all of them involve “bifurcations from infinity”, i.e., the pulses come inward from an infinite distance as the exponent σ increases past the critical point. The position of the pulses is quantified and the stability of the waveforms is also systematically examined in the so-called “co-exploding frame”. Both the equilibrium distance between the pulse peaks and the point spectrum eigenvalues associated with the multi-hump configurations are obtained as a function of the blowup rate G theoretically, and these findings are supported by detailed numerical computations. Finally, some prototypical dynamical scenarios are explored, and an outlook towards such multi-hump solutions in higher dimensions is provided.

I. INTRODUCTION

The nonlinear Schrödinger (NLS) model is undoubtedly one of the quintessential ones within the realm of dispersive nonlinear partial differential equations [1–4]. It arises as a canonical or as an envelope model description in a diverse range of physical settings ranging from the evolution of optical beams in fibers and lasers [5, 6] to the description of atomic wavefunctions in ultracold Bose-Einstein condensates [7–9] and from plasmas [10] to water waves [2].

While the focus of a large number of studies on the NLS model concerns the dynamics of its solitary wave solutions (either bright [6] or dark [9, 11]), the presence of *collapse* is another key feature of the equation when nonlinear effects overcome dispersive ones. In this case, the relevant ground state solution to the NLS becomes (orbitally) unstable leading to the formation of singular solutions [3, 12]. From a physical perspective, the focusing nature of the problem induces self-similar collapse when the nonlinearity becomes “too strong” (e.g., considering a power nonlinearity $|u|^{2\sigma}u$ for a sufficiently large σ) [13–15], or when the dimensionality of the problem increases for fixed nonlinearity (e.g., considering a radially symmetric problem where the Laplacian reads $\Delta u = u_{rr} + (d-1)u_r/r$ for sufficiently large d [3, 12, 16–18]).

There has been a series of classic experiments that address relevant collapse features in NLS-type models, such as ones in nonlinear optics [19] observing the famous Townes soliton and its collapse, or more recent

ones examining the collapse of structures with topological charge [20]. Intriguingly, after numerous years, experiments in other fields such as ultracold atomic systems have also been catching up, and have enabled alternative Bose-Einstein condensate (BEC) realizations of Townes solitons in two separate recent experiments [21, 22]. Indeed, additional directions related to collapse have also been recently explored. These include the collapse of copropagating beams with different wavelengths in so-called two-color systems [23], as well as the consideration of vortical beams quenched from repulsive to attractive interactions in BECs and thus accordingly led to collapse [24].

It is some aspects of this very recent experimental endeavor of [24] that have motivated the present work. Indeed, in that work it was found that the original ring of atomic mass, prevented by the vortical structure from collapsing in the center of the condensate system, broke into a necklace structure consisting of individual (Townes-like) blobs which subsequently collapsed in the periphery of the ring pattern. This is also reminiscent of a scenario proposed earlier in the context of azimuthal modulational instability of a vortex solitary wave, e.g., in [25]. This scenario produces multiple concurrently collapsing structures, a setting that has, indeed, been theoretically considered earlier in the work of [26]. Arguably, the simplest setup enabling the study of such multi-bump states potentially leading to multiple concurrent blowups arises in one spatial dimension, i.e., $d = 1$. Indeed, the earlier work of [17] has partially examined such states in the realm of variable dimension d (i.e., used as a bifurcation parameter), which is rather unphysical (albeit interesting from a bifurcation perspective).

Here, motivated from our earlier studies which have considered the mathematically equivalent, yet more tractable setting of a variable nonlinear exponent σ , we revisit the examination of multi-pulse self-similarly exploding solutions. Firstly, we provide the mathematical setup (in Section II) that facilitates the numerical computation of these solutions, as a systematic bifurcation problem from the critical point of $\sigma d = 2$. Varying the nonlinear exponent σ with fixed $d = 1$, we construct the full bifurcation diagrams of such multi-pulse collapsing states, observing all of them emerging from *infinity* at the respective bifurcation point. As part of our analytical considerations, we derive the asymptotic distance of the pulses as a function of the deviation from the critical point. Moreover, following up on the analysis of the stability of the single-bump collapsing branch that appeared in our earlier works [14, 15], here we provide a systematic spectral analysis of the multi-bump branches, examining how the number of unstable modes of the solutions grows as a function of the blowup rate G . The summary of our theoretical and numerical results is provided in section III. Section IV focuses on the details of the theoretical analysis for the steady problem; the corresponding stability analysis is considered in Section V. Indeed, we have identified some unexpected dependencies of the relevant eigenvalues and explain the systematics of how the relevant power laws on G emerge. Both the eigenvalues and the eigenvectors of the resulting instabilities are provided together with a number of direct numerical computations performed on the half domain. The latter showcase the destabilization of the relevant multi-humped solutions towards the single-humped one. Finally, we summarize our findings and conclusions in Section VI, and discuss exciting avenues of future research emanating from the present work. A number of technical details concerning the numerical computations (involving, e.g., the comparison with alternative numerical approaches, as well as the dynamics in the full domain), and the analysis (such as the consideration of higher order terms in the bifurcation diagram) are presented in suitable Appendices.

II. THEORETICAL AND NUMERICAL SETUP

Our starting point for the examination of the multi-pulse collapse solutions will be the one-dimensional, nonlinear Schrödinger (NLS) equation with a power-law nonlinearity [14, 15] given by:

$$i\frac{\partial\psi}{\partial z} + \frac{\partial^2\psi}{\partial x^2} + |\psi|^{2\sigma}\psi = 0, \quad (1)$$

where $\psi := \psi(x, z)$ is the complex-valued wavefunction, and σ , the strength of the (power-law) nonlinearity. The Hamiltonian associated with the NLS reads:

$$H = \int_{-\infty}^{\infty} \left(\left| \frac{\partial\psi}{\partial x} \right|^2 - \frac{1}{\sigma+1} |\psi|^{2\sigma+2} \right) dx, \quad (2)$$

and satisfies:

$$i \frac{\partial \psi}{\partial z} = \frac{\delta H}{\delta \psi^*}, \quad i \frac{\partial \psi^*}{\partial z} = -\frac{\delta H}{\delta \psi},$$

where $*$ stands for complex conjugation. It should be noted that H is finite for the Cauchy problem of the NLS.

The study of self-similar blowup solutions to the NLS necessitates the introduction of the so-called stretched variables:

$$\xi := \frac{x}{L}, \quad \tau := \int_0^z \frac{dz'}{L^2(z')}, \quad \psi(x, z) := L^{-1/\sigma} v(\xi, \tau)$$

whose substitution to the NLS and Hamiltonian [cf. Eqs. (1) and (2)] gives respectively

$$i \frac{\partial v}{\partial \tau} + \frac{\partial^2 v}{\partial \xi^2} + |v|^{2\sigma} v - i \xi L L_z \frac{\partial v}{\partial \xi} - \frac{i L L_z}{\sigma} v = 0, \quad (3)$$

and

$$H = L^{-2/\sigma-2} \int_{-\infty}^{\infty} \left(\left| \frac{\partial v}{\partial \xi} \right|^2 - \frac{1}{\sigma+1} |v|^{2\sigma+2} \right) d\xi.$$

We will refer to Eq. (3) as the NLS in the co-exploding frame hereafter, and define $G := -L L_z$ corresponding to the blowup rate. This way, Eq. (3) is conveniently written as

$$i \frac{\partial v}{\partial \tau} + \frac{\partial^2 v}{\partial \xi^2} + |v|^{2\sigma} v - v + i G \left(\xi \frac{\partial v}{\partial \xi} + \frac{1}{\sigma} v \right) = 0, \quad (4)$$

where we have factored out phase rotations via the transformation of the (complex-valued) field $v \mapsto v^{i\tau}$. Self-similar blowup solutions to Eq. (4) are identified as *stationary* solutions therein, that is, $v(\xi, \tau) \mapsto v(\xi)$ when $\sigma > 2$ corresponding to the supercritical case for the one-dimensional NLS.

Indeed, we are able to numerically identify self-similar solutions by posing Eq. (4) on a computational yet finite spatial domain $[-K, K] \ni \xi$ supplemented with homogeneous Neumann boundary conditions, i.e., $v_\xi|_{\xi=\pm K} = 0, \forall \tau$. We consider a uniform spatial discretization with resolution $d\xi$, and replace the spatial derivatives with respect to ξ in Eq. (4) with a centered, fourth-order accurate finite difference scheme. We further validated our numerical findings in this work by employing the finite element method as implemented in the open-source software **FreeFem++** [27] (see also Sec. A in the Appendix).

Then, the identification of stationary solutions, i.e., self-similar ones to Eq. (4) involves the following twofold process. At first, we perform time-stepping using the BDF1 (i.e., backward Euler) scheme in order the self-similar dynamics to approach a stationary solution, i.e., $v(\xi, \tau) \mapsto v(\xi)$. We note that we corroborated our simulations here by using MATLAB's **ode23t** ODE solver (employing the trapezoidal method). Since the blowup rate G is an extra unknown to the problem, we close the system by imposing a pointwise, i.e., pinning condition of the form: $\text{Im}[v(\xi = 0, \tau)] = C \equiv \text{const.}$ stemming from:

$$\int_{-K}^K \text{Im}[v(\xi, \tau)] T(\xi) d\xi = C, \quad (5)$$

where $T(\xi)$ is the so-called template function [28]. For the pointwise condition given by Eq. (5), we choose $T(\xi) = \delta(\xi)$, and in most of our numerical computations, we set $C = 0$, thus seeking for a self-similar profile v satisfying: $\text{Im}[v(0, \tau)] = 0$. We would like to note at this point that our numerical experimentation has suggested that pointwise conditions may be a bit restrictive (especially during parametric continuations), and thus as an alternative, we have also employed alternative phase conditions obtaining the same results in terms of the amplitude $|v|$ (and density $|v|^2$) of the solution although the real and imaginary parts of v may be different. This is not surprising as each such approach respectively “pins down” a solution out of the group orbit of self-similar transformations.

Once the self-similar dynamics approaches a stationary profile $v(\xi)$ (and fixed blowup rate G), the second step “corrects” the solution by seeking to identify it as a numerically exact solution using Newton’s method. The waveform obtained from the self-similar dynamics is fed as an initial guess to the Newton solver, and it converges typically, within 2-3 iterations with very high accuracy. The resulting numerically exact solution (up to a prescribed accuracy) enables us subsequently to perform its spectral stability analysis in the co-exploding frame. For our stability computations and the results shown next, we use MATLAB’s `eigs` (sparse matrix) eigenvalue solver. Our stability results are corroborated using also the FreeFEM’s eigenvalue solver [27] (see also Sec. A in the Appendix). The spectral stability results we obtained using both eigensolvers match precisely with each other. The above described process works very well for the fundamental (single hump) self-similar solution of Eq. (4).

Our primary focus, however, in this work is on multi-humped, self-similar solutions of the NLS for $\sigma > 2$. Since these solutions are dynamically unstable, an alternative approach is required, as self-similar dynamics will not (typically) converge to a stable stationary profile. To identify suitable profiles that can serve as initial guesses for Newton’s method in solving the stationary two-point boundary value problem, we adopt the approach (known as zero-Hamiltonian solutions method) introduced in [17] (see, also [12]). In brief, we consider the radially symmetric case (for $d = 1$ in [17]) that renders Eq. (4) now defined on the half-line, i.e., $[0, \infty) \ni \xi$ with v_+ being the symmetric solution. For computational purposes, we truncate the semi-infinite domain to a finite one $[0, K]$ with K typically being 200 to 1000. The stationary problem that we aim to solve is:

$$v_+'' - v_+ + iG \left(\frac{1}{\sigma} v_+ + \xi v_+' \right) + |v_+|^{2\sigma} v_+ = 0, \quad (6)$$

supplemented with boundary conditions:

$$v_+'(0) = 0, \quad \text{Im}[v_+(0)] = 0, \quad \left| K v_+'(K) + (1 + i/G) v_+(K) \right| = 0, \quad (7)$$

where primes stand for (total) differentiation with respect to ξ .

The above boundary value problem is solved by a combination of a shooting method and a (gradient-free) minimization technique that ultimately determines the unknown parameters $(\text{Re}[v_+(0)], G)$, and thus the profile of interest. Indeed, starting from an initial guess $(\text{Re}[v_+^{(0)}(0)], G^{(0)})$, the latter is treated as an initial condition to Eq. (6) which itself is viewed as an initial-value problem. Upon performing a forward integration in ξ up to $\xi = K$, we treat the boundary condition at $\xi = K$ in Eq. (7) as our objective function we want to minimize. For our purposes, we used MATLAB’s `fminsearch` function (combined with the `ode23t` integrator), and corroborated our results using NAG’s `e04jyf` minimization routine (and `dop853` integrator). Upon convergence, we determine $(\text{Re}[v_+(0)], G)$ and the profile $v_+(\xi)$ of interest. Then, the solution $v(\xi)$ on $[-K, K]$ is constructed via symmetrization:

$$v(\xi) = \begin{cases} v_+(\xi), & \text{for } 0 \leq \xi \leq K \\ v_+(-\xi), & \text{for } -K \leq \xi \leq 0 \end{cases} \quad (8)$$

and fed to our Newton solver in order to obtain the numerically exact solution. We performed a systematic scan of different initial guesses $(\text{Re}[v_+^{(0)}(0)], G^{(0)})$ taken from the $(\text{Re}[v_+(0)], G)$ -plane, that gave us a plethora of multi-bump solutions to the NLS. Then, those were continued over σ parametrically by using pseudo-arclength continuation [29], thus obtaining branches of self-similar, multi-humped solutions, and constructing the respective bifurcation diagrams, i.e., G vs σ . For illustration purposes, Figure 1 displays an example of a double-humped solution to the boundary-value problem of Eqs. (6)-(7) obtained on $[0, 200]$, where its amplitude $|v_+|$ is depicted as a function of ξ . The localized bump is located around $\xi \approx 2.05$. For this particular solution, the determined parameters are: $\text{Re}[v_+(0)] = 0.4836$ and $G = 0.275549$.

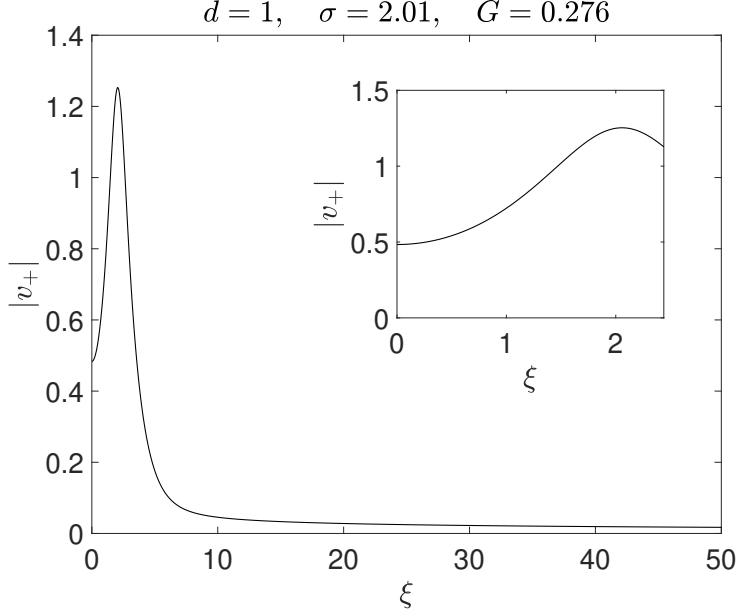


FIG. 1: The amplitude $|v_+|$ of a double-humped solution to the boundary value problem of Eqs. (6)-(7) for $\sigma = 2.01$ and $K = 200$. The blowup rate for this solution is $G \approx 0.276$, and the bump, i.e., the highest in-amplitude peak appears at $\xi \approx 2.05$. To ease visualization, the amplitude $|v_+|$ is shown on $[0, 50]$. The inset displays a zoom of $|v_+|$ near the origin confirming the vanishing derivative of the amplitude.

III. MULTIHUMPED 1D SELF-SIMILAR SOLUTIONS: PRINCIPAL EXISTENCE AND STABILITY RESULTS

A. Existence Results

Our prototypical results in terms of the existence of multi-pulse collapse states are presented in Figures 2 and 3. More specifically, Figure 2 presents the spatial profiles of self-similar solutions with $n = 1, 2, 3$ and 4 humps, and blowup rate $G = 0.01$ ($\sigma > 2$). Indeed, we have identified even higher order states (not shown here), always coming in two sets of families (see also the relevant discussion of [17]), namely ones with odd numbers of peaks (featuring a peak at the center of symmetry of the configuration), as well as ones with an even number of peaks, *which are symmetric around a local minimum of the profile density*.

The variation of hump positions with blowup rate, G is displayed in Fig. 3. This is a point of contact and indeed of excellent agreement with our theoretical analysis that we now summarize (the analysis is presented in full detail in Section IV). For the case of $n = 2$ equations, the theoretical prediction for the equilibrium positions of the two-pulse configurations is given (symmetrically around 0) by the G -dependent expressions:

$$X_1 = -\frac{32}{\pi G^2} e^{-X_2 + X_1}, \quad X_2 = \frac{32}{\pi G^2} e^{-X_2 + X_1},$$

so that $X_2 = -X_1 = X$, say, with

$$X = \frac{32}{\pi G^2} e^{-2X}.$$

The case of $n = 3$ equations leads our general expression detailed in section IV to result in the predictions of:

$$X_1 = -\frac{32}{\pi G^2} e^{-X_2 + X_1}, \quad X_2 = \frac{32}{\pi G^2} (e^{-X_2 + X_1} - e^{-X_3 + X_2}), \quad X_3 = \frac{32}{\pi G^2} e^{-X_3 + X_2},$$

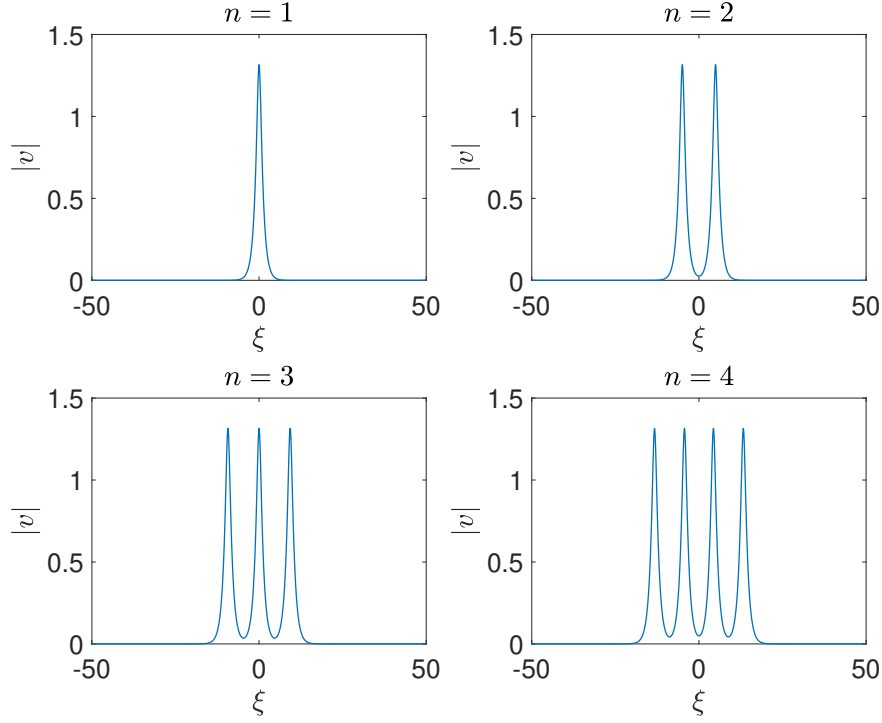


FIG. 2: Comparison of self-similar blowup solutions with $n = 1, 2, 3$ and 4 humps for $G = 0.01$ and $K = 50$.

so that $X_3 = -X_1 = X$, say, $X_2 = 0$, with

$$X = \frac{32}{\pi G^2} e^{-X}.$$

Finally, among the cases shown in Fig. 3, for $n = 4$, our theoretical predictions yield:

$$\begin{aligned} X_1 &= -\frac{32}{\pi G^2} e^{-X_2+X_1}, & X_2 &= \frac{32}{\pi G^2} (e^{-X_2+X_1} - e^{-X_3+X_2}), \\ X_3 &= \frac{32}{\pi G^2} (e^{-X_3+X_2} - e^{-X_4+X_3}), & X_4 &= \frac{32}{\pi G^2} e^{-X_4+X_3}, \end{aligned}$$

so that, with $X_3 = -X_2 = Y_1$, $X_4 = -X_1 = Y_2$, say, with

$$Y_1 = \frac{32}{\pi G^2} (e^{-2Y_1} - e^{-Y_2+Y_1}), \quad Y_2 = \frac{32}{\pi G^2} e^{-Y_2+Y_1}.$$

We can observe that Fig. 3 presents *excellent agreement* with the observed numerical results throughout the interval of consideration for the values of G . Similar predictions can be made for arbitrary values of n , as will be seen in Section IV.

Moreover, having the positions of the pulses, we also derive in section IV a systematic expression that provides the corresponding branch's bifurcation diagram, i.e., connects the blowup rate G with the nonlinearity power σ in line with our earlier calculation in [14]. More specifically:

$$\sigma - 2 = \frac{8\sigma}{n\pi} (e^{2X_n} + e^{-2X_1}) \frac{e^{-\pi/G}}{G}. \quad (9)$$

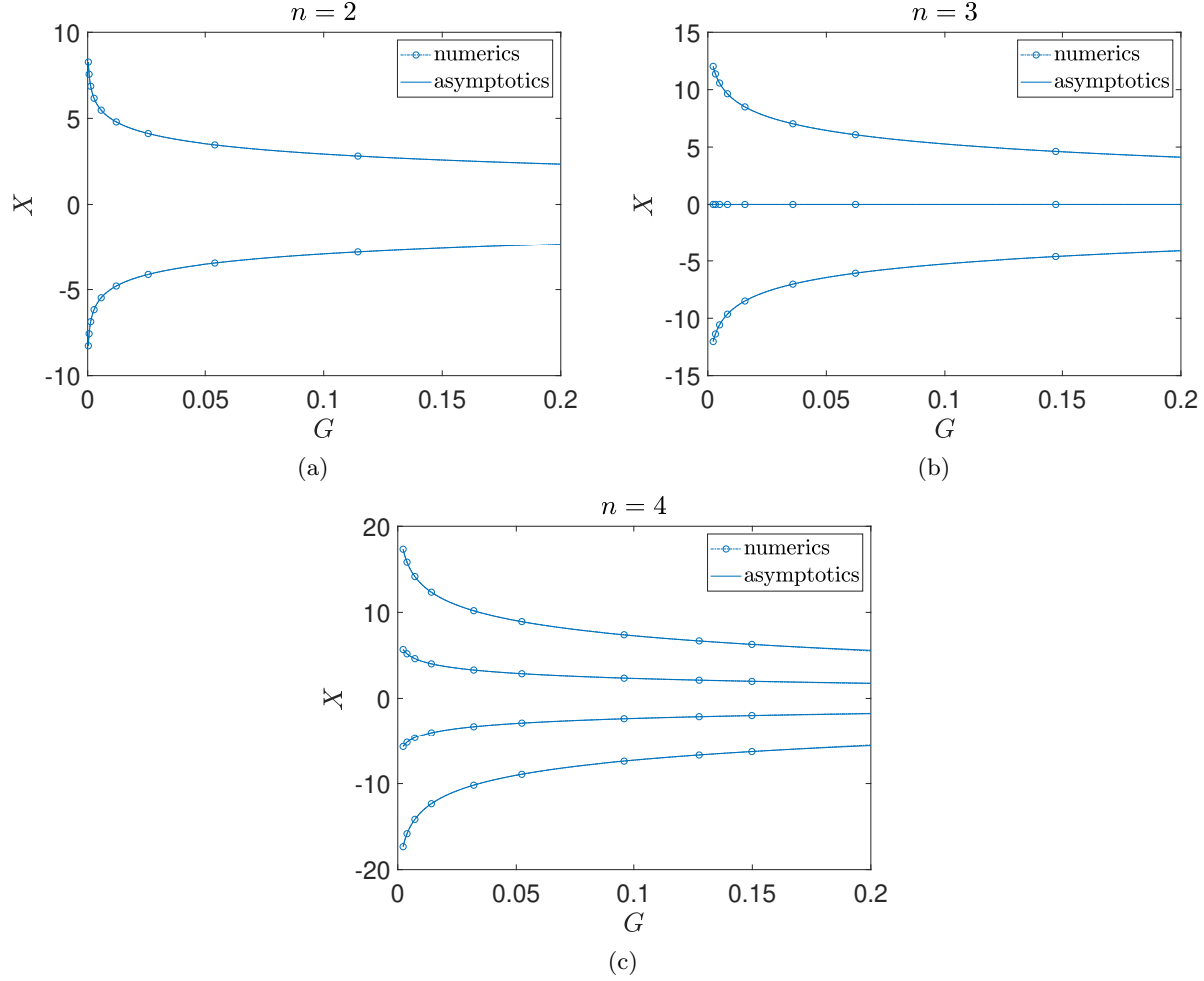


FIG. 3: Variation of hump positions, X , with blowup rate, G for two, three and four-humped self-similar solutions. The dash-dotted lines with open circles lines correspond to numerical solutions with $K = 50$. The full lines represent the asymptotic prediction of hump positions.

Note that with $n = 1$ and $X_1 = X_n = 0$ this reduces to the formula in [14], and also that we anticipate the solutions of (9) to satisfy $X_1 = -X_n$ so that

$$\sigma - 2 = \frac{16\sigma}{n\pi} \frac{e^{2X_n - \pi/G}}{G}. \quad (10)$$

Figure 4 illustrates the dependence of G with the parameter σ for self-similar solutions of different numbers of humps, as obtained through our numerical computations. Among all self-similar profiles, only the single-humped ($n=1$) solution with $G > 0$ is found to be stable (as will be discussed below). However, importantly for all the branches considered, we find again excellent agreement between the theoretical bifurcation curve prediction and the numerically obtained one. Only in the case of $n = 4$ can we detect a nearly imperceptible discrepancy at the level of the figure (at least with the eyeball metric) between theory and computation. While this discrepancy is modestly amplified as n becomes higher, it is clear that all the relevant branches are accurately captured by our asymptotics. Moreover, and quite importantly, this bifurcation analysis definitively shows that all of the relevant solutions emerge *concurrently* at the blowup threshold of $\sigma d = 2$. Indeed, as our position diagrams clearly indicate, the relevant waveforms constitute an example of

“bifurcation from infinity”, with the relevant pulses being “summoned back” (from an infinite) to a finite distance from each other as the blowup rate G increases.

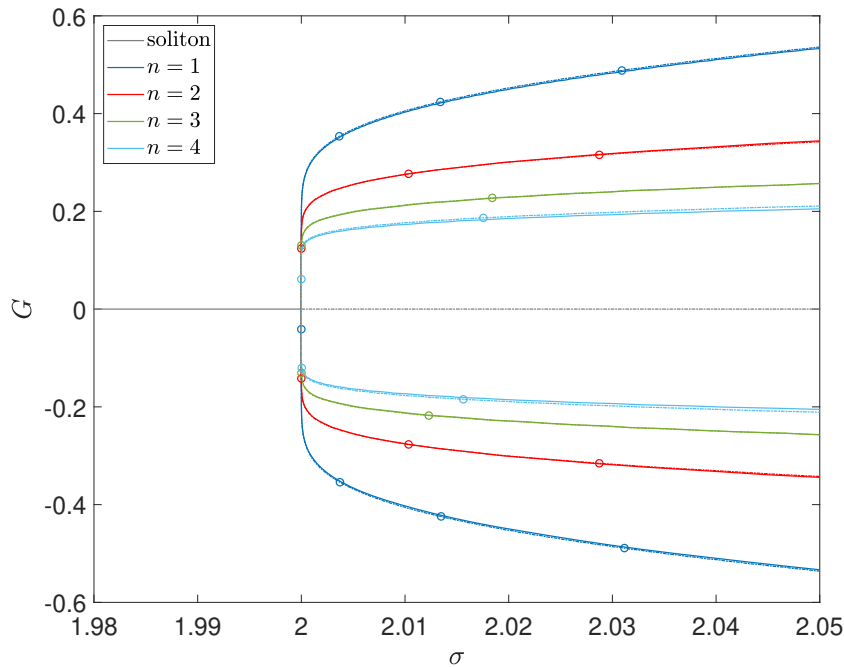


FIG. 4: Variation of the blowup rate G as a function of σ for domain size, $K = 50$. The gray lines represent the blowup rate of soliton solutions, and the blue line displays the blowup rate of $n = 1$ -humped self-similar solutions. The blowup rates of self-similar solutions with $n = 2, 3, 4$ humps are depicted with red, green, and cyan lines, respectively. The dot-dashed lines with open circles represent the numerical computations, and the solid lines show the asymptotic prediction for the blowup rate G .

B. Spectral Properties

We now turn to the examination of the stability features of each one of the branches that are identified herein. Before we do so, it is instructive to remind ourselves of the findings for the single-hump $n = 1$ branch as obtained earlier in [15]. In the relevant case, as the destabilization of the relevant solitonic branch proceeds (for the $G = 0$ solution), we have identified 6 point spectrum eigenvalues, i.e., 3-pairs near the origin. When we move to the co-exploding frame to obtain the self-similarly collapsing solution as a stationary state, it was argued in [15] that two exact eigenvalues can be computed ($\lambda = 2G$ and $\lambda = G$) associated with the symmetries of rescaling and of translation, respectively, in the case of the infinite domain. One more eigenvalue was found to stay at $\lambda = 0$, while 3 negative real eigenvalues slightly deviating from the opposites of the above values (as the system is no longer Hamiltonian) were also identified.

To consider the stability problem in further mathematical detail, we first perform a transformation: $v(\xi, \tau) = V(\xi, \tau)e^{i\tau - iG(\tau)\xi^2/4}$ to turn our PDE problem to:

$$i\frac{\partial V}{\partial \tau} + \frac{G'\xi^2}{4}V + \frac{\partial^2 V}{\partial \xi^2} + |V|^{2\sigma}V - V - \frac{i(\sigma - 2)G}{2\sigma}V + \frac{G^2\xi^2}{4}V = 0,$$

where $G' = dG/d\tau$.

Then, the steady state solutions satisfy:

$$\frac{d^2 V_s}{d\xi^2} + |V_s|^{2\sigma} V_s - V_s - \frac{i(\sigma-2)G}{2\sigma} V_s + \frac{G^2 \xi^2}{4} V_s = 0, \quad (11)$$

with G constant equal to $G(\sigma)$. We linearize about the steady state by writing

$$V(\xi, \tau) = V_s(\xi) + \epsilon \left(f(\xi) e^{\lambda \tau} + g^*(\xi) e^{\lambda^* \tau} \right) \quad (12)$$

and accordingly obtain the eigenvalue problem

$$i\lambda f + \frac{d^2 f}{d\xi^2} + \sigma |V_s|^{2\sigma-2} V_s^2 g + (\sigma+1) |V_s|^{2\sigma} f - f - \frac{i(\sigma-2)G}{2\sigma} f + \frac{G^2 \xi^2}{4} f = 0, \quad (13)$$

$$-i\lambda g + \frac{d^2 g}{d\xi^2} + \sigma |V_s|^{2\sigma-2} (V_s^*)^2 f + (\sigma+1) |V_s|^{2\sigma} g - g + \frac{i(\sigma-2)G}{2\sigma} g + \frac{G^2 \xi^2}{4} g = 0. \quad (14)$$

Then, the two exact eigenvalues and their corresponding eigenvectors —for the infinite domain case— can be explicitly written as: $\lambda = 2G$,

$$f = iV_s + G \left(\frac{V_s}{\sigma} + \xi \frac{dV_s}{d\xi} - \frac{iG\xi^2 V_s}{2} \right), \quad g = -iV_s^* + G \left(\frac{V_s^*}{\sigma} + \xi \frac{dV_s^*}{d\xi} + \frac{iG\xi^2 V_s^*}{2} \right). \quad (15)$$

and $\lambda = G$,

$$f = \frac{dV_s}{d\xi} - \frac{iG\xi V_s}{2}, \quad g = \frac{dV_s^*}{d\xi} + \frac{iG\xi V_s^*}{2}. \quad (16)$$

What we find in the case of the multi-bump collapse solutions is that the number of eigenvalues is effectively doubled when we consider two-pulse solutions instead of one. I.e., in the case of $n = 2$ we need to account for 12 point spectrum eigenvalues instead of 6. In the case of 3-pulse solutions this number rises to 18 and for $n = 4$ to 24. Remarkably (for us!) we have been able to fully categorize the eigenvalues of each one of these scenarios. Indeed, what we find in each case of n -pulse states is the following: the configuration ends up possessing *exactly* $n - 1$ real eigenvalues that, to leading order, depend on the blowup rate in a predominantly square root form, i.e., $\lambda \propto G^{1/2}$. There are similarly $n + 1$ real eigenvalues that end up with a dependence $\lambda \propto G$. Then, there exist $n - 1$ pairs that end up being purely imaginary for an n -pulse state. Finally, one pair ends up near the origin. Given that, for each of the real eigenvalues, nearly the opposite λ is also (very close) to an eigenvalue, this accounts for $(n - 1) + (n + 1) + (n - 1) + 1$ i.e., $3n$ (approximate) pairs, i.e., $6n$ eigenvalues in total, which is what we observe for solutions consisting of n -copies of the original pulse. The spectra of the multi-humped self-similar solutions are illustrated in Fig. 5 for $G = 0.01$. In all cases, one can observe that a vertical part of each spectrum aligns at $-G$. In all cases, one can observe the existence of real positive eigenvalues, the number of which changes with the number of humps, n . In particular, single-humped solutions have two dominant real eigenvalues, $n = 2$ solutions have four, $n = 3$ have six, and $n = 4$ have eight dominant real eigenvalues. All multi-humped self-similar solution have two real eigenvalues $\lambda_1 \approx G$, and $\lambda_2 \approx 2G$ [rather than equal to G or $2G$ as our computations are affected by the finiteness of the computational domain]. The relevant count is fully in line with our qualitative discussion above.

Importantly, our methodology does not only provide the qualitative theoretical backdrop for the eigenvalue dependence on G . It provides, as will be evident in section V, detailed quantitative estimates for the relevant eigenvalues. Moreover, it provides explicit predictions for the corresponding eigenfunctions. These can be seen in comparison to the numerically obtained eigenvectors in Fig. 6 and to the corresponding numerical eigenvalues in Fig. 7. The former are in excellent agreement with the numerical computations. For the latter, the $G^{1/2}$ dependence of $n - 1$ real eigenvalues, and the G dependence of another $n + 1$ ones is evident, and we see that for most of them the agreement is also quantitatively very accurate. For some of the eigenvalues, we observe a slight disparity (e.g., for λ_3 (green) one for the $n = 2$ case, λ_4 and λ_6 (black and red) for $n = 3$ and perhaps most notably λ_5 and λ_8 (purple and pink ones) for $n = 4$). This is, however, chiefly true when

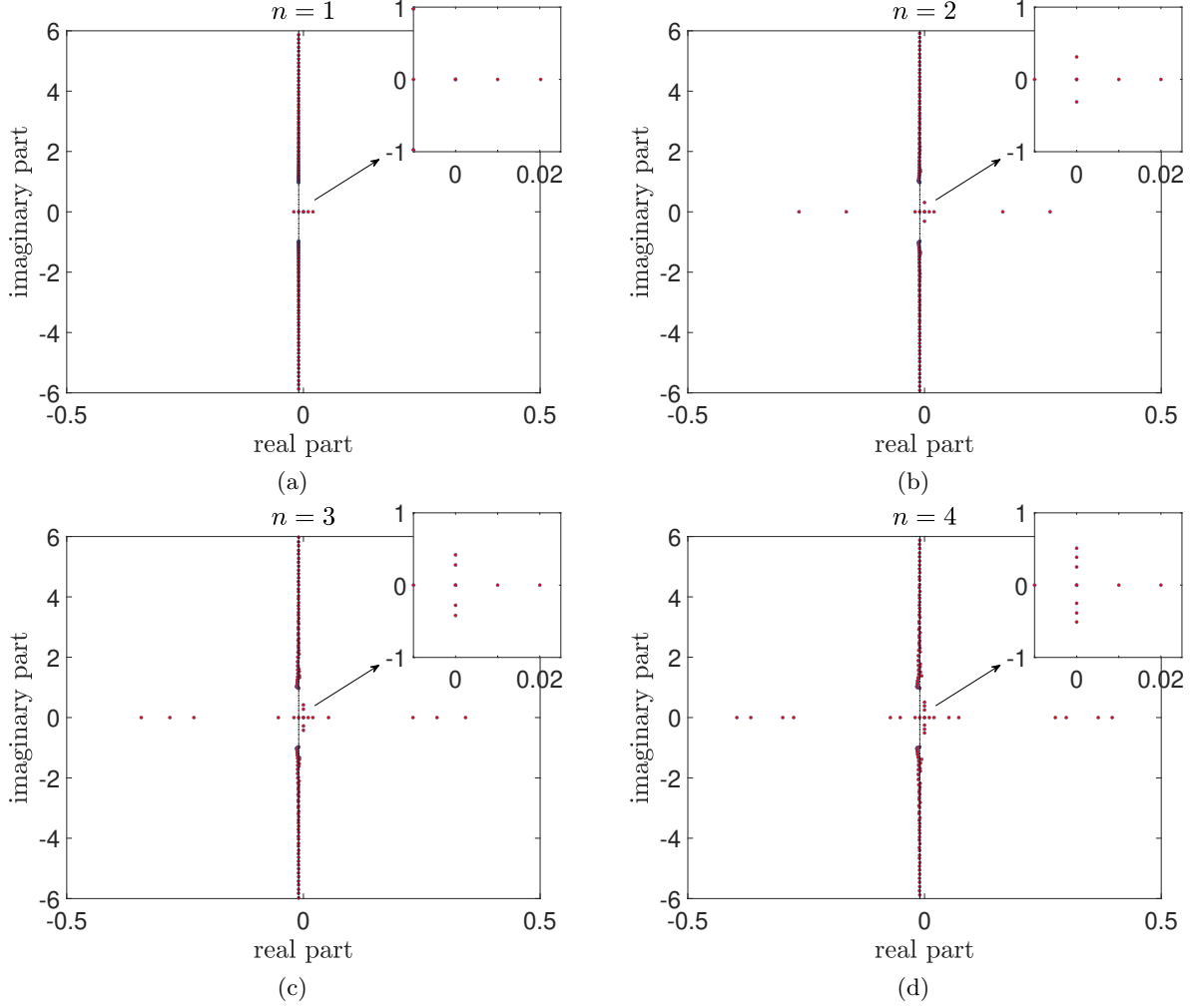


FIG. 5: Single ($n = 1$) and multi-humped ($n = 2, 3, 4$) self-similar solution spectra for $G = 0.01$. The vertical part of the spectra align at $-G = -0.01$ for all cases (black dash-dotted lines). The insets illustrate real eigenvalues $\lambda \approx G$, $\lambda \approx 2G$, and eigenvalues with zero real part. One can observe the existence of a single conjugate pair of eigenvalues with zero real part for self-similar solutions with $n = 2$ humps, two pairs for $n = 3$, and three pairs for $n = 4$. For single-humped self-similar solutions there is only an eigenvalue at the origin.

the eigenvalues are sufficiently large and takes place due to higher order corrections not accounted for in our theory. Interestingly, for some other eigenvalues, these higher order corrections appear to be negligible and the prediction remains highly accurate throughout the interval of considered values of G . At the moment, we do not have an explanation about why this takes place for some of the eigenvalues but not for others, other than to allude to reasons of symmetry. However, this is a potential interesting topic for further exploration.

C. Dynamics in the Self-similar Frame

Our methodology captures the associated dynamics in the rescaled $\xi - \tau$ spatio-temporal domain. In particular, we aim to validate the instability of multi-humped self-similar NLS solutions –discussed in the previous sections– in contrast to the stable single-humped self-similar solutions. For this purpose, we solve

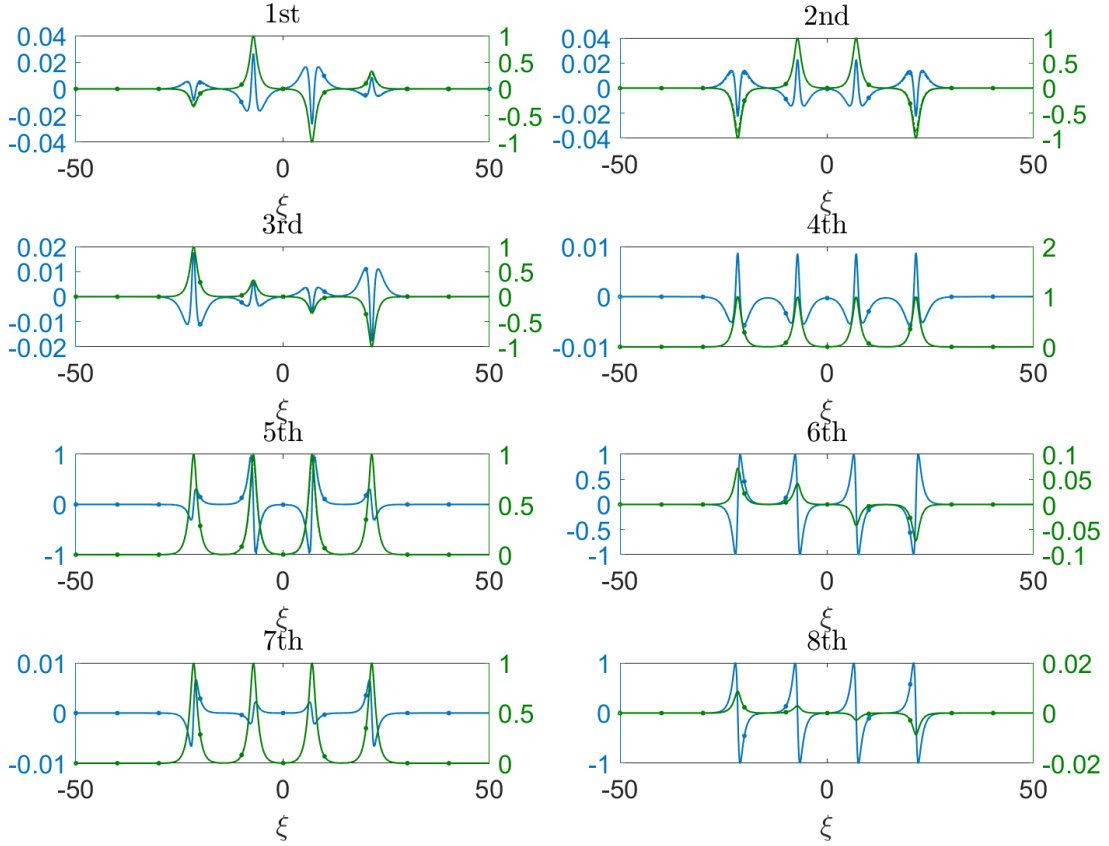


FIG. 6: Eigenfunctions for 4-humped solutions and $G = 5 \times 10^{-4}$. Blue depicts the real part and green corresponds to the imaginary parts. The numerical eigenfunctions are displayed with dash-dotted lines with open circles and asymptotic predictions (from §V, truncated at $O(G)$) are displayed with solid lines. The two are practically coincident with each other.

Eq. (4) in $\xi \in [0, K]$ with zero flux boundary conditions at both ends of the domain. The blowup rate, G , is computed by imposing a pinning condition, which “freezes” the imaginary part of v at $\xi = 0$ to a constant value, C , i.e.: $\text{Im}[v(0, \tau)] = C$, in line with the above discussion. Time-stepping is performed by applying the backward Euler scheme, as also discussed above.

Figure 8(a)-(b) illustrates the evolution of unstable two-humped and three-humped self-similar solutions toward a stable single-humped self-similar state. The insets display the evolution of the blowup rate, G , with both cases achieving convergence after $\tau \approx 40$. For the two-humped case (Fig. 8(a)), the initial condition is the self-similar solution at $\sigma = 2.011$ which is perturbed by decreasing σ by 10^{-4} , i.e., setting $\sigma = 2.0109$. For the three-humped case (Fig. 8(b)), we start with the self-similar solution computed at $\sigma = 2.011$ and perturb it by increasing σ by 10^{-4} , i.e., using $\sigma = 2.0111$ in the dynamical integration. In both cases, it is clear that asymptotically once some of the system’s “mass” is ejected outward, the profiles can converge to the single-hump state.

However, it is important to note that convergence to the stable single-humped self-similar solution is not always guaranteed, and depends on the nature of the initial perturbation. For instance, reversing the sign of the σ perturbation in the two previous simulations prevents the dynamics from converging to a stable single-humped solution, as shown in Figs. 9(a)-(b). Specifically, Fig. 9(a) illustrates the evolution of the

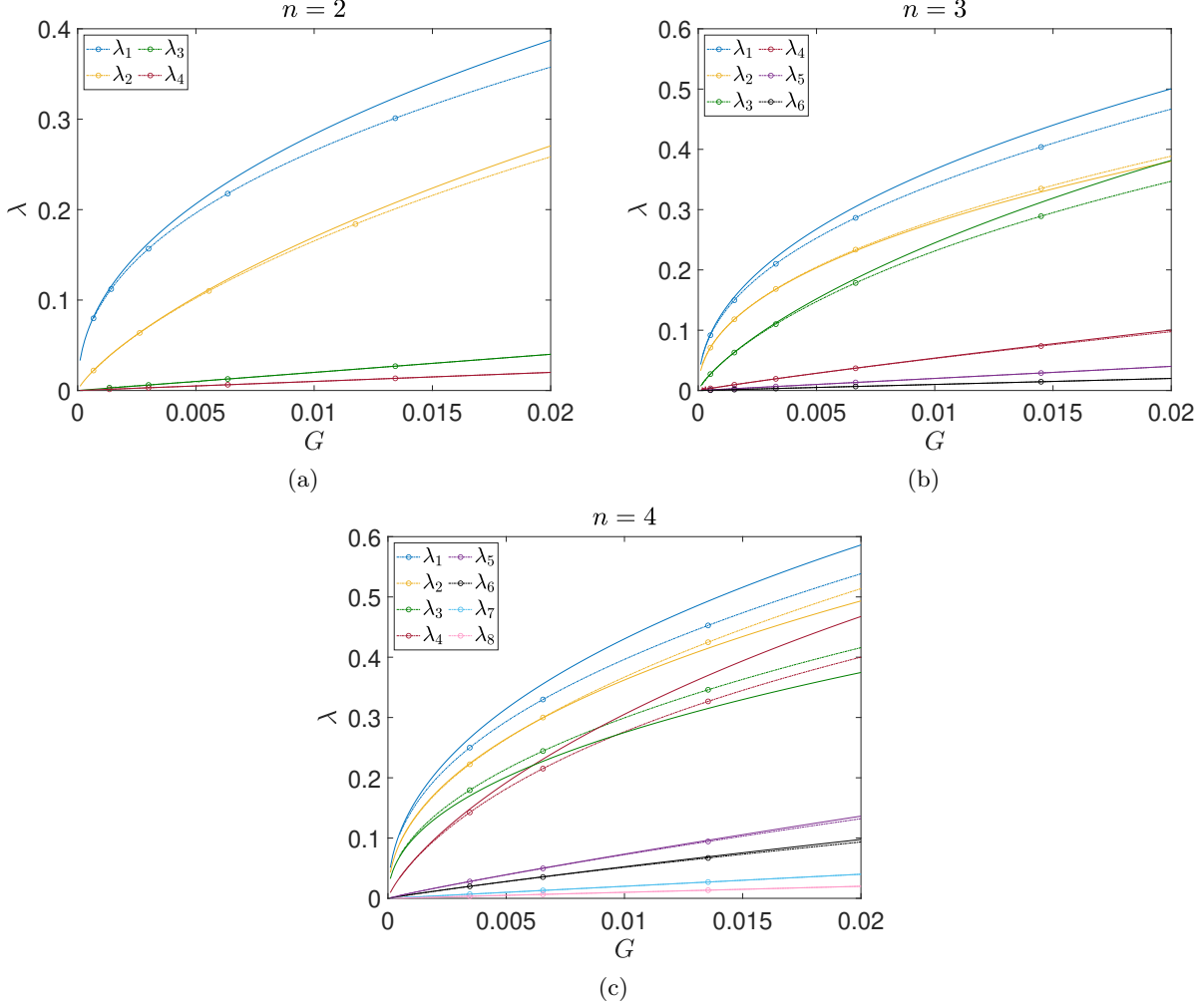


FIG. 7: Variation of dominant real eigenvalues with blowup rate, G for (a) two, (b) three, and (c) four humped self-similar solutions. All multi-humped solutions share the $\lambda \approx G$ and $\lambda \approx 2G$ eigenvalues (λ_4 and λ_3 for $n = 2$, λ_6 and λ_5 for $n = 3$, and λ_8 and λ_7 for $n = 4$, respectively). Numerical computations for each eigenvalue are displayed with dash-dotted lines with open circles and asymptotic predictions are depicted with solid lines of the same color for each eigenvalue.

two-humped solution computed at $\sigma = 2.011$ and perturbed by increasing σ by 10^{-4} (i.e., $\sigma = 2.011$). Similarly, Fig. 9(b) depicts the evolution of the three-humped solution, also computed at $\sigma = 2.011$, this time perturbed by decreasing σ to 2.0109. In both cases, the rescaled dynamics fail to reach a stable single-humped self-similar state.

To further reinforce our statement we perform additional simulations, where the initial multi-humped state is perturbed along an unstable eigenvector associated with one of the dominant real eigenmodes. Here, we apply perturbations along the eigenmode corresponding to the largest real eigenvalue. In Figs. 10(a)-(b), we present the spatio-temporal evolution of v starting from perturbed (a) two-humped, and (b) three-humped self-similar solutions computed at $\sigma = 2.001$. All different multi-modal self-similar states *are expected to evolve toward the same stable single-humped self-similar solution*. This is illustrated in Fig. 10(c), where we show the initial state for each simulation (2-humped and 3-humped at $\tau = 0$) alongside the final, stable single-humped self-similar state at $\tau = 200$ for $\sigma = 2.001$. The converged blow-up rate ($G(\tau = 200) \approx 0.302$) is identical across all three simulations.

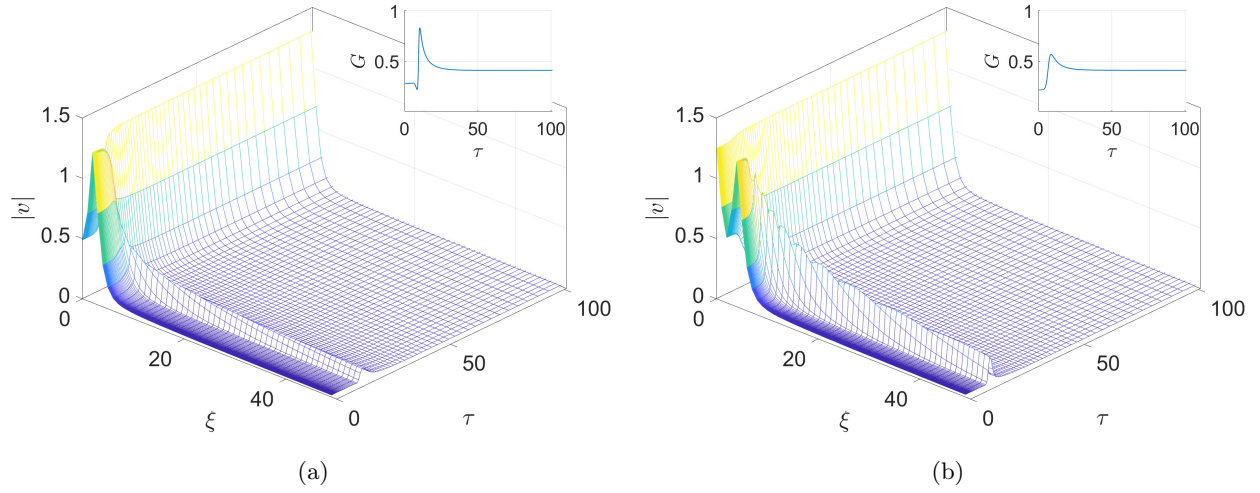


FIG. 8: Long time stability of single-humped self-similar solutions in dynamical simulations. (a) A two-humped self-similar solution, initially computed at $\sigma = 2.011$, evolves toward a stable single-humped self-similar solution after a slight decrease to $\sigma = 2.0109$. (b) A three-humped self-similar solution ($\sigma = 2.011$) transitions to a stable single-humped self-similar state when σ is increased to $\sigma = 2.0111$. The insets display the corresponding evolution of the blowup rate G . Simulations are performed in the domain $\xi \in [0, 50]$, with a nodal distance of $\Delta\xi = 0.002$.

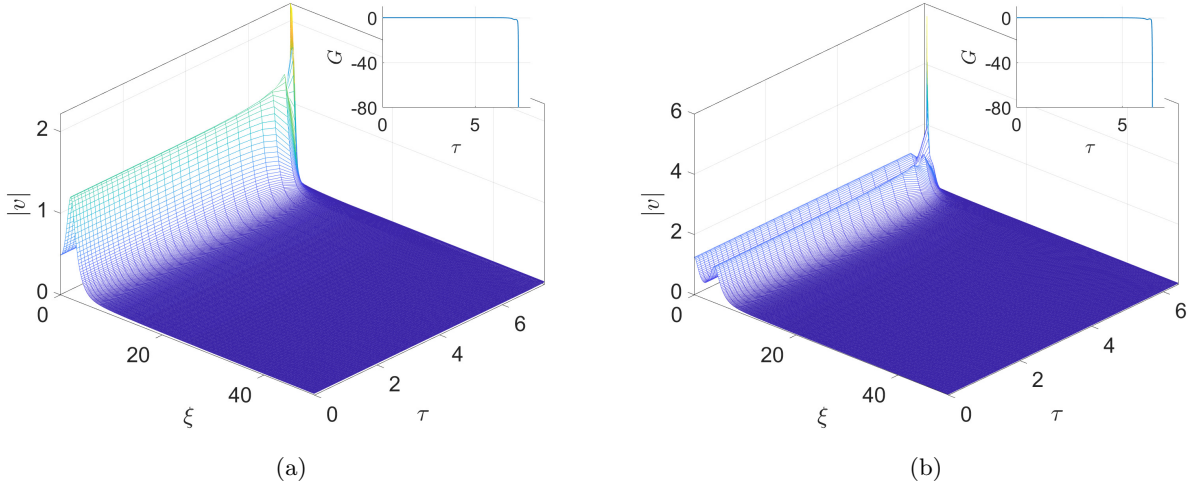


FIG. 9: (a) Dynamical simulation starting from a two-humped self-similar solution at $\sigma = 2.011$; the σ value is now slightly increased to $\sigma = 2.0111$, and dynamics evolve away from the stable single-humped self-similar solution. (b) An initial three-humped self-similar solution computed at $\sigma = 2.011$ is now perturbed setting $\sigma = 2.0109$. Again, one observes that rescaled dynamics fail to converge to a stable self-similar state. The insets display the corresponding evolution of the blowup rate G . Simulations are performed in the domain $\xi \in [0, 50]$, with a nodal distance of $\Delta\xi = 0.002$.

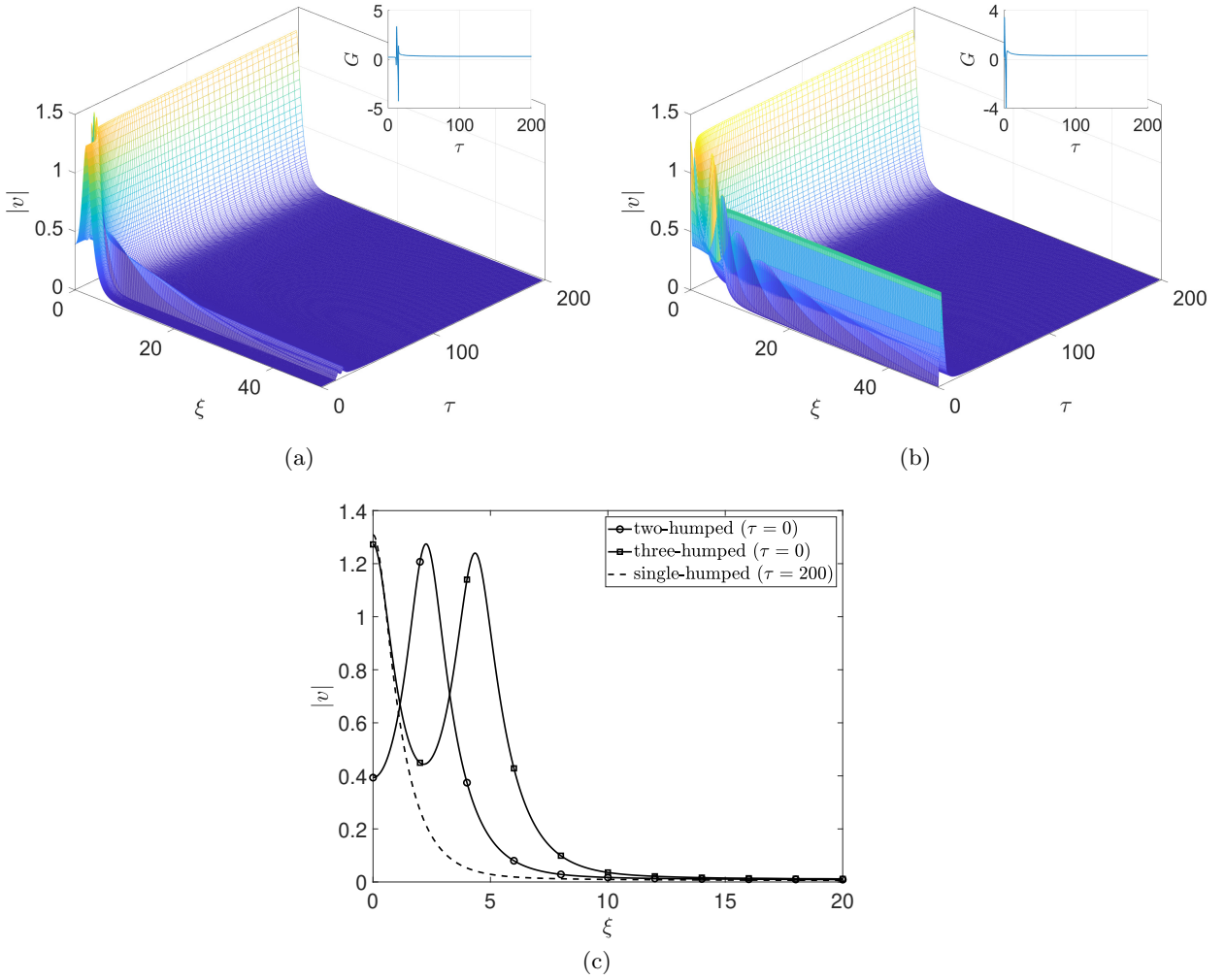


FIG. 10: Dynamical simulations starting from (a) two-humped, and (b) three-humped self-similar solutions at $\sigma = 2.001$. By perturbing the initial condition along an unstable eigendirection (the one associated with the second largest real eigenvalue), the self-similar dynamics converged to the corresponding stable single-humped solution at large τ . The inset of each figure shows the corresponding evolution of the blow-up rate G . (d) The two different multi-humped states (2-humped and 3-humped) ultimately converge to the same stable single-humped self-similar profile (dashed line).

IV. DETAILED ASYMPTOTIC ANALYSIS OF THE MULTI-HUMP STEADY STATE

We suppose that σ is exponentially close to 2 as $G \rightarrow 0$ so that, in steady state,

$$\frac{d^2 V_s}{d\xi^2} + |V_s|^4 V_s - V_s + \frac{G^2 \xi^2}{4} V_s + \text{T.S.T.} = 0,$$

where T.S.T. represents transcendentally small terms. We look for a general multi-hump solution, with humps located at $\xi = X_i(G)$ with $|X_i| \gg 1$, $i = 1, \dots, n$, where we label such that $X_i < X_{i+1}$. We aim to determine the X_i along with the dependence of G on σ . We will find that each $X_i = O(\log G)$. By symmetry we expect to find $X_i = -X_{n+1-i}$, though we will not assume it. We use the pinning condition $\text{Im}(V_s(0)) = 0$, for which we will find V_s is real to all algebraic orders in G .

For the single hump we found in [14] that the solution comprised a near field in the vicinity of the hump and a far field away from the hump. The far field contained a turning point, so there was also an inner region in the vicinity of the turning point which gave an exponentially-small reflection back towards the near field. This exponentially small component ultimately led to the relationship between σ and G describing the bifurcation. In the multi-hump case we will find that there is again a near field in the vicinity of each hump, along with new regions between adjacent humps. The far field, including the turning point, remains largely the same as in the single-hump case. We will detail the asymptotic solution in each region in turn, matching them to obtain the positions of the humps and the relationship between σ and G .

A. Near field of the i th hump

We write $\xi = X_i + x$ to give

$$\frac{d^2 V_s}{dx^2} + |V_s|^4 V_s - V_s + \frac{G^2(x + X_i)^2}{4} V_s = 0. \quad (17)$$

Now expand

$$V_s = \sum_{n=0}^{\infty} G^{2n} V_n \quad (18)$$

to give the leading-order equation

$$\frac{d^2 V_0}{dx^2} + |V_0|^4 V_0 - V_0 = 0, \quad (19)$$

where we have assumed (and will verify a posteriori) that $G^2 X_i^2 \ll 1$. The relevant solution is the soliton,

$$V_0 = 3^{1/4} \operatorname{sech}^{1/2}(2x) = 3^{1/4} \operatorname{sech}^{1/2}[2(\xi - X_i)]. \quad (20)$$

B. Solution in between the humps

Consider the gap between X_i and X_{i+1} . In this region V_s is (algebraically) small, so we can neglect the nonlinear terms at leading order. Then, expanding again as in (18) gives

$$\frac{d^2 V_0}{d\xi^2} - V_0 = 0. \quad (21)$$

The inner solution (20) near X_{i+1} written in terms of ξ is

$$V_0 = 3^{1/4} \operatorname{sech}^{1/2}[2(\xi - X_{i+1})].$$

For large X_{i+1} with $\xi \ll X_{i+1}$ this is

$$V_0 \sim 12^{1/4} e^{\xi - X_{i+1}}. \quad (22)$$

Similarly the inner solution near X_i written in terms of ξ is

$$V_0 = 3^{1/4} \operatorname{sech}^{1/2}[2(\xi - X_i)].$$

For large X_i with $X_i \ll \xi$ this is

$$V_0 \sim 12^{1/4} e^{-\xi + X_i}. \quad (23)$$

Imposing these two matching conditions the solution of (21) for $X_i \ll \xi \ll X_{i+1}$ yields

$$V_0 = 12^{1/4} e^{-\xi + X_i} + 12^{1/4} e^{\xi - X_{i+1}}. \quad (24)$$

There is an exponentially small (in $X_i - X_{i+1}$) interaction term from each hump on the other. We will see that this term will match with the next term in the inner expansion, which is $O(G^2)$, so that $X_i - X_{i+1}$ will be logarithmically large in G . Writing (24) in terms of the inner variable $x = \xi - X_{i+1}$ gives

$$V_0 = 12^{1/4} e^x + 12^{1/4} e^{-x + X_i - X_{i+1}}; \quad (25)$$

thus the extra interaction term corresponds to an exponentially growing term leaving the inner region near X_{i+1} . Similarly, in terms of the inner variable $x = \xi - X_i$ we have

$$V_0 = 12^{1/4} e^{-x} + 12^{1/4} e^{x + X_i - X_{i+1}}, \quad (26)$$

again corresponding to an exponentially growing term leaving the inner region near X_i .

In the regions $\xi > X_n$ and $\xi < X_1$ there is no additional interaction term—the solution to (21) is a single exponential which decays at $\pm\infty$ respectively. We may include these regions in the general framework by adopting the convention that $X_0 = -\infty$, $X_{n+1} = \infty$, in which case (24) holds in these regions also.

C. Next order in the near field

Equating coefficients of G^2 in (17) gives

$$\frac{d^2 V_1}{dx^2} + 5V_0^4 V_1 - V_1 = -\frac{(x + X_i)^2}{4} V_0. \quad (27)$$

The homogeneous version of (27) is satisfied by V_0' , so that there is a solvability condition. Multiplying by V_0' and integrating gives, on the LHS,

$$\int_{-R}^R \frac{dV_0}{dx} \left(\frac{d^2 V_1}{dx^2} + 5V_0^4 V_1 - V_1 \right) dx = \left[\frac{dV_0}{dx} \frac{dV_1}{dx} - \frac{d^2 V_0}{dx^2} V_1 \right]_{-R}^R + \int_{-R}^R \left(\frac{\partial^3 V_0}{\partial x^3} + 5V_0^4 \frac{dV_0}{dx} - \frac{dV_0}{dx} \right) V_1 dx$$

so that the solvability condition is (when accounting for the vanishing of the integral term upon differentiation of the expression for V_0 in Eq. (19))

$$-\int_{-R}^R \frac{dV_0}{dx} \frac{(x + X_i)^2}{4} V_0 dx = \left[\frac{dV_0}{dx} \frac{dV_1}{dx} - \frac{d^2 V_0}{dx^2} V_1 \right]_{-R}^R. \quad (28)$$

Since V_0 is even the LHS may be simplified to

$$-X_i \int_{-R}^R \frac{dV_0}{dx} \frac{x}{2} V_0 dx = X_i \int_{-R}^R \frac{V_0^2}{4} dx \rightarrow \frac{\sqrt{3} \pi X_i}{8} \text{ as } R \rightarrow \infty.$$

For the RHS we evaluate the boundary terms by matching with (25) and (26). As $x \rightarrow \infty$,

$$G^2 V_1 \sim 12^{1/4} e^{-X_{i+1} + X_i} e^x, \quad V_0 \sim 12^{1/4} e^{-x}, \quad (29)$$

so that

$$\frac{dV_0}{dx} \frac{dV_1}{dx} - \frac{d^2 V_0}{dx^2} V_1 \sim -4\sqrt{3} \frac{e^{-X_{i+1} + X_i}}{G^2}.$$

Similarly, as $x \rightarrow -\infty$,

$$G^2 V_1 \sim 12^{1/4} e^{-X_i + X_{i-1}} e^{-x}, \quad V_0 \sim 12^{1/4} e^x, \quad (30)$$

so that

$$\frac{dV_0}{dx} \frac{dV_1}{dx} - \frac{d^2V_0}{dx^2} V_1 \sim -4\sqrt{3} \frac{e^{-X_i+X_{i-1}}}{G^2}.$$

Thus the solvability condition (28) is, as $R \rightarrow \infty$,

$$X_i = \frac{32}{\pi G^2} (e^{-X_i+X_{i-1}} - e^{-X_{i+1}+X_i}). \quad (31)$$

Equations (31) form a closed system of n equations for the n unknowns X_1, \dots, X_n . It is relevant to note here that this set of equations (that is sometimes referred to as the —steady state form of— Toda lattice with nonzero masses) has appeared in other settings recently, such as, e.g., the case of N dark solitary waves in the presence of a parabolic confinement applicable to atomic Bose-Einstein condensates [30]. In the latter case, the exponential tail-tail interaction of the solitary waves is balanced by the presence of the parabolic trap (onsite) effect on each of the solitary waves. On the other hand, here the linear effective potential stems from the role of the phase of the complex wavefunction past the critical point of collapse. For the present case, we still need to identify σ , and to do so we need to consider the regions $\xi > X_n$ and $\xi < X_1$ more carefully.

D. Far field

Consider first the region $\xi > X_n$. When ξ is large the term $G^2 \xi^2 V_s/4$ can no longer be neglected. Thus there is a different balance in the equation in the far field. The solution is almost exactly the same as for the single-hump soliton reported in [14], so we merely sketch the analysis here.

We rescale $\xi = \rho/G$ to give

$$G^2 \frac{\partial^2 V_s}{\partial \rho^2} + |V_s|^4 V_s - V_s + \frac{\rho^2}{4} V_s = 0.$$

Since V_s is exponentially small in the far field we can neglect the nonlinear term. We look for a WKB solution in the form

$$V_s \sim e^{\phi(\rho)/G} \sum_{n=0}^{\infty} A_n(\rho) G^n. \quad (32)$$

At leading order this gives

$$(\phi')^2 = 1 - \frac{\rho^2}{4}.$$

Note the turning point at $\rho = 2$. For $\rho < 2$ the relevant solution is

$$\phi' = - \left(1 - \frac{\rho^2}{4}\right)^{1/2}$$

so that ϕ is decreasing (and V is exponentially decaying) as ρ increases. Let us fix the constant by writing

$$\phi = - \int_0^\rho \left(1 - \frac{\bar{\rho}^2}{4}\right)^{1/2} d\bar{\rho}.$$

The leading-order amplitude equation is

$$2\phi' A_0' + \phi'' A_0 = 0$$

so that

$$A_0 = \frac{a_0}{(-\phi')^{1/2}} = \frac{2^{1/2} a_0}{(4 - \rho^2)^{1/4}}.$$

The constant a_0 is determined by matching with the near field solution in the vicinity of X_i . As $\rho \rightarrow 0$

$$e^{\phi(\rho)/G} A_0 \sim a_0 e^{-\rho/G}. \quad (33)$$

Since the right-most soliton is not positioned at the origin, the matching condition is slightly different to that in [14]. Writing (20) (or indeed (24)) in terms of ρ and expanding for small G gives

$$V_0 \sim 12^{1/4} e^{-\rho/G + X_n}.$$

Matching with (33) gives

$$a_0 = 12^{1/4} e^{X_n}.$$

Beyond the turning point, as $\rho \rightarrow \infty$ only the solution in which

$$\phi' = i \left(\frac{\rho^2}{4} - 1 \right)^{1/2}$$

has a finite Hamiltonian. Thus for $\rho > 2$, the WKB solution is

$$V_s = \alpha e^{i\phi_2(\rho)/G} \sum_{n=0}^{\infty} A_n(\rho) (iG)^n,$$

for some constant α , where

$$\phi_2 = \int_2^\rho \left(\frac{\bar{\rho}^2}{4} - 1 \right)^{1/2} d\bar{\rho}, \quad A_0(\rho) = \frac{2^{1/2} a_0}{(\rho^2 - 4)^{1/4}}.$$

The turning point causes an exponentially small reflection back into the near field. The solution in the turning point region is exactly the same as in [14], with the result that $\alpha = e^{i\pi/4}$ and the WKB solution in $\rho < 2$ is modified to

$$V_s = e^{\phi(\rho)/G} \sum_{n=0}^{\infty} A_n(\rho) G^n + \gamma e^{-\phi(\rho)/G} \sum_{n=0}^{\infty} A_n(\rho) (-G)^n \quad \rho < 2,$$

where, for an infinite domain,

$$\gamma = \frac{i}{2} e^{2\phi(2)/G} = \frac{i}{2} e^{-\pi/G}.$$

E. Matching back into the near field

We have found that the exponentially small correction to the far field in $0 < \rho < 2$ is

$$V_{\text{exp}} = \gamma e^{-\phi(\rho)/G} \sum_{n=0}^{\infty} A_n(\rho) (-G)^n$$

As $\rho \rightarrow 0$

$$V_{\text{exp}} \sim a_0 \gamma e^{\rho/G}. \quad (34)$$

Writing $V_s = V_G + V_{\text{exp}}$ where V_G is the original (multi-hump) algebraic expansion, and neglecting quadratic terms in V_{exp} but keeping now the term involving $\sigma - 2$ gives, noting that V_G is real, we obtain

$$\frac{d^2 V_{\text{exp}}}{d\xi^2} + V_G^4(2V_{\text{exp}}^* + 3V_{\text{exp}}) - V_{\text{exp}} + \frac{G^2 \xi^2}{4} V_{\text{exp}} = -2(\sigma - 2)V_G^5 \log V_G + \frac{i(\sigma - 2)G}{2\sigma} V_G.$$

We separate into real and imaginary parts. Writing $V_{\text{exp}} = U_{\text{exp}} + iW_{\text{exp}}$ gives

$$\frac{d^2 U_{\text{exp}}}{d\xi^2} + 5V_G^4 U_{\text{exp}} - U_{\text{exp}} + \frac{G^2 \xi^2}{4} U_{\text{exp}} = -2(\sigma - 2)V_G^5 \log V_G, \quad (35)$$

$$\frac{d^2 W_{\text{exp}}}{d\xi^2} + V_G^4 W_{\text{exp}} - W_{\text{exp}} + \frac{G^2 \xi^2}{4} W_{\text{exp}} = \frac{(\sigma - 2)G}{2\sigma} V_G. \quad (36)$$

Note that V_G satisfies the homogeneous version of (36). The resulting solvability condition will determine σ . Unlike §IV A–§IV C, it is easiest now to consider this equation throughout the whole near-field region, rather than considering each hump separately. Multiplying (36) by V_G and integrating from $-R$ to R , while also using the equation satisfied by V_G , gives

$$\begin{aligned} & \int_{-R}^R \left(V_G \frac{d^2 W_{\text{exp}}}{d\xi^2} + V_G^5 W_{\text{exp}} - V_G W_{\text{exp}} + \frac{G^2 \xi^2}{4} V_G W_{\text{exp}} \right) d\xi \\ &= \left[V_G \frac{dW_{\text{exp}}}{d\xi} - W_{\text{exp}} \frac{dV_G}{d\xi} \right]_{-R}^R + \int_{-R}^R \left(W_{\text{exp}} \frac{d^2 V_G}{d\xi^2} + V_G^5 W_{\text{exp}} - V_G W_{\text{exp}} + \frac{G^2 \xi^2}{4} V_G W_{\text{exp}} \right) d\xi \\ &= \left[V_G \frac{dW_{\text{exp}}}{d\xi} - W_{\text{exp}} \frac{dV_G}{d\xi} \right]_{-R}^R = \frac{(\sigma - 2)G}{2\sigma} \int_{-R}^R V_G^2 dx \end{aligned} \quad (37)$$

As $R \rightarrow \infty$ we evaluate the boundary terms by matching using (34). We find

$$V_G(R) \frac{dW_{\text{exp}}}{dx}(R) - W_{\text{exp}}(R) \frac{dV_G}{dx}(R) = 2\sqrt{3} e^{2X_n} e^{-\pi/G} \quad \text{as } R \rightarrow \infty.$$

A similar calculation in $\xi < X_1$ shows that

$$V_G(-R) \frac{dW_{\text{exp}}}{dx}(-R) - W_{\text{exp}}(-R) \frac{dV_G}{dx}(-R) = -2\sqrt{3} e^{-2X_1} e^{-\pi/G} \quad \text{as } R \rightarrow \infty.$$

The dominant contribution to the RHS of (37) comes from each of the humps, since V_G is $O(G^2)$ in between the humps. Since

$$\int_{-\infty}^{\infty} V_0(x)^2 dx = \frac{\sqrt{3}\pi}{2},$$

we find, finally

$$\sigma - 2 = \frac{8\sigma}{n\pi} (e^{2X_n} + e^{-2X_1}) \frac{e^{-\pi/G}}{G}. \quad (38)$$

Note that with $n = 1$ and $X_1 = X_n = 0$ this reduces to the formula in [14], and also that we anticipate the solutions of (38) to satisfy $X_1 = -X_n$ so that

$$\sigma - 2 = \frac{16\sigma}{n\pi} \frac{e^{2X_n - \pi/G}}{G}. \quad (39)$$

V. DETAILED ASYMPTOTIC ANALYSIS OF THE MULTI-HUMP EIGENVALUES

Since V_s is real to all orders, and σ is exponentially close to 2, we may write the linearization problem of Eqs. (13)-(14) as

$$i\lambda f + \frac{d^2 f}{d\xi^2} + 2V_s^4 g + 3V_s^4 f - f + \frac{G^2 \xi^2}{4} f = \text{T.S.T.}, \quad (40)$$

$$-i\lambda g + \frac{d^2 g}{d\xi^2} + 2V_s^4 f + 3V_s^4 g - g + \frac{G^2 \xi^2}{4} g = \text{T.S.T.}. \quad (41)$$

We aim to find asymptotic approximations to the real eigenvalues found numerically in §III. Since V_s is real to all orders, when λ is real we may write $g = f^* + \text{T.S.T.}$, so that

$$i\lambda f + \frac{d^2 f}{d\xi^2} + 2V_s^4 f^* + 3V_s^4 f - f + \frac{G^2 \xi^2}{4} f = \text{T.S.T.} \quad (42)$$

Anticipating that λ is small when G is small, the leading-order eigenfunctions satisfy

$$\frac{d^2 f_0}{d\xi^2} + 2V_0^4 f_0^* + 3V_0^4 f_0 - f_0 = 0. \quad (43)$$

There are two solutions to this equation, namely

$$f_0 = \frac{dV_0}{d\xi}, \quad f_0 = iV_0.$$

For a multi-hump steady state we may take a different multiple of $dV_0/d\xi$ or iV_0 at each hump. We begin in §V A by analysing the eigenfunctions which are proportional to iV_0 near each hump, which give the dominant eigenvalues. We then, in §V B, analyse those eigenfunctions which are proportional to $dV_0/d\xi$, which are much more difficult to find.

Throughout the analysis we will encounter inhomogeneous versions of (43) in the form

$$\frac{d^2 f}{dx^2} + 2V_0^4 f^* + 3V_0^4 f - f = \rho. \quad (44)$$

Since the imaginary part of the homogeneous equation has the nontrivial solution V_0 , and the real part of the homogeneous equation has the nontrivial solution dV_0/dx , there are two solvability conditions on (44), namely,

$$\text{Im} \left[\frac{df}{dx} V_0 - f \frac{dV_0}{dx} \right]_{-R}^R = \int_{-R}^R \text{Im}(\rho) V_0 dx, \quad (45)$$

$$\text{Re} \left[\frac{df}{dx} \frac{dV_0}{dx} - f \frac{d^2 V_0}{dx^2} \right]_{-R}^R = \int_{-R}^R \text{Re}(\rho) \frac{dV_0}{dx} dx, \quad (46)$$

for all R . We will of course be interested in the limit $R \rightarrow \infty$.

A. Perturbation of $f = iV_0$: eigenvalues of $O(G^{1/2})$.

Guided by our numerical results let us anticipate that $\lambda = O(G^{1/2})$ and write $\lambda = G^{1/2} \lambda_1$. We will perturb in powers of $G^{1/2}$. The expansion has a similar structure to that of §IV—there are inner regions in the vicinity of each hump, and outer regions between humps, which much be matched together to give λ .

1. Inner expansion near the i th hump

With $\xi = X_i + x$, we expand

$$f = b_i \sum_{k=0}^{\infty} G^{k/2} f_k,$$

with $f_0 = iV_0$. At $O(G^{1/2})$ we have

$$\frac{d^2 f_1}{dx^2} + V_0^4(2f_1^* + 3f_1) - f_1 = \lambda_1 V_0.$$

The solvability conditions (45), (46) are automatically satisfied, so that λ_1 is undetermined, and

$$f_1 = \lambda_1 \left(\frac{V_0}{4} + \frac{x}{2} \frac{dV_0}{dx} \right).$$

At $O(G)$ we find [31]

$$\frac{d^2 f_2}{dx^2} + V_0^4(2f_2^* + 3f_2) - f_2 = -i\lambda_1^2 \left(\frac{V_0}{4} + \frac{x}{2} \frac{dV_0}{dx} \right).$$

Again the solvability conditions (45), (46) are automatically satisfied, so that λ_1 is still undetermined, and the solution is

$$f_2 = -\frac{i\lambda_1^2}{8} x^2 V_0.$$

At $O(G^{3/2})$ we find

$$\frac{d^2 f_3}{dx^2} + V_0^4(2f_3^* + 3f_3) - f_3 = -\frac{\lambda_1^3 x^2}{8} V_0.$$

As before, the solvability conditions are automatically satisfied, and the solution is

$$f_3 = \frac{\lambda_1^3}{2} \hat{V}_1, \quad g_3 = \frac{\lambda_1^3}{2} \hat{V}_1,$$

where \hat{V}_1 satisfies

$$\frac{d^2 \hat{V}_1}{dx^2} + 5V_0^4 \hat{V}_1 - \hat{V}_1 = -\frac{x^2 V_0}{4}, \quad \hat{V}_1 \rightarrow 0 \text{ as } x \rightarrow \pm\infty,$$

that is, \hat{V}_1 is the next term in the expansion of the standard single hump solution [14] (i.e. not accounting for the shift in origin). At $O(G^2)$ we find

$$\frac{d^2 f_4}{dx^2} + V_0^4(2f_4^* + 3f_4) - f_4 = -\frac{i\lambda_1^4}{2} \hat{V}_1 - \frac{i(x + X_i)^2}{4} V_0 - 4iV_1 V_0^4. \quad (47)$$

Here at last the solvability condition (45) is not automatically satisfied, and will determine λ_1 . Note that V_1 grows exponentially as $x \rightarrow \pm\infty$ (in contrast to \hat{V}_1)—see (29), (30)—so that we must be careful in evaluating the solvability condition. Multiplying (27) by V_0 and integrating gives

$$\begin{aligned} -\int_{-R}^R \frac{(x + X_i)^2}{4} V_0^2 dx &= \int_{-R}^R \left(\frac{d^2 V_1}{dx^2} + 5V_0^4 V_1 - V_1 \right) V_0 dx \\ &= \int_{-R}^R \left(\frac{d^2 V_0}{dx^2} + 5V_0^5 - V_0 \right) V_1 dx + \left[\frac{dV_1}{dx} V_0 - V_1 \frac{dV_0}{dx} \right]_{-R}^R \\ &= \int_{-R}^R 4V_0^5 V_1 dx + \left[\frac{dV_1}{dx} V_0 - V_1 \frac{dV_0}{dx} \right]_{-R}^R. \end{aligned}$$

Thus the solvability conditions on (47) may be written as

$$\text{Im} \left[\frac{df_4}{dx} V_0 - f_4 \frac{dV_0}{dx} \right]_{-R}^R = -\frac{\lambda_1^4}{2} \int_{-R}^R \hat{V}_1 V_0 dx + \left[\frac{dV_1}{dx} V_0 - V_1 \frac{dV_0}{dx} \right]_{-R}^R \quad (48)$$

$$\text{Re} \left[\frac{df_4}{dx} \frac{dV_0}{dx} - f_4 \frac{d^2 V_0}{dx^2} \right]_{-R}^R = 0. \quad (49)$$

The boundary terms on the RHS can be evaluated using (29), (30). To evaluate the boundary terms on the LHS we need to consider f in the region between humps.

2. In between the humps

Consider the gap between X_i and X_{i+1} . In this region $V_s = O(G^2 \log G)$ so that we can neglect the nonlinear term. Thus

$$iG^{1/2} \lambda_1 f + \frac{d^2 f}{d\xi^2} - f + \frac{G^2 \xi^2}{4} f = O(f G^8 \log^4 G), \quad (50)$$

Expanding

$$f = \sum_{k=0}^{\infty} G^{k/2} f_k,$$

gives

$$\frac{d^2 f_0}{d\xi^2} - f_0 = 0, \quad (51)$$

at leading order. Matching requires

$$f_0 \sim 12^{1/4} i b_{i+1} e^{\xi - X_{i+1}} \quad \text{as } \xi \rightarrow X_{i+1}, \quad f_0 \sim 12^{1/4} i b_i e^{-\xi + X_i} \quad \text{as } \xi \rightarrow X_i.$$

Thus

$$f_0 = 12^{1/4} i b_{i+1} e^{\xi - X_{i+1}} + 12^{1/4} i b_i e^{-\xi + X_i}.$$

In terms of $\xi = X_{i+1} + x$ this is

$$f_0 = 12^{1/4} i b_{i+1} e^x + 12^{1/4} i b_i e^{-x + X_i - X_{i+1}}.$$

Since $e^{X_i - X_{i+1}} = O(G^2)$ the additional term must match with $G^2 f_4$ from the $(i+1)$ th hump solution, giving

$$b_{i+1} f_4 G^2 \sim 12^{1/4} i b_i e^{-x + X_i - X_{i+1}} \quad (52)$$

as $x \rightarrow -\infty$. Similarly, in terms of $\xi = X_i + x$,

$$f_0 = 12^{1/4} i b_{i+1} e^{x + X_i - X_{i+1}} + 12^{1/4} i b_i e^{-x},$$

giving the matching condition on the i th hump solution

$$b_i f_4 G^2 \sim 12^{1/4} i b_{i+1} e^{x + X_i - X_{i+1}}, \quad (53)$$

as $x \rightarrow \infty$. Under our convention that $X_0 = -\infty$, $X_{n+1} = \infty$ equations (52), (53) can be extended to include $i = 0$ and $i = n$, respectively.

3. Solvability condition

We now have enough information to evaluate the solvability conditions (48), (49). Using (52), (53), (29) and (30) gives

$$\lim_{R \rightarrow \infty} \operatorname{Re} \left[\frac{df_4}{dx} \frac{dV_0}{dx} - f_4 \frac{d^2 V_0}{dx^2} \right]_{-R}^R = 0, \quad (54)$$

$$\lim_{R \rightarrow \infty} \operatorname{Im} \left[b_i \frac{df_4}{dx} V_0 - b_i f_4 \frac{dV_0}{dx} \right]_{-R}^R = 4\sqrt{3} i b_{i+1} \frac{e^{X_i - X_{i+1}}}{G^2} + 4\sqrt{3} i b_{i-1} \frac{e^{X_{i-1} - X_i}}{G^2}, \quad (55)$$

$$\lim_{R \rightarrow \infty} \left[\frac{dV_1}{dx} V_0 - V_1 \frac{dV_0}{dx} \right]_{-R}^R = 4\sqrt{3} \frac{e^{X_i - X_{i+1}}}{G^2} + 4\sqrt{3} \frac{e^{X_{i-1} - X_i}}{G^2}. \quad (56)$$

Thus, letting $R \rightarrow \infty$, (49) is satisfied, and, since

$$\int_{-\infty}^{\infty} \hat{V}_1 V_0 dx = \frac{\sqrt{3} \pi^3}{256},$$

the remaining condition (48) is

$$\frac{b_i \lambda_1^4 \pi^3}{2048} = (b_i - b_{i+1}) \frac{e^{X_i - X_{i+1}}}{G^2} + (b_i - b_{i-1}) \frac{e^{X_{i-1} - X_i}}{G^2}, \quad i = 1, \dots, n. \quad (57)$$

Equation (57) is a set of n homogeneous linear equations for the n coefficients b_i , $i = 1, \dots, n$. For a nontrivial solution the determinant must vanish, and it is this condition that determines the eigenvalue λ_1 . Note that $b_i = b$ for all i , $\lambda_1 = 0$ is a solution of (57) for any n . This corresponds to global phase invariance, with corresponding eigenvalue $\lambda = 2G$ (we would need to include λ_2 and proceed to higher orders to see that through this expansion, but fortunately we have an exact eigenfunction for $\lambda = 2G$ in (15)). Thus we expect that there are $n - 1$ remaining eigenvalues which are $O(G^{1/2})$. Note also that the eigenvalues appear in pairs—for each positive eigenvalue there is a corresponding negative eigenvalue with the same (leading order) weights b_i .

4. Examples

a. Two humps: With $-X_1 = X_2 = X$, (57) is

$$\lambda_1^4 = \frac{2048}{\pi^3 G^2} \left(1 - \frac{b_2}{b_1} \right) e^{-2X} = \frac{2048}{\pi^3 G^2} \left(1 - \frac{b_1}{b_2} \right) e^{-2X},$$

Thus $b_2^2 = b_1^2$ so that $b_2 = \pm b_1$. The additional solution $b_2 = -b_1$ has positive eigenvalue

$$\lambda = \frac{8e^{-X/2}}{\pi^{3/4}} = \frac{2^{7/4} X^{1/4}}{\pi^{1/2}} G^{1/2}.$$

b. Three humps: With $X_2 = 0$, $-X_1 = X_3 = X$, (57) is

$$\frac{\pi^3 G^2 \lambda_1^4}{2048} = \left(1 - \frac{b_2}{b_1} \right) e^{-X} = \left(1 - \frac{b_3}{b_1} \right) e^{-X} + \left(1 - \frac{b_1}{b_2} \right) e^{-X} = \left(1 - \frac{b_2}{b_3} \right) e^{-X},$$

with solution $(b_1, b_2, b_3) = (1, 1, 1)$ as expected along with the additional solutions

$$(b_1, b_2, b_3) = (1, -2, 1), \quad (1, 0, -1),$$

which have corresponding positive eigenvalues

$$\lambda = \frac{2^{3/2} 3^{1/4} X^{1/4}}{\pi^{1/2}} G^{1/2}, \quad \lambda = \frac{2^{3/2} X^{1/4}}{\pi^{1/2}} G^{1/2}.$$

c. Four humps: With $-X_1 = X_4 = Y_2$, $-X_2 = X_3 = Y_1$, in addition to $\mathbf{b} = (b_1, b_2, b_3, b_4) = (1, 1, 1, 1)$ the solutions of (57) are

$$\begin{aligned}\mathbf{b} &= (-1, 1, 1, -1), \\ \mathbf{b} &= \left(1 + r - (r^2 + 2r + 2)^{1/2}, 1, -1, -1 - r + (r^2 + 2r + 2)^{1/2}\right), \\ \mathbf{b} &= \left(1 + r + (r^2 + 2r + 2)^{1/2}, 1, -1, -1 - r - (r^2 + 2r + 2)^{1/2}\right),\end{aligned}$$

where $r = Y_1/Y_2$, with corresponding positive eigenvalues

$$\begin{aligned}\lambda &= \frac{2^{7/4} Y_2^{1/4}}{\pi^{1/2}} G^{1/2}, \\ \lambda &= \frac{2^{3/2}}{\pi^{1/2}} \left(2Y_2 + Y_1 + (Y_1^2 + 2Y_1Y_2 + 2Y_2^2)^{1/2}\right)^{1/4} G^{1/2}, \\ \lambda &= \frac{2^{3/2}}{\pi^{1/2}} \left(2Y_2 + Y_1 - (Y_1^2 + 2Y_1Y_2 + 2Y_2^2)^{1/2}\right)^{1/4} G^{1/2}.\end{aligned}$$

B. Perturbation of $f = V_0'$: eigenvalues of $O(G)$.

Let us anticipate that $\lambda = O(G)$ and write $\lambda = G\lambda_1$. We will see that these eigenvalues are much more difficult to approximate, and that there is some subtlety in the calculation which is not immediately apparent. In order to motivate the rather detailed calculation which follows later, we first present a plausible analysis along the same lines as §V A, which will turn out to be incorrect.

1. Inner expansion near the i th hump

With $\xi = X_i + x$, we try an expansion near the i th hump of the form

$$f = a_i \sum_{k=0}^{\infty} G^k f_k,$$

with $f_0 = dV_0/dx$. At $O(G)$ we have

$$\frac{d^2 f_1}{dx^2} + V_0^4 (2f_1^* + 3f_1) - f_1 = -i\lambda_1 \frac{dV_0}{dx}.$$

The solvability conditions are automatically satisfied, λ_1 is undetermined, and

$$f_1 = -\frac{\lambda_1 i x}{2} V_0.$$

At $O(G^2)$

$$\frac{d^2 f_2}{dx^2} + V_0^4 (2f_2^* + 3f_2) - f_2 = -\frac{\lambda_1^2 x}{2} V_0 - \frac{(x + X_i)^2}{4} \frac{dV_0}{dx} - 20V_1 V_0^3 \frac{dV_0}{dx}. \quad (58)$$

The solvability condition (46) is not automatic, and will determine λ_1 . We can simplify the right-hand side of (46) using (27). Differentiating (27) gives

$$\frac{d^3 V_1}{dx^3} + 5V_0^4 \frac{dV_1}{dx} + 20V_0^3 V_1 \frac{dV_0}{dx} - \frac{dV_1}{dx} = -\frac{(x + X_i)}{2} V_0 - \frac{(x + X_i)^2}{4} \frac{dV_0}{dx}.$$

Thus

$$\begin{aligned}
\int_{-R}^R \left(\frac{(x+X_i)^2}{4} \frac{dV_0}{dx} + 20V_1V_0^3 \frac{dV_0}{dx} \right) \frac{dV_0}{dx} dx &= \int_{-R}^R \left(-\frac{(x+X_i)}{2} V_0 - \frac{d^3V_1}{dx^3} - 5V_0^4 \frac{dV_1}{dx} + \frac{dV_1}{dx} \right) \frac{dV_0}{dx} dx \\
&= \int_{-R}^R -\frac{(x+X_i)}{2} V_0 \frac{dV_0}{dx} - \left(\frac{d^3V_0}{dx^3} + 5V_0^4 \frac{dV_0}{dx} - \frac{dV_0}{dx} \right) \frac{dV_1}{dx} dx - \left[\frac{d^2V_1}{dx^2} \frac{dV_0}{dx} - \frac{dV_1}{dx} \frac{d^2V_0}{dx^2} \right]_{-R}^R \\
&= \int_{-R}^R \frac{1}{4} V_0^2 dx - \left[\frac{d^2V_1}{dx^2} \frac{dV_0}{dx} - \frac{dV_1}{dx} \frac{d^2V_0}{dx^2} \right]_{-R}^R
\end{aligned}$$

Thus the solvability conditions on (58) may be written

$$\text{Im} \left[\frac{df_2}{dx} V_0 - f_2 \frac{dV_0}{dx} \right]_{-R}^R = 0, \quad (59)$$

$$\text{Re} \left[\frac{df_2}{dx} \frac{dV_0}{dx} - f_2 \frac{d^2V_0}{dx^2} \right]_{-R}^R = \frac{(\lambda_1^2 - 1)}{4} \int_{-R}^R V_0^2 dx + \left[\frac{d^2V_1}{dx^2} \frac{dV_0}{dx} - \frac{dV_1}{dx} \frac{d^2V_0}{dx^2} \right]_{-R}^R. \quad (60)$$

To evaluate the left-hand we need to consider the region between the humps.

2. In between the humps

As usual consider the gap between X_i and X_{i+1} . In this region

$$iG\lambda_1 f + \frac{d^2 f}{d\xi^2} - f + \frac{G^2 \xi^2}{4} f = O(fG^8 \log^4 G), \quad (61)$$

Expanding

$$f = \sum_{k=0}^{\infty} G^k f_k,$$

gives

$$\frac{d^2 f_0}{d\xi^2} - f_0 = 0, \quad (62)$$

at leading order. Matching requires

$$f \sim 12^{1/4} a_{i+1} e^{\xi - X_{i+1}} \quad \text{as } \xi \rightarrow X_{i+1}, \quad f \sim -12^{1/4} a_i e^{-\xi + X_i} \quad \text{as } \xi \rightarrow X_i.$$

Thus

$$f_0 = 12^{1/4} a_{i+1} e^{\xi - X_{i+1}} - 12^{1/4} a_i e^{-\xi + X_i}.$$

In terms of $\xi = X_{i+1} + x$ this is

$$f_0 = 12^{1/4} a_{i+1} e^x - 12^{1/4} a_i e^{-x + X_i - X_{i+1}}.$$

Since $e^{X_i - X_{i+1}} = O(G^2)$ the additional term matches with $G^2 f_2$ from the $(i+1)$ th hump, giving the matching condition

$$a_{i+1} f_2 G^2 \sim -12^{1/4} a_i e^{-x + X_i - X_{i+1}},$$

as $x \rightarrow -\infty$ for the near-hump solution. In terms of $\xi = X_i + x$ the between-hump solution is

$$f_0 = 12^{1/4} a_{i+1} e^{x+X_i-X_{i+1}} - 12^{1/4} a_i e^{-x},$$

giving the matching condition

$$a_i f_2 G^2 \sim 12^{1/4} a_{i+1} e^{x+X_i-X_{i+1}},$$

as $x \rightarrow \infty$ for the near-hump solution. Thus

$$\lim_{R \rightarrow \infty} \operatorname{Im} \left[\frac{df_2}{dx} V_0 - f_2 \frac{dV_0}{dx} \right]_{-R}^R = 0, \quad (63)$$

$$\lim_{R \rightarrow \infty} \operatorname{Re} \left[a_i \frac{df_2}{dx} \frac{dV_0}{dx} - a_i f_2 \frac{d^2 V_0}{dx^2} \right]_{-R}^R = -4\sqrt{3} a_{i+1} \frac{e^{-X_{i+1}+X_i}}{G^2} - 4\sqrt{3} a_{i-1} \frac{e^{-X_i+X_{i-1}}}{G^2}, \quad (64)$$

$$\lim_{R \rightarrow \infty} \left[\frac{d^2 V_1}{dx^2} \frac{dV_0}{dx} - \frac{dV_1}{dx} \frac{d^2 V_0}{dx^2} \right]_{-R}^R = -4\sqrt{3} \frac{e^{-X_{i+1}+X_i}}{G^2} - 4\sqrt{3} \frac{e^{-X_i+X_{i-1}}}{G^2}. \quad (65)$$

3. Solvability condition

Letting $R \rightarrow \infty$, the solvability condition (59) is satisfied, and, noting that

$$\int_{-\infty}^{\infty} V_0^2 dx = \frac{\sqrt{3}\pi}{2},$$

(60) becomes

$$(\lambda_1^2 - 1) \frac{\pi}{32} a_i = (a_i - a_{i+1}) \frac{e^{X_i-X_{i+1}}}{G^2} + (a_i - a_{i-1}) \frac{e^{X_{i-1}-X_i}}{G^2}, \quad i = 1, \dots, n. \quad (66)$$

Equations (66) are a homogeneous set of linear equations for a_i , $i = 1, \dots, n$. For a non-trivial solution the determinant must vanish, which determines the eigenvalue λ_1 . Note that $\lambda_1 = \pm 1$, $a_i = a$ for all i , is always a solution, corresponding to a global translation. Note also that the eigenvalues again come in pairs—for every positive eigenvalue there is a negative eigenvalue of equal modulus.

4. Examples

a. Two humps With $-X_1 = X_2 = X$ equation (66) gives

$$\lambda_1^2 = 1 + \left(1 - \frac{a_2}{a_1}\right) X = 1 + \left(1 - \frac{a_1}{a_2}\right) X.$$

Thus $a_1 = \pm a_2$, and it appears there are solutions

$$(a_1, a_2) = (1, 1), \quad (a_1, a_2) = (-1, 1),$$

with corresponding positive eigenvalues

$$\lambda = G, \quad \lambda = (1 + 2X)^{1/2} G.$$

b. *Three humps* For the three-bump case with $-X_1 = X_3 = X$, $X_2 = 0$, equation (66) gives

$$\lambda_1^2 = 1 + \left(1 - \frac{a_2}{a_1}\right) X = 1 + \left(1 - \frac{a_3}{a_2}\right) X + \left(1 - \frac{a_1}{a_2}\right) X = 1 + \left(1 - \frac{a_2}{a_3}\right) X.$$

Writing $(a_1, a_2, a_3) = \mathbf{a}$ the solutions are

$$\mathbf{a} = (1, 1, 1), \quad \mathbf{a} = (1, 0, -1) \quad \text{and} \quad \mathbf{a} = (1, -2, 1),$$

with corresponding positive eigenvalues

$$\lambda = G, \quad \lambda = (1 + X)^{1/2} G, \quad \lambda = (1 + 3X)^{1/2} G. \quad (67)$$

c. *Four humps* With $-X_1 = X_4 = Y_2$, $-X_2 = X_3 = Y_1$, equation (66) gives

$$\begin{aligned} \lambda_1^2 &= 1 + \left(1 - \frac{a_2}{a_1}\right) Y_2 = 1 + \left(1 - \frac{a_3}{a_2}\right) (Y_1 + Y_2) + \left(1 - \frac{a_1}{a_2}\right) Y_2 \\ &= 1 + \left(1 - \frac{a_4}{a_3}\right) Y_2 + \left(1 - \frac{a_2}{a_3}\right) (Y_1 + Y_2) = 1 + \left(1 - \frac{a_3}{a_4}\right) Y_2. \end{aligned}$$

With $\mathbf{a} = (a_1, a_2, a_3, a_4)$, there are solutions

$$\begin{aligned} \mathbf{a} &= (1, 1, 1, 1), \\ \mathbf{a} &= (-1, 1, 1, -1), \\ \mathbf{a} &= \left(1 + r - (r^2 + 2r + 2)^{1/2}, 1, -1, -1 - r + (r^2 + 2r + 2)^{1/2}\right), \\ \mathbf{a} &= \left(1 + r + (r^2 + 2r + 2)^{1/2}, 1, -1, -1 - r - (r^2 + 2r + 2)^{1/2}\right), \end{aligned}$$

where $r = Y_1/Y_2$, with corresponding positive eigenvalues

$$\begin{aligned} \lambda &= G, \\ \lambda &= (1 + 2Y_2)^{1/2} G, \\ \lambda &= \left(1 + 2Y_2 + Y_1 + (Y_1^2 + 2Y_1Y_2 + 2Y_2^2)^{1/2}\right)^{1/2} G, \\ \lambda &= \left(1 + 2Y_2 + Y_1 - (Y_1^2 + 2Y_1Y_2 + 2Y_2^2)^{1/2}\right)^{1/2} G. \end{aligned}$$

In Fig. 11 we show a comparison between the predictions of equation (66) and our numerical solutions.

We see that some of the eigenvalues are well approximated, but in each case there is a large eigenvalue that the asymptotic prediction misses, and there is a predicted eigenvalue which is not present numerically. To understand why this is the case we have to return to our assumptions about the form of the eigenfunctions.

C. Why the naive asymptotic solution fails

Having determined that both iV_0 and dV_0/dx satisfy the leading-order problem when λ is small, we should really consider a leading order solution in the near-hump region of the form

$$f_0 = a_i \frac{dV_0}{dx} + b_i iV_0, \quad (68)$$

i.e. we should combine both solutions rather than considering them separately. For the single-hump solution these eigenfunctions can be considered independently, but for the multi-hump solutions they interact with

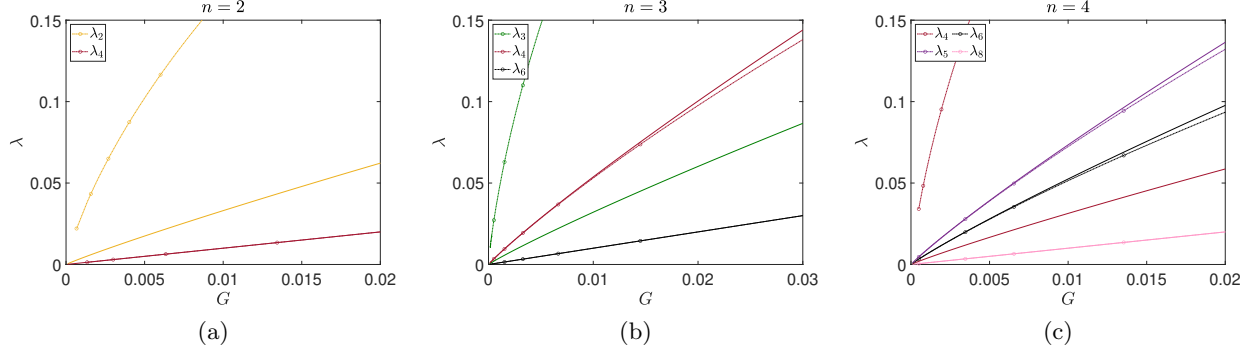


FIG. 11: Comparison of the eigenvalues proportional to G . The solid lines are the asymptotic predictions of (66); the lines with circles correspond to the numerically calculated values.

each other. Let us suppose that $\lambda = \lambda_1 G$ and proceed using (68) as the first term in the expansion near the i th hump. Then we would find that there are solvability conditions at $O(G^2)$, which are of the form

$$\begin{bmatrix} A(\lambda_1) & 0 \\ 0 & B \end{bmatrix} \begin{bmatrix} \mathbf{a} \\ \mathbf{b} \end{bmatrix} = \begin{bmatrix} \mathbf{0} \\ \mathbf{0} \end{bmatrix},$$

where \mathbf{a} and \mathbf{b} are vectors with components a_i and b_i respectively, A is the matrix representing the linear equations (66), and B is the matrix representing the linear equations (57) but with λ_1 set to zero, i.e.

$$(b_i - b_{i+1}) \frac{e^{X_i - X_{i+1}}}{G^2} + (b_i - b_{i-1}) \frac{e^{X_{i-1} - X_i}}{G^2} = 0. \quad (69)$$

In our analysis in §V B we set $\det(A) = 0$ to determine the eigenvalue λ_1 , and assumed that $\mathbf{b} = \mathbf{0}$. However, as we observed when writing down (57), the matrix B is singular, with null vector $(1, 1, \dots, 1)$. Thus there is still a degree of freedom which is undetermined at this order, which will be determined at the next order in the expansions. This means that we can no longer ignore the fact that \mathbf{a} , \mathbf{b} and λ should also be expanded in powers of G .

If we do so, following the scheme above, then we find that the leading-order solvability condition is

$$\begin{bmatrix} A(\lambda_1) & 0 \\ 0 & B \end{bmatrix} \begin{bmatrix} \mathbf{a}^{(0)} \\ \mathbf{b}^{(0)} \end{bmatrix} = \begin{bmatrix} \mathbf{0} \\ \mathbf{0} \end{bmatrix},$$

so that λ_1 is an eigenvalue of A , with $\mathbf{a}^{(0)}$ the corresponding normalised eigenvector, and $\mathbf{b}^{(0)} = b^{(0)}(1, 1, \dots, 1)$ with $b^{(0)}$ still undetermined. Proceeding with the expansion we would find solvability conditions at the next order of the form

$$\begin{bmatrix} A(\lambda_1) & 0 \\ 0 & B \end{bmatrix} \begin{bmatrix} \mathbf{a}^{(1)} \\ \mathbf{b}^{(1)} \end{bmatrix} = \begin{bmatrix} \lambda_2 C_1 \mathbf{a}^{(0)} + C_2 \mathbf{b}^{(0)} \\ C_3 \mathbf{a}^{(0)} \end{bmatrix}, \quad (70)$$

for some matrices C_1, C_2, C_3 . Note in particular that terms involving $\mathbf{b}^{(0)}$ appear on the right-hand side of the equation for $\mathbf{a}^{(1)}$ while terms involving $\mathbf{a}^{(0)}$ appear on the right-hand side of the equation for $\mathbf{b}^{(1)}$. Now both the matrix $A(\lambda_1)$ and the matrix B are singular, so there are solvability conditions on the two right-hand sides. But both the degrees of freedom we have— λ_2 and $b^{(0)}$ —appear on the RHS of the equation for $\mathbf{a}^{(1)}$. The solvability condition for $B\mathbf{b}^{(1)} = C_3\mathbf{a}^{(0)}$ may or may not be satisfied; we have no parameter in the equation to adjust to ensure that it is. This explains why the naive asymptotic approximation in §V B predicted solutions which were not found numerically—if we had continued to the next order in the expansion we would have found a solvability condition that we could not satisfy.

In order to solve the problem of both remaining degrees of freedom appearing in the same block of (70) we need to make \mathbf{b} an order of G larger than \mathbf{a} . Suppose, therefore, that $\mathbf{a}^{(0)} = \mathbf{0}$. Then the leading-order

solvability conditions give

$$B\mathbf{b}^{(0)} = \mathbf{0}, \quad (71)$$

so that $\mathbf{b}^{(0)} = b^{(0)}(1, 1, \dots, 1)$. At next order we will find

$$\begin{bmatrix} A(\lambda_1) & 0 \\ 0 & B \end{bmatrix} \begin{bmatrix} \mathbf{a}^{(1)} \\ \mathbf{b}^{(1)} \end{bmatrix} = \begin{bmatrix} C_2 \mathbf{b}^{(0)} \\ 0 \end{bmatrix}. \quad (72)$$

Since $\mathbf{b}^{(0)}$ is non-zero there is a non-trivial solution $\mathbf{a}^{(1)} = A^{-1}C_2\mathbf{b}^{(0)}$ when A is non-singular. Thus λ_1 is still undetermined, but the relative scaling of $\mathbf{a}^{(1)}$ and $\mathbf{b}^{(0)}$ is determined. Now, at next order, we will find

$$\begin{bmatrix} A(\lambda_1) & 0 \\ 0 & B \end{bmatrix} \begin{bmatrix} \mathbf{a}^{(2)} \\ \mathbf{b}^{(2)} \end{bmatrix} = \begin{bmatrix} \lambda_2 C_1 \mathbf{a}^{(1)} + C_2 \mathbf{b}^{(1)} \\ C_3 \mathbf{a}^{(1)} + C_4 \mathbf{b}^{(0)} \end{bmatrix}. \quad (73)$$

Crucially, since $\mathbf{a}^{(0)}$ is a function of λ_1 , the solvability condition on the second block can be satisfied and determines the eigenvalue λ_1 . Now that we know schematically the structure of the expansions, let us work through some of the details.

D. More careful analysis of the eigenvalues $\lambda = O(G)$.

We suppose that

$$\lambda = \sum_{k=1}^{\infty} \lambda_k G^k. \quad (74)$$

Near the i th hump, with $\xi = X_i + x$, we set

$$f = a_i U + b_i W \quad (75)$$

where

$$f = \sum_{k=0}^{\infty} G^k f_k, \quad U = \sum_{k=0}^{\infty} G^k U_k, \quad W = \sum_{k=0}^{\infty} G^k W_k, \quad (76)$$

with

$$U_0 = \frac{dV_0}{dx}, \quad W_0 = iV_0. \quad (77)$$

We also expand a_i and b_i in powers of G , anticipating the interleaving expansions,

$$a_i = G a_i^{(1)} + G^3 a_i^{(3)} + \dots, \quad b_i = b_i^{(0)} + G^2 b_i^{(2)} + \dots. \quad (78)$$

Since the analysis gets now very technical, and we need to match many orders of inner and outer expansions, we defer many of the details to an appendix, and here simply pick out some of the key equations. At $O(G^2)$ in the inner expansion near the i th hump we find the solvability condition (D8),

$$b_i^{(0)} \left(\frac{4\sqrt{3}}{G^2} e^{-X_{i+1}+X_i} + \frac{4\sqrt{3}}{G^2} e^{-X_i+X_{i-1}} \right) = \frac{4\sqrt{3} b_{i+1}^{(0)}}{G^2} e^{X_i-X_{i+1}} + \frac{4\sqrt{3} b_{i-1}^{(0)}}{G^2} e^{X_{i-1}-X_i}. \quad (79)$$

As anticipated, this is (57) with λ_1 set to zero, and is equation (71), $B\mathbf{b}^{(0)} = \mathbf{0}$, from §V C. Equation (79) fixes $b_i^{(0)} = b^{(0)}$ for all i .

At $O(G^3)$ in the inner expansion near the i th hump we find the solvability condition (D22),

$$\begin{aligned} \frac{\pi a_i^{(1)}(\lambda_1^2 - 1)}{32} + (a_{i+1}^{(1)} - a_i^{(1)}) \frac{e^{X_i - X_{i+1}}}{G^2} + (a_{i-1}^{(1)} - a_i^{(1)}) \frac{e^{-X_i + X_{i-1}}}{G^2} \\ = \frac{3\pi}{64} \lambda_1 b^{(0)} X_i - \frac{\lambda_1 b^{(0)}}{2} (X_i - X_{i+1}) \frac{e^{X_i - X_{i+1}}}{G^2} - \frac{\lambda_1 b^{(0)}}{2} (X_i - X_{i-1}) \frac{e^{-X_i + X_{i-1}}}{G^2}. \end{aligned} \quad (80)$$

Equation (80) is equation (72), $A(\lambda_1)\mathbf{a}^{(1)} = C_2\mathbf{b}^{(0)}$, from §V C. When $b^{(0)}$ is non-zero it gives $a_i^{(1)}$ in terms of $b^{(0)}$, with no restriction on λ_1 . To determine λ_1 we need to go to one more order. Note that there is still the possibility that $b^{(0)} = 0$, in which case λ_1 is determined by $\det A = 0$ and $\mathbf{a}^{(1)}$ is a null vector of A .

At $O(G^4)$ in the inner expansion near the i th hump we find the solvability condition (D29),

$$\begin{aligned} \frac{b^{(0)}\lambda_1^2(\lambda_1^2 - 4)\pi^3}{512} + \frac{3\pi\lambda_1 X_i}{64} (b^{(0)}\lambda_1 X_i - 2a_i^{(1)}) + 4(b_{i+1}^{(2)} - b_i^{(2)}) \frac{e^{X_i - X_{i+1}}}{G^2} \\ + 4(b_{i-1}^{(2)} - b_i^{(2)}) \frac{e^{X_{i-1} - X_i}}{G^2} + 2a_{i+1}^{(1)}(X_{i+1} - X_i)\lambda_1 \frac{e^{X_i - X_{i+1}}}{G^2} + 2a_{i-1}^{(1)}(X_{i-1} - X_i)\lambda_1 \frac{e^{X_{i-1} - X_i}}{G^2} \\ - 3a_{i+1}^{(1)}\lambda_1 \frac{e^{X_i - X_{i+1}}}{G^2} + 3a_{i-1}^{(1)}\lambda_1 \frac{e^{X_{i-1} - X_i}}{G^2} + \frac{\lambda_1^2}{2} b^{(0)} \frac{e^{X_i - X_{i+1}}}{G^2} (-X_i^2 + 3X_{i+1} + 2X_i X_{i+1} - X_{i+1}^2) \\ + \frac{\lambda_1^2}{2} b^{(0)} \frac{e^{X_{i-1} - X_i}}{G^2} (-X_i^2 - 3X_{i-1} + 2X_i X_{i-1} - X_{i-1}^2) = 0. \end{aligned} \quad (81)$$

This is equation (73), $B\mathbf{b}^{(2)} = C_3\mathbf{a}^{(1)} + C_4\mathbf{b}^{(0)}$, from §V C. Since B has the null vector $(1, 1, \dots, 1)$ these equations for $b_i^{(2)}$ have a solvability condition: if we sum over i then $b_i^{(2)}$ vanishes. This sum over i is the equation which determines λ_1 .

Let us first identify which of the eigenvalues of §V B survive the new solvability condition (81).

1. Eigenvalues which follow the old scheme of §V B

We found some numerically determined eigenvalues did match the predictions of §V B. If $b^{(0)} = 0$ then the eigenvalue is determined by requiring a non-trivial solution of (80),

$$\frac{\pi a_i^{(1)}(\lambda_1^2 - 1)}{32} + (a_{i+1}^{(1)} - a_i^{(1)}) \frac{e^{X_i - X_{i+1}}}{G^2} + (a_{i-1}^{(1)} - a_i^{(1)}) \frac{e^{-X_i + X_{i-1}}}{G^2} = 0, \quad (82)$$

as in §V B, but the extra solvability condition given by (81) must also be satisfied, which is

$$\begin{aligned} \sum_{i=1}^n -\frac{3\pi\lambda_1 X_i}{32} a_i^{(1)} + 2a_{i+1}^{(1)}(X_{i+1} - X_i)\lambda_1 \frac{e^{X_i - X_{i+1}}}{G^2} \\ + 2a_{i-1}^{(1)}(X_{i-1} - X_i)\lambda_1 \frac{e^{X_{i-1} - X_i}}{G^2} - 3a_{i+1}^{(1)}\lambda_1 \frac{e^{X_i - X_{i+1}}}{G^2} + 3a_{i-1}^{(1)}\lambda_1 \frac{e^{X_{i-1} - X_i}}{G^2} = 0. \end{aligned} \quad (83)$$

In general we would not expect this to be satisfied, but certain symmetries of the $a_i^{(1)}$ may mean it is satisfied automatically. In particular, with some index relabelling, (83) is

$$\begin{aligned} \sum_{i=1}^n -\frac{3\pi X_i}{32} a_i^{(1)} + 2(a_i^{(1)} - a_{i-1}^{(1)}) X_i \frac{e^{X_{i-1} - X_i}}{G^2} \\ + 2(a_i^{(1)} - a_{i+1}^{(1)}) X_i \frac{e^{X_i - X_{i+1}}}{G^2} - 3a_i^{(1)} \frac{e^{X_{i-1} - X_i}}{G^2} + 3a_i^{(1)} \frac{e^{X_i - X_{i+1}}}{G^2} = 0. \end{aligned}$$

Simplifying using (82) and (31) gives

$$\sum_{i=1}^n -3X_i a_i^{(1)} + (\lambda_1^2 - 1)a_i^{(1)} = 0. \quad (84)$$

Since, by symmetry, $\sum_{i=1}^n X_i = 0$ we find the eigenvalue $\lambda_1 = \pm 1$ with eigenvector $a_i^{(1)} = 1$ for $i = 1, \dots, n$ always works as it should.

a. Two humps With $-X_1 = X_2 = X$ we found

$$\mathbf{a} = (-1, 1), \quad \mathbf{a} = (1, 1),$$

with corresponding positive eigenvalues

$$\lambda = (1 + 2X)^{1/2}G, \quad \lambda = G.$$

The second satisfies (84) but the first does not, in agreement with Fig. 11(a).

b. Three humps For the three-bump case with $-X_1 = X_3 = X$, $X_2 = 0$, we found

$$\mathbf{a} = (1, -2, 1), \quad \mathbf{a} = (1, 0, -1) \quad \text{and} \quad \mathbf{a} = (1, 1, 1),$$

with corresponding positive eigenvalues

$$\lambda = (1 + 3X)^{1/2}G, \quad \lambda = (1 + X)^{1/2}G, \quad \lambda = G. \quad (85)$$

The first and third satisfy (84), but the second does not, in agreement with Fig. 11(b).

c. Four humps With $-X_1 = X_4 = Y_2$, $-X_2 = X_3 = Y_1$, we found

$$\begin{aligned} \mathbf{a} &= \left(1 + r - (r^2 + 2r + 2)^{1/2}, 1, -1, -1 - r + (r^2 + 2r + 2)^{1/2}\right), \\ \mathbf{a} &= (-1, 1, 1, -1), \\ \mathbf{a} &= \left(1 + r + (r^2 + 2r + 2)^{1/2}, 1, -1, -1 - r - (r^2 + 2r + 2)^{1/2}\right), \\ \mathbf{a} &= (1, 1, 1, 1), \end{aligned}$$

where $r = Y_1/Y_2$, with corresponding positive eigenvalues

$$\begin{aligned} \lambda &= \left(1 + 2Y_2 + Y_1 + (Y_1^2 + 2Y_1Y_2 + 2Y_2^2)^{1/2}\right)^{1/2}G, \\ \lambda &= (1 + 2Y_2)^{1/2}G, \\ \lambda &= \left(1 + 2Y_2 + Y_1 - (Y_1^2 + 2Y_1Y_2 + 2Y_2^2)^{1/2}\right)^{1/2}G, \\ \lambda &= G. \end{aligned}$$

The second and fourth satisfy (84), but the first and third do not. It appears in Fig. 11(c) that we correctly predicted the first eigenvalue also. However, this was merely a coincidence, and the first eigenfunction in fact follows the new scheme with nonzero $b^{(0)}$.

2. Eigenvalues which follow the new scheme

a. Two humps With $-X_1 = X_2 = X$ the sum over i of (D29) is

$$\frac{\lambda_1^2(\lambda_1^2 - 4)\pi(\pi^2(\lambda_1^2 - 1 - 2X) + 8X^2(3 - 4X))}{256(\lambda_1^2 - 1 - 2X)} = 0. \quad (86)$$

We see the positive eigenvalue $\lambda_1 = 2$, and also a singularity at the false eigenvalue $\lambda_1 = (1 + 2X)^{1/2}$ of §V B. There is one other positive eigenvalue given by

$$\lambda_1 = \left(1 + 2X + \frac{8X^2(4X - 3)}{\pi^2}\right)^{1/2}. \quad (87)$$

The corresponding eigenvector is

$$\mathbf{b}^{(0)} = (1, 1), \quad \mathbf{a}^{(1)} = \frac{\lambda_1 X(2X - 3)}{2(\lambda_1^2 - 1 - 2X)}(1, -1).$$

b. Three humps With $-X_1 = X_3 = X$, $X_2 = 0$, the sum over i of (D29) is

$$\frac{\lambda_1^2(\lambda_1^2 - 4)\pi(3\pi^2(\lambda_1^2 - 1 - X) + 16X^2(3 - 2X))}{512(\lambda_1^2 - 1 - X)} = 0. \quad (88)$$

We see the positive eigenvalue $\lambda_1 = 2$, and also a singularity at the false eigenvalue $\lambda_1 = (1 + X)^{1/2}$ of §V B. There is one other positive eigenvalue given by

$$\lambda_1 = \left(1 + X + \frac{16X^2(2X - 3)}{3\pi^2}\right)^{1/2}. \quad (89)$$

The corresponding eigenvector is

$$\mathbf{b}^{(0)} = (1, 1, 1), \quad \mathbf{a}^{(1)} = \frac{\lambda_1 X(X - 3)}{2(\lambda_1^2 - 1 - X)}(1, 0, -1).$$

c. Four humps With $-X_1 = X_4 = Y_2$, $-X_2 = X_3 = Y_1$, the sum over i of (D29) has two positive solutions in addition to $\lambda_1 = 2$.

VI. CONCLUSIONS AND FUTURE CHALLENGES

In the present work we have revisited the topic of multi-pulse collapsing solutions in the context of the one-dimensional nonlinear Schrödinger equation with a power-law nonlinearity. Returning to the results of [17] from a novel perspective, we have showcased not only in a qualitative, but also in a quantitative way, how *countably infinitely many* branches of such solutions bifurcate from the critical point, along with their most well-known cousin, namely the stationary single collapse point waveform. We have shown that all of these solutions emerge from an infinite distance between the pulses in an example of “bifurcation from infinity” with the distance between the pulses shrinking as the growth rate of the collapse increases. We have provided quantitative characterizations both for the bifurcation curve of the relevant waveforms for the blowup rate G as a function of σ , as well as for the separation between their peaks as a function of G . Importantly, we have also tackled both qualitatively and quantitatively the spectral stability analysis of the relevant states. Indeed, we have found all of them to be unstable, bearing $n - 1$ pairs of eigenvalues of practically of size $G^{1/2}$, another $n + 1$ pairs of size practically proportional to G , while $n - 1$ pairs emerge on the imaginary axis, and one remains in the vicinity of the origin. We have verified the relevant count for cases of $n = 1$ to $n = 4$ and indeed examined cases even up to $n = 6$. While some of the $O(G^{1/2})$ eigenvalues were less accurately captured when G was large, generally our predictions were found to be in excellent qualitative and good quantitative agreement with the numerical observations. Finally, some select dynamical simulations gave us the opportunity to observe the symmetry breaking events leading to the instability of the multi-pulse configurations and the eventual predominance of a single pulse, in line with the expectations associated with stability based on our eigenvector analysis.

Naturally, this study paves the way for a number of directions of future study. Arguably, the most canonical of these concerns whether such multi-bump collapsing solutions can be systematically found in higher

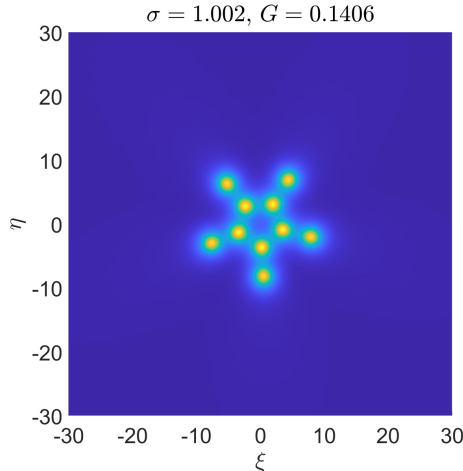


FIG. 12: Star-shaped self-similar profile, $|v(\xi, \eta)|$, for the 2D NLS equation. Here, $\sigma = 1.002$ and the computed blow-up rate is $G = 0.1406$.

dimensions. Our preliminary considerations along this vein suggest the existence of a wide range of possible higher-dimensional waveforms. For instance, in Fig. 12, we illustrate a prototypical star-shaped self-similar waveform computed in the rescaled $(\xi, \eta) \equiv (x/L, y/L)$ space for the 2D NLS equation. Generalizations of the analytical considerations herein enable the consideration of multiple collapse “spots” as an intriguing interacting particle system in the higher-dimensional setting meriting investigation (in terms of its equilibria) in its own right. These can then potentially be associated with the recent experiments of [24] and offer a systematic explanation for the observations therein. These can also potentially be connected to the stability analysis of the *ring type solutions* that have been discovered in the work of [32, 33]. It would be particularly interesting to explore the spectral stability of the ring in terms of its eigenvalues in the co-exploding frame and the conditions under which these may potentially give rise to multi-pulse configurations as the parameters of the system (such as the nonlinearity exponent) may vary. From a computational perspective, and especially for such higher-dimensional PDEs, domain decomposition methods [34, 35] together with the parallelization features provided by the Portable, Extensible Toolkit for Scientific Computation (PETSc) [36] already embedded in FreeFEM [37] (and references therein) have provided us with the necessary computational environment to efficiently and reliably study these types of problems.

It is also relevant to point out here that recent experimental developments in optics have enabled the realization of fractional derivatives (in the form of derivatives of the Riesz type) which, in turn, allow for the manipulation of dispersion [38]. Considering the fractional Laplacian operator $(-\Delta)^{\alpha/2}$, with the Lévy index $0 < \alpha < 2$, this experimental realization has made considerations in the vicinity of $\alpha = 1$ possible. This constitutes (even for the cubic nonlinearity) a critical point for transition to collapse-type solutions and hence represents an additional area of possible future research for the waveforms and phenomena identified herein. Such studies are currently underway and the reporting of associated findings is deferred to future publications.

ACKNOWLEDGEMENTS

This work has been supported by the U.S. National Science Foundation under Grants DMS-2204782 (EGC), and PHY-2110030, PHY-2408988 and DMS-2204702 (PGK), and by the US National Science Foundation (IGK). EGC expresses his gratitude to Prof. Hannes Uecker (University of Oldenburg) for fruitful discussions related to the finite-element implementation of phase conditions in `pde2path` [39]. Also, EGC thanks Profs. Christopher Douglas (Duke), Pierre Jolivet (Sorbonne Université), Georges Sadaka (University

of Rouen Normandie) for their continuing support and encouragement on technical aspects on FreeFEM.

-
- [1] M. J. Ablowitz and H. Segur, *Solitons and the inverse scattering transform* (SIAM, 1981).
 - [2] M. Ablowitz, *Nonlinear Dispersive Waves, Asymptotic Analysis and Solitons* (Cambridge University Press, Cambridge, 2011).
 - [3] C. Sulem and P. Sulem, *The nonlinear Schrödinger equation: self-focusing and wave collapse* (Springer, New York, 1999).
 - [4] M. Ablowitz, B. Prinari, and A. Trubatch, *Discrete and Continuous Nonlinear Schrödinger Systems* (Cambridge University Press, Cambridge, 2004).
 - [5] A. Hasegawa and Y. Kodama, *Solitons in Optical Communications* (Clarendon Press, Oxford, 1995).
 - [6] Y. S. Kivshar and G. P. Agrawal, *Optical Solitons: From Fibers to Photonic Crystals* (Academic Press, 2003) pp. 1–540.
 - [7] L. P. Pitaevskii and S. Stringari, *Bose-Einstein Condensation*, Oxford Science Publications No. 116 (Clarendon Press, Oxford ; New York, 2003).
 - [8] C. J. Pethick and H. Smith, *Bose-Einstein Condensation in Dilute Gases*, 2nd ed. (Cambridge University Press, Cambridge, 2008).
 - [9] P. G. Kevrekidis, D. J. Frantzeskakis, and R. Carretero-González, *The Defocusing Nonlinear Schrödinger Equation* (SIAM, Philadelphia, 2015).
 - [10] M. Kono and M. Skorić, *Nonlinear Physics of Plasmas* (Springer-Verlag, Heidelberg, 2010).
 - [11] D. J. Frantzeskakis, *Journal of Physics A: Mathematical and Theoretical* **43**, 213001 (2010).
 - [12] G. Fibich, *The Nonlinear Schrödinger Equation: Singular Solutions and Optical Collapse*, Applied Mathematical Sciences, Vol. 192 (Springer, New York, 2015).
 - [13] C. I. Siettos, I. G. Kevrekidis, and P. G. Kevrekidis, *Nonlinearity* **16**, 497 (2003).
 - [14] S. J. Chapman, M. Kavousanakis, I. G. Kevrekidis, and P. G. Kevrekidis, *Phys. Rev. E* **104**, 044202 (2021).
 - [15] S. Chapman, M. Kavousanakis, E. Charalampidis, I. Kevrekidis, and P. Kevrekidis, *Physica D: Nonlinear Phenomena* **439**, 133396 (2022).
 - [16] M. J. Landman, G. C. Papanicolaou, C. Sulem, and P. L. Sulem, *Phys. Rev. A* **38**, 3837 (1988).
 - [17] C. J. Budd, S. Chen, and R. D. Russell, *Journal of Computational Physics* **152**, 756 (1999).
 - [18] P. Amodio, C. J. Budd, O. Koch, V. Rottschäfer, G. Settanni, and E. Weinmüller, *Physica D: Nonlinear Phenomena* **401**, 132179 (2020).
 - [19] K. D. Moll, A. L. Gaeta, and G. Fibich, *Phys. Rev. Lett.* **90**, 203902 (2003).
 - [20] L. T. Vuong, T. D. Grow, A. Ishaaya, A. L. Gaeta, G. W. 't Hooft, E. R. Eliel, and G. Fibich, *Phys. Rev. Lett.* **96**, 133901 (2006).
 - [21] B. Bakkali-Hassani, C. Maury, Y.-Q. Zou, E. Le Cerf, R. Saint-Jalm, P. C. M. Castilho, S. Nascimbene, J. Dalibard, and J. Beugnon, *Phys. Rev. Lett.* **127**, 023603 (2021).
 - [22] C.-A. Chen and C.-L. Hung, *Phys. Rev. Lett.* **125**, 250401 (2020).
 - [23] A. Sukhinin, A. B. Aceves, J.-C. Diels, and L. Arissian, *Phys. Rev. A* **95**, 031801 (2017).
 - [24] S. Banerjee, K. Zhou, S. K. Tiwari, H. Tamura, R. Li, P. Kevrekidis, S. I. Mistakidis, V. Walther, and C.-L. Hung, “Collapse of a quantum vortex in an attractive two-dimensional bose gas,” (2024), arXiv:2406.00863 [cond-mat.quant-gas].
 - [25] R. Caplan, Q. Hoq, R. Carretero-González, and P. Kevrekidis, *Optics Communications* **282**, 1399 (2009).
 - [26] H. Nawa, *Journal of Statistical Physics* **91**, 439 (1998).
 - [27] F. Hecht, *J. Numer. Math.* **20**, 251 (2012).
 - [28] C. W. Rowley, I. G. Kevrekidis, J. E. Marsden, and K. Lust, *Nonlinearity* **16**, 1257 (2003).
 - [29] Y. Kuznetsov, *Elements of Bifurcation Theory (4th Edition)* (Springer-Verlag (New York), 2023).
 - [30] M. P. Coles, D. E. Pelinovsky, and P. G. Kevrekidis, *Nonlinearity* **23**, 1753 (2010).
 - [31] Really we should expand λ (and b_i) in powers of G , so that there would be additional terms on the RHS due to λ_2 . However, these terms will simply mirror the terms involving λ_1 at the previous order, and we can ignore them if we are only interested in the leading approximation of the eigenvalue.
 - [32] G. Fibich, N. Gavish, and X.-P. Wang, *Physica D: Nonlinear Phenomena* **231**, 55 (2007).
 - [33] G. Baruch, G. Fibich, and N. Gavish, *Physica D: Nonlinear Phenomena* **239**, 1968 (2010).
 - [34] V. Dolean, P. Jolivet, and F. Nataf, *An Introduction to Domain Decomposition Methods* (Society for Industrial and Applied Mathematics, Philadelphia, PA, 2015) <https://epubs.siam.org/doi/pdf/10.1137/1.9781611974065>.
 - [35] A. Toselli and O. B. Widlund, *Domain Decomposition Methods - Algorithms and Theory* (Springer-Verlag (Berlin), 2005).

- [36] S. Balay and et. al., *PETSc/TAO Users Manual* (Argonne National Laboratory-21/39, <https://petsc.org/release/docs/manual/manual.pdf>, 2022).
- [37] G. Sadaka, P. Jolivet, E. G. Charalampidis, and I. Danaila, *Computer Physics Communications* **306**, 109378 (2025).
- [38] V. T. Hoang, J. Widjaja, Y. L. Qiang, M. Liu, T. J. Alexander, A. F. J. Runge, and C. M. de Sterke, “Observation of fractional evolution in nonlinear optics,” (2024), arXiv:2410.23671 [physics.optics].
- [39] H. Uecker, *Numerical Continuation and Bifurcation in Nonlinear PDEs* (SIAM (Philadelphia), 2021).

Appendix A: Comparison with finite element computations

In this section, we compare numerical computations presented in the main text of our manuscript with those obtained using the open-source, finite-element software, **FreeFEM** [27]. Figure A1 shows a comparison of two-humped solutions computed numerically with finite differences and P3 finite elements. The blow-up rate is $G = 0.01$ and the computational domain: $\xi \in [-300, 300]$. Both solutions appear visually indistinguishable. For the finite-difference computation, the domain is discretized using equidistant nodes with a nodal spacing of $\Delta\xi = 0.06$ (i.e., 10,000 points) whereas for the finite-element, 10,000 nodes were considered on $[-300, 300]$. In addition to the solution comparison, we also present the spectra computed using MATLAB’s **eigs** function and **FreeFEM**’s eigensolver (ARPACK). This comparison demonstrates that both eigensolvers yield nearly identical eigenvalues.

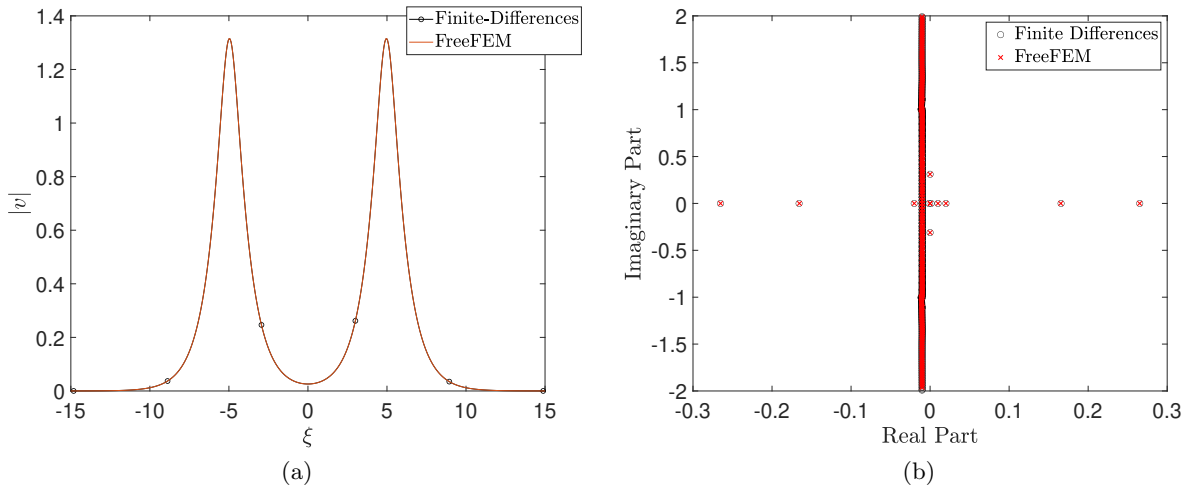


FIG. A1: (a) Finite-difference (black line with open circles) and finite-element (red line) two-humped solutions with a blow-up rate of $G = 0.01$. The two solutions are visually indistinguishable. The computational domain $\xi \in [-300, 300]$ is discretized using equidistant nodes with a spacing of $\Delta\xi = 0.06$ (10,000 nodes). (b) Spectra comparison between the finite-difference discretization and MATLAB’s **eigs** function (black circles) and **FreeFEM**’s ARPACK eigensolver (red crosses).

Appendix B: Full domain dynamical simulations

In this section, we present dynamical simulations performed on the full domain, i.e., $\xi \in [-K, K]$. When simulations are performed on $[-K, K]$, convergence of an unstable multi-hump state to a steady-state corresponding to a single-humped solution is not observed. The initial data evolves toward the corresponding single-humped self-similar state; however the $\lambda = G$ associated eigenmode drives the solution away from this final state. Figure A2 illustrates the $\xi - \tau$ spatiotemporal evolution of an initial two-humped self-similar

solution computed at $\sigma = 2.01$, slightly perturbed along the symmetric eigenmode corresponding to the second largest eigenvalue. After an initial τ period spanning approximately $[0, 6]$, where the solution visibly restructures toward a single-humped state, then at $\tau \approx 40$, v starts shifting from the origin to positive ξ values. This shift is attributed to the $\lambda = G$ eigenvalue of the single-humped self-similar solution. In Fig. A3(a)-(b), we compare the numerically approximated value of $\frac{\partial v}{\partial \tau}$ at $\tau = 48$ with the $\lambda = G$ -associated eigenmode of the single-humped self-similar solution ((a) real part and (b) imaginary part). The comparison shows good agreement, indicating that v shifts in the direction of the $\lambda = G$ -associated eigenmode. The blow-up rate for a single-humped solution at $\sigma = 2.01$ is $G = 0.403$. In Fig. A3(c), we plot the evolution of the deviation $\|v(\xi, \tau) - v^*\|$, with v^* the single-humped self-similar solution at $\sigma = 2.01$. Our starting point for measuring the deviation is $\tau_0 = 40$. This deviation is expected to grow exponentially in rescaled time, following: $\|v(\xi, \tau) - v^*\| \sim e^{a(\tau - \tau_0)}$, where $a \approx G$. Indeed, fitting yields $a \approx 0.4085$ which is close to the expected value of the blow-up rate for a single-humped solution at $\sigma = 2.01$ (which, as mentioned above, is $G = 0.403$).

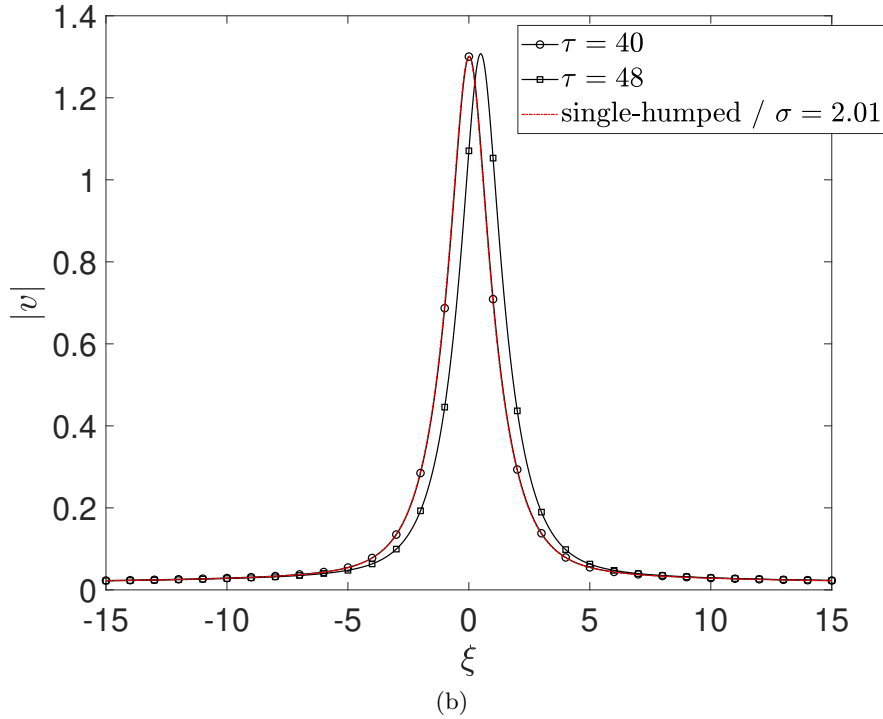
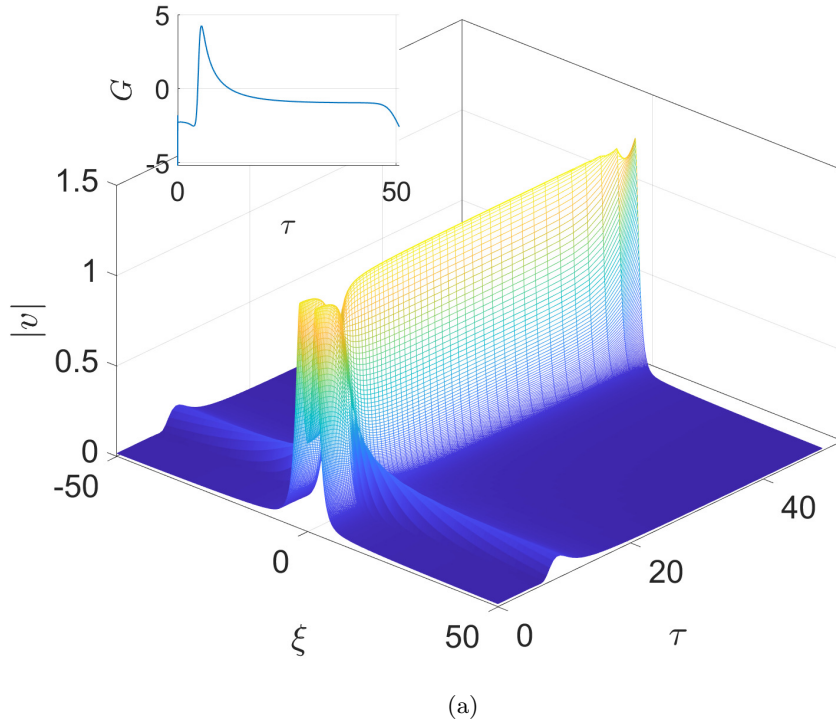


FIG. A2: (a) Dynamics in the renormalized/rescaled spatio-temporal framework $\xi - \tau$: Starting from a two-humped solution at $\sigma = 2.01$ and perturbing along the eigenfunction that corresponds to the second largest real eigenvalue the solution evolves toward the corresponding single-humped solution after an initial “restructuring” τ -period. Convergence is lost at around $\tau = 50$. The inset illustrates the evolution of blow-up rate, G . (b) To enhance visualization of the shift from the origin at later stages of the simulation, we plot two snapshots: one at $\tau = 40$ (solid line with open circles), where the solution is visually indistinguishable from the single-humped self-similar solution (red dashed line), and one at $\tau = 48$, where the solution has visibly shifted from the origin. $\xi \in [-50, 50]$, nodal distance: $\delta x = 0.001$, and $dt = 0.01$.

H

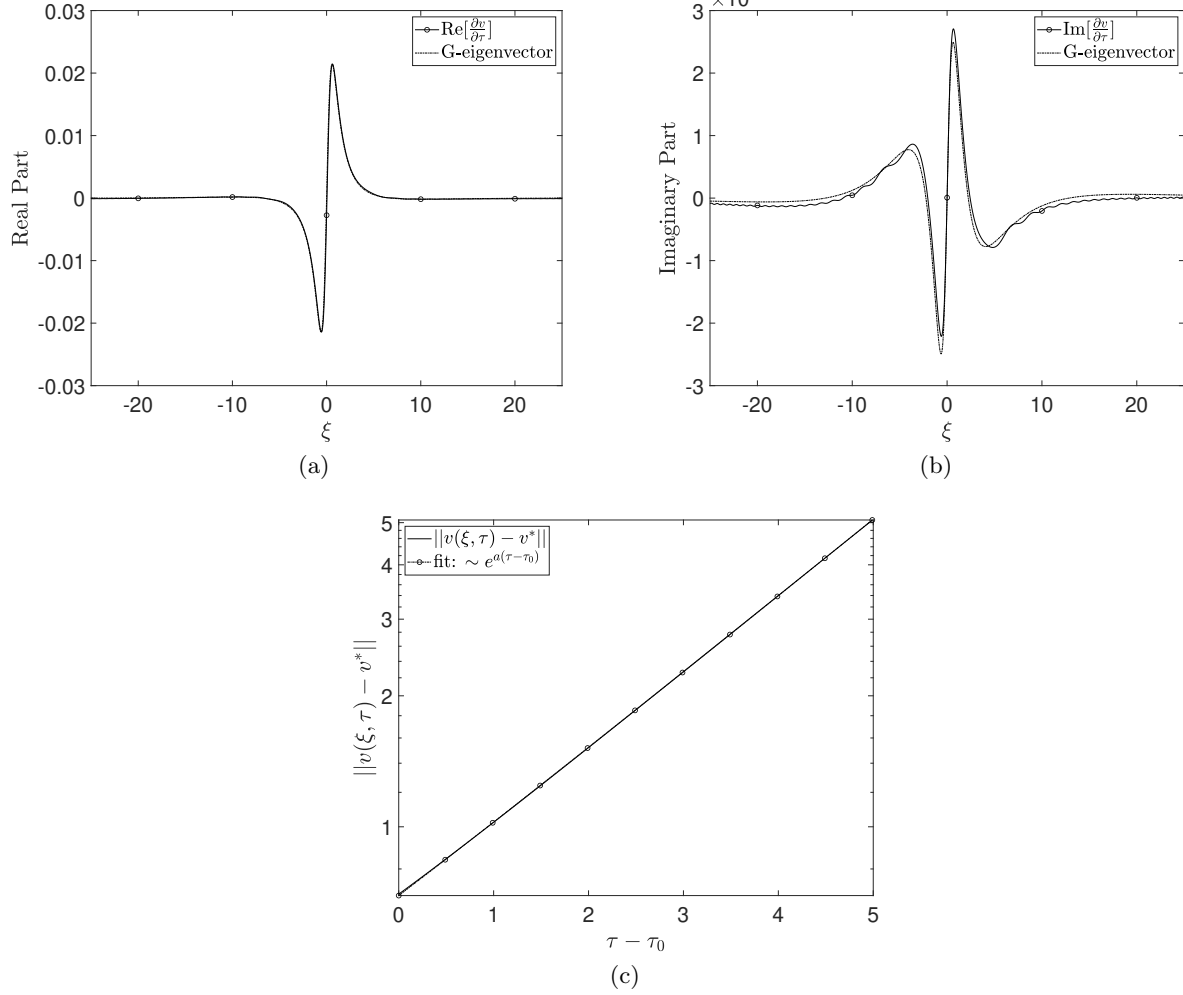


FIG. A3: Comparison of solution's (a) real part and (b) imaginary part, partial τ derivative (computed at $\tau = 42$) with the real and imaginary part of the G -eigenvector indicating that the instability presented in Fig. A2 leads to growth along the direction of the G -eigenvector. (c) Exponential evolution of solution's v deviation from the single-humped solution, v^* , $\|v(\xi, \tau) - v^*\|$. The starting time to measure deviation is $\tau_0 = 40$. Here, $a \approx 0.4085$, which is close to the blow-up rate of the single-humped solution: $G = 0.403$.

In Fig. A4(a), we present a second simulation initialized with the two-humped solution for $\sigma = 2.01$. This time, no perturbation is directly applied to the initial condition, and we perform a direct numerical simulation with the roundoff error providing the initial perturbation. The unstable self-similar solution retains its initial shape for a time interval $\tau \in [0, 18]$ before gradually losing its symmetry in the later stages of the simulation. At this point, we observe an asymmetric shape for v and the blow-up rate that trends toward large negative values. The solution begins to deviate in the direction of the largest real eigenvalue of the two-humped solution. This behavior is illustrated in Fig. A4(b)-(c), where we plot the time-derivative of v (real and imaginary part) computed at $\tau = 18$ and compare against the eigenmode which is associated with the largest real eigenvalue of the two-humped solution. If we fit the exponential growth of the deviation from the two-humped solution v_{2h}^* , $E \equiv \|v(\xi, \tau) - v_{2h}^*\| \sim e^{a(\tau - \tau_0)}$, then a is expected to be close to λ_1 . This fitting is shown in Fig. A4(d), where $a = 1.2606$ close enough to $\lambda_1 = 1.245$. We start measuring the deviation at $\tau_0 = 18$.

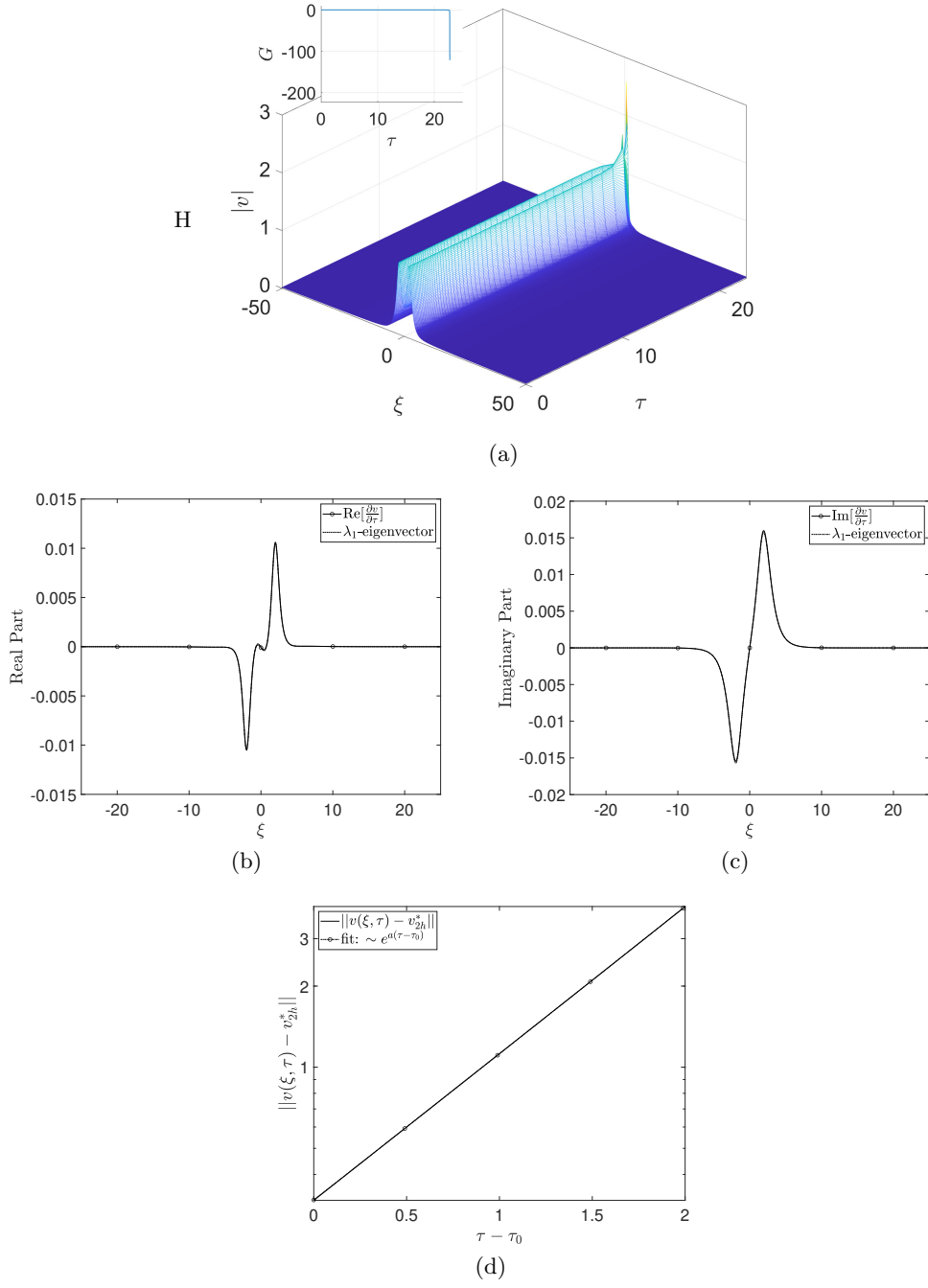


FIG. A4: (a) Dynamics in the renormalized/rescaled spatio-temporal framework $\xi - \tau$: Starting from a two-humped solution at $\sigma = 2.01$, we observe that the dynamics for the time interval $[0, 18]$ are slow. The accumulation of numerical errors drives the solution to asymmetric profiles for $\tau > 20$, while the blow-up rate, G (shown in the inset) shifts towards large negative values, and convergence is lost at around $\tau \approx 23$ [in line with the blow-up of such solutions also reported in [17]]. (b)-(c) Comparison of solution's (rescaled- τ) time derivative ((b) real part and (c) imaginary part) computed at $\tau = 18$ with the real and imaginary part of the eigenvector associated with the largest real eigenvalue of the two-humped solution, $\lambda_1 = 1.245$. The agreement indicates that the deviation grows along the direction of the λ_1 eigenvector. (d) Exponential evolution of solution's v deviation from the two-humped solution, v_{2h}^* , $\|v(\xi, \tau) - v_{2h}^*\|$. The starting time to measure deviation is $\tau_0 = 18$. Here, $a \approx 1.26$, which is close to the largest real eigenvalue, λ_1 of the two-humped solution.

Appendix C: Higher order terms in the bifurcation diagram

To get a good quantitative analysis in Figure 4 when G is not so small we need to include higher-order terms in equation (39). We can do so by following a similar procedure to that by which we determined the higher-order terms for the one-hump solution in [14].

1. Higher-order terms in the far field

We proceed to calculate more terms in the expansion (32) of §IV D. The calculation is similar to that in [14]. The equation for A_1 is

$$2A_1'\phi' + A_0'' + A_1\phi'' = 0,$$

i.e.,

$$\frac{d}{d\rho} A_1(-\phi')^{1/2} = \frac{A_0''}{2(-\phi')^{1/2}} = \frac{a_0(8 + 3\rho^2)}{4(4 - \rho^2)^{5/2}}.$$

Thus,

$$A_1 = \frac{a_0\rho(24 - \rho^2)}{24\sqrt{2}(4 - \rho^2)^{7/4}} + \frac{2^{1/2}a_1}{(4 - \rho^2)^{1/4}}.$$

Matching the near field gives $a_1 = 0$. At the next order

$$2A_2'\phi' + A_1'' + A_2\phi'' = 0,$$

i.e.

$$\frac{d}{d\rho} A_2(-\phi')^{1/2} = \frac{A_1''}{2(-\phi')^{1/2}} = \frac{a_0\rho(3648 + 640\rho^2 - 3\rho^4)}{192(\rho^2 - 4)^4}.$$

Thus

$$A_2 = \frac{a_0(2320 - 996\rho^2 + 9\rho^4)}{576\sqrt{2}(4 - \rho^2)^{13/4}} + \frac{2^{1/2}a_2}{(4 - \rho^2)^{1/4}}.$$

As $\rho \rightarrow 0$,

$$A_2 \rightarrow \frac{145a_0}{4608} + a_2. \quad (C1)$$

2. Higher-order terms in outer limit of the inner

From §E as $x \rightarrow \infty$, the asymptotic behaviour of $V_1 = V_o + V_e$ is given by

$$V_o \sim 3^{1/4} \frac{X_i}{16} \sqrt{2} e^{-x} (2x^2 + 2x - 2\log 2 + 1), \quad (C2)$$

$$V_e \sim 12^{1/4} (\alpha_0 + \alpha_1 x + \alpha_2 x^2 + \alpha_3 x^3) e^{-x} - \frac{X_i^2}{16} 3^{1/4} \sqrt{2} (1 - 2x) e^{-x}, \quad (C3)$$

with α_i , $i = 0, 1, 2, 3$ given by (E9). With $x = \xi - X_i$, The coefficient of $e^{-\xi}$ is

$$\left(3^{1/4} \frac{X_i}{16} \sqrt{2} (2X_i^2 - 2X_i - 2\log 2 + 1) + 12^{1/4} (\alpha_0 - \alpha_1 X_i + \alpha_2 X_i^2 - \alpha_3 X_i^3) - \frac{X_i^2}{16} 3^{1/4} \sqrt{2} (1 + 2X_i) \right) e^{X_i}.$$

Matching with (C1) gives

$$a_2 = \left(3^{1/4} \frac{X_i}{16} \sqrt{2} (2X_i^2 - 2X_i - 2\log 2 + 1) + 12^{1/4} (\alpha_0 - \alpha_1 X_i + \alpha_2 X_i^2 - \alpha_3 X_i^3) - \frac{X_i^2}{16} 3^{1/4} \sqrt{2} (1 + 2X_i) \right) e^{X_i} - \frac{145a_0}{4608}.$$

3. Higher-order terms in the integral of V_s^2

The final step in finding higher-order terms in (37) is to get a better approximation to the right-hand side, for which we need the integral of V_s^2 . If we spilt the integral we have

$$\int_{-\infty}^{\infty} = \int_{-\infty}^{X_1-R} + \int_{X_1-R}^{X_1+R} + \int_{X_1+R}^{X_2-R} + \cdots + \int_{X_n+R}^{\infty}$$

Now, using the inner expansion,

$$\begin{aligned} \int_{X_i-R}^{X_i+R} V_s^2 d\xi &= \int_{-R}^R (V_0^2 + 2G^2 V_0 V_1 + \cdots) dx \\ &\sim \frac{\sqrt{3}\pi}{2} + 2G^2 \int_{-R}^R V_{\text{even}} V_0 dx \\ &\sim \frac{\sqrt{3}\pi}{2} + 2G^2 \int_{-R}^R \left(\frac{3^{1/4}}{2} \left(\frac{e^{X_i-X_{i+1}}}{G^2} + \frac{e^{X_{i-1}-X_i}}{G^2} \right) v_2(x) + \hat{V}_1(x) - \frac{X_i^2}{4} \left(\frac{V_0}{4} + \frac{x}{2} \frac{dV_0}{dx} \right) \right) V_0 dx \\ &= \frac{\sqrt{3}\pi}{2} + 2G^2 \frac{\sqrt{3}\pi^3}{256} + 3^{1/4} (e^{X_i-X_{i+1}} + e^{X_{i-1}-X_i}) \int_{-R}^R v_2 V_0 dx \\ &= \frac{\sqrt{3}\pi}{2} + 2G^2 \frac{\sqrt{3}\pi^3}{256} + 3^{1/4} (e^{X_i-X_{i+1}} + e^{X_{i-1}-X_i}) \left[2 \times 3^{1/4} (x - \tanh 2x) \right]_{-R}^R \\ &= \frac{\sqrt{3}\pi}{2} + G^2 \frac{\sqrt{3}\pi^3}{128} + 4\sqrt{3} (e^{X_i-X_{i+1}} + e^{X_{i-1}-X_i}) (R-1). \end{aligned}$$

using the outer (between humps) expansion,

$$\begin{aligned} \int_{X_i+R}^{X_{i+1}-R} V_s^2 d\xi &= \int_{X_i+R}^{X_{i+1}-R} (V_0^2 + 2G^2 V_1 V_0 + \cdots) d\xi \\ &= \int_{X_i+R}^{X_{i+1}-R} 2\sqrt{3} (e^{-\xi+X_i} + e^{\xi-X_{i+1}})^2 + 2G^2 12^{1/4} V_1 (e^{-\xi+X_i} + e^{\xi-X_{i+1}}) + \cdots d\xi \\ &\sim -8\sqrt{3} R e^{X_i-X_{i+1}} + 4\sqrt{3} (X_{i+1} - X_i) e^{X_i-X_{i+1}} + \cdots \end{aligned}$$

Thus, together

$$\begin{aligned}
\int_{-\infty}^{\infty} V_s^2 dx &\sim \frac{\sqrt{3}\pi}{2} \left(1 + \frac{G^2\pi^2}{64}\right) n + 4\sqrt{3}(R-1) \sum_{i=1}^n (e^{X_i-X_{i+1}} + e^{X_{i-1}-X_i}) \\
&\quad - 8\sqrt{3}R \sum_{i=1}^{n-1} e^{X_i-X_{i+1}} + 4\sqrt{3} \sum_{i=1}^{n-1} (X_{i+1} - X_i) e^{X_i-X_{i+1}} \\
&\sim \frac{\sqrt{3}\pi}{2} \left(1 + \frac{G^2\pi^2}{64}\right) n + 4\sqrt{3}(R-1) \sum_{i=1}^{n-1} e^{X_i-X_{i+1}} + 4\sqrt{3}(R-1) \sum_{i=1}^{n-1} e^{X_i-X_{i+1}} \\
&\quad - 8\sqrt{3}R \sum_{i=1}^{n-1} e^{X_i-X_{i+1}} + 4\sqrt{3} \sum_{i=1}^{n-1} (X_{i+1} - X_i) e^{X_i-X_{i+1}} \\
&\sim \frac{\sqrt{3}\pi}{2} \left(1 + \frac{G^2\pi^2}{64}\right) n + 4\sqrt{3} \sum_{i=1}^{n-1} (X_{i+1} - X_i - 2) e^{X_i-X_{i+1}}
\end{aligned}$$

4. Normal form

With $X_1 = -X_n$ equation (37) now becomes

$$\begin{aligned}
4\sqrt{3}e^{2X_n}e^{-\pi/G} &\left(1 + G^2 \left(\frac{X_i}{16}(2X_i^2 - 2X_i - 2\log 2 + 1) \right. \right. \\
&\quad \left. \left. + (\alpha_0 - \alpha_1 X_i + \alpha_2 X_i^2 - \alpha_3 X_i^3) - \frac{X_i^2}{16}(1 + 2X_i) \right) e^{X_i} - \frac{145G^2}{4608} \right)^2 \\
&= \frac{(\sigma - 2)G}{2\sigma} \left(\frac{\sqrt{3}\pi}{2} \left(1 + \frac{G^2\pi^2}{64}\right) n + 4\sqrt{3} \sum_{i=1}^{n-1} (X_{i+1} - X_i - 2) e^{X_i-X_{i+1}} \right) \quad (C4)
\end{aligned}$$

This is what is plotted in Figure 4.

Appendix D: Detailed asymptotic analysis of the eigenvalues $\lambda = O(G)$.

With the expansions (74)-(78), equating coefficients at $O(G)$ we have

$$f_1 = a_i^{(1)}U_0 + b_i^{(0)}W_1,$$

where

$$\frac{d^2 W_1}{dx^2} + 2V_0^4 W_1^* + 3V_0^4 W_1 - W_1 = \lambda_1 V_0.$$

The solvability conditions on W_1 are satisfied automatically, and

$$W_1 = \lambda_1 \left(\frac{V_0}{4} + \frac{x}{2} \frac{dV_0}{dx} \right).$$

Equating coefficients at $O(G^2)$ we have

$$f_2 = a_i^{(1)}U_1 + b_i^{(2)}W_0 + b_i^{(0)}W_2,$$

where

$$\begin{aligned}\frac{d^2 U_1}{dx^2} + 2V_0^4 U_1^* + 3V_0^4 U_1 - U_1 &= -i\lambda_1 \frac{dV_0}{dx}, \\ \frac{d^2 W_2}{dx^2} + V_0^4(2W_2^* + 3W_2) - W_2 &= -i\lambda_1^2 \left(\frac{V_0}{4} + \frac{x}{2} \frac{dV_0}{dx} \right) + \lambda_2 V_0 - i \frac{(x + X_i)^2}{4} V_0 - 4iV_1 V_0^4.\end{aligned}$$

The solvability conditions on U_1 are automatically satisfied, while those on W_2 are

$$\text{Im} \left[\frac{dW_2}{dx} V_0 - W_2 \frac{dV_0}{dx} \right]_{-R}^R = \left[\frac{dV_1}{dx} V_0 - V_1 \frac{dV_0}{dx} \right]_{-R}^R, \quad (\text{D1})$$

$$\text{Re} \left[\frac{dW_2}{dx} \frac{dV_0}{dx} - W_2 \frac{d^2 V_0}{dx^2} \right]_{-R}^R = 0. \quad (\text{D2})$$

The solutions are

$$U_1 = -\frac{i\lambda_1 x}{2} V_0, \quad W_2 = -\frac{i\lambda_1^2 x^2 V_0}{8} + iV_1 + \lambda_2 \left(\frac{V_0}{4} + \frac{x}{2} \frac{dV_0}{dx} \right). \quad (\text{D3})$$

Note that W_2 grows at infinity, as does V_1 , so that to evaluate (D1) we need to match with the region between humps. In preparation for matching we list the limiting behaviour of the near-hump solutions as $x \rightarrow \pm\infty$:

$$\begin{aligned}U_0 &\sim \mp 12^{1/4} e^{\mp x} \quad \text{as } x \rightarrow \pm\infty, & W_0 &\sim 12^{1/4} i e^{\mp x} \quad \text{as } x \rightarrow \pm\infty, \\ U_1 &\sim -\frac{12^{1/4} i}{2} x e^{\mp x} \quad \text{as } x \rightarrow \pm\infty, & W_1 &\sim 12^{1/4} \left(\frac{1}{4} \mp \frac{x}{2} \right) e^{\mp x} \quad \text{as } x \rightarrow \mp\infty,\end{aligned}$$

Thus,

$$f_0 \sim 12^{1/4} i b_i^{(0)} e^{\mp x} \quad \text{as } x \rightarrow \pm\infty, \quad f_1 \sim 12^{1/4} b_i^{(0)} \left(\frac{1}{4} \mp \frac{x}{2} \right) e^{\mp x} \mp 12^{1/4} a_i^{(1)} e^{\mp x} \quad \text{as } x \rightarrow \pm\infty.$$

1. In between the humps

As usual, away from the humps,

$$i\lambda f + \frac{d^2 f}{d\xi^2} - f + \frac{G^2 \xi^2}{4} f = O(G^8 \log G^4 f).$$

Consider the gap between X_i and X_{i+1} . At leading order

$$\frac{d^2 f_0}{d\xi^2} - f_0 = 0.$$

Matching requires

$$f_0 \sim 12^{1/4} i b_{i+1}^{(0)} e^{\xi - X_{i+1}} \quad \text{as } \xi \rightarrow X_{i+1}, \quad f_0 \sim 12^{1/4} i b_i^{(0)} e^{-\xi + X_i} \quad \text{as } \xi \rightarrow X_i.$$

Thus,

$$f_0 = 12^{1/4} i b_{i+1}^{(0)} e^{\xi - X_{i+1}} + 12^{1/4} i b_i^{(0)} e^{-\xi + X_i}.$$

In terms of $\xi = X_{i+1} + x$ this is

$$f_0 = 12^{1/4} i b_{i+1}^{(0)} e^x + 12^{1/4} i b_i^{(0)} e^{-x + X_i - X_{i+1}},$$

giving the matching condition (translating to $i + 1 \rightarrow i$)

$$G^2 f_2 \sim 12^{1/4} i b_{i-1}^{(0)} e^{-x+X_{i-1}-X_i} \quad \text{as } x \rightarrow -\infty \quad (\text{D4})$$

on the local solution near the i th hump. Similarly we find

$$G^2 f_2 \sim 12^{1/4} i b_{i+1}^{(0)} e^{x+X_i-X_{i+1}} \quad \text{as } x \rightarrow \infty. \quad (\text{D5})$$

on the local solution near the i th hump. Since

$$f_2 = a_i^{(1)} U_1 + b_i^{(2)} W_0 + b_i^{(0)} W_2,$$

and the local hump solutions for U_1 and W_0 decay at infinity, matching gives

$$\text{Im} \left[b_i^{(0)} \frac{dW_2}{dx} V_0 - b_i^{(0)} W_2 \frac{dV_0}{dx} \right]_{-R}^R = \frac{4\sqrt{3} b_{i+1}^{(0)}}{G^2} e^{X_i-X_{i+1}} + \frac{4\sqrt{3} b_{i-1}^{(0)}}{G^2} e^{X_{i-1}-X_i}, \quad (\text{D6})$$

$$\text{Re} \left[b_i^{(0)} \frac{dW_2}{dx} \frac{dV_0}{dx} - b_i^{(0)} W_2 \frac{d^2 V_0}{dx^2} \right]_{-R}^R = 0. \quad (\text{D7})$$

Using (D6), (D7) and (56) in (D1)-(D2) gives

$$b_i^{(0)} \left(\frac{4\sqrt{3}}{G^2} e^{-X_{i+1}+X_i} + \frac{4\sqrt{3}}{G^2} e^{-X_i+X_{i-1}} \right) = \frac{4\sqrt{3} b_{i+1}^{(0)}}{G^2} e^{X_i-X_{i+1}} + \frac{4\sqrt{3} b_{i-1}^{(0)}}{G^2} e^{X_{i-1}-X_i}. \quad (\text{D8})$$

This is equation (79) from the main text. Equation (D8) fixes $b_i^{(0)} = b^{(0)}$ for all i .

2. The outer limit of f_2

We will need to know the outer limit of f_2 , for which we need to know the behaviour of W_2 as $x \rightarrow \pm\infty$. We have just evaluated the exponentially growing component by matching, but we will find that unfortunately we need also the exponentially decaying component. This requires the asymptotic behaviour of V_1 . Note that there are also higher-order terms arising from the expansion of f_0 and f_1 as $x \rightarrow \pm\infty$, but these don't contribute until $O(e^{-5x}) = O(G^{10})$ so we will ignore them.

We show in §E that, as $x \rightarrow -\infty$,

$$V_1 \sim 3^{1/4} \frac{X_i}{16} \sqrt{2} e^x (-2x^2 + 2x + 2 \log 2 - 1) + 3^{1/4} \frac{e^{X_{i-1}-X_i}}{G^2} \sqrt{2} e^{-x} + 12^{1/4} (\alpha_0 - \alpha_1 x + \alpha_2 x^2 - \alpha_3 x^3) e^x - \frac{X_i^2}{16} 3^{1/4} \sqrt{2} (1 + 2x) e^x, \quad (\text{D9})$$

while, as $x \rightarrow \infty$,

$$V_1 \sim 3^{1/4} \frac{X_i}{16} \sqrt{2} e^{-x} (2x^2 + 2x - 2 \log 2 + 1) + 3^{1/4} \sqrt{2} \frac{e^{X_i-X_{i+1}}}{G^2} e^x + 12^{1/4} (\alpha_0 + \alpha_1 x + \alpha_2 x^2 + \alpha_3 x^3) e^{-x} - \frac{X_i^2}{16} 3^{1/4} \sqrt{2} (1 - 2x) e^{-x}. \quad (\text{D10})$$

Thus

$$\begin{aligned} W_2 &\sim -\frac{i\lambda_1^2 x^2}{8} 12^{1/4} e^{-x} + 12^{1/4} i \frac{X_i}{16} e^{-x} (2x^2 + 2x - 2 \log 2 + 1) + 12^{1/4} i \frac{e^{X_i-X_{i+1}}}{G^2} e^x \\ &\quad + 12^{1/4} i (\alpha_0 + \alpha_1 x + \alpha_2 x^2 + \alpha_3 x^3) e^{-x} - i \frac{X_i^2}{16} 12^{1/4} (1 - 2x) e^{-x} + \frac{\lambda_2}{4} 12^{1/4} (1 - 2x) e^{-x} \quad \text{as } x \rightarrow \infty, \\ W_2 &\sim -\frac{i\lambda_1^2 x^2}{8} 12^{1/4} e^x + 12^{1/4} i \frac{X_i}{16} e^x (-2x^2 + 2x + 2 \log 2 - 1) + 12^{1/4} i \frac{e^{X_{i-1}-X_i}}{G^2} e^{-x} \\ &\quad + 12^{1/4} i (\alpha_0 - \alpha_1 x + \alpha_2 x^2 - \alpha_3 x^3) e^x - i \frac{X_i^2}{16} 12^{1/4} (1 + 2x) e^x + \frac{\lambda_2}{4} 12^{1/4} (1 + 2x) e^x \quad \text{as } x \rightarrow -\infty. \end{aligned}$$

Thus

$$\begin{aligned}
f_2 \sim & 12^{1/4} b_i^{(2)} i e^{-x} - 12^{1/4} a_i^{(1)} \frac{i \lambda_1 x}{2} e^{-x} - b^{(0)} \frac{i \lambda_1^2 x^2}{8} 12^{1/4} e^{-x} + 12^{1/4} i b^{(0)} \frac{X_i}{16} e^{-x} (2x^2 + 2x - 2 \log 2 + 1) \\
& + 12^{1/4} i b^{(0)} \frac{e^{X_i - X_{i+1}}}{G^2} e^x + 12^{1/4} i b^{(0)} (\alpha_0 + \alpha_1 x + \alpha_2 x^2 + \alpha_3 x^3) e^{-x} - i \frac{X_i^2}{16} 12^{1/4} b^{(0)} (1 - 2x) e^{-x} \\
& + \frac{\lambda_2}{4} 12^{1/4} b^{(0)} (1 - 2x) e^{-x} \quad \text{as } x \rightarrow \infty, \quad (D11)
\end{aligned}$$

$$\begin{aligned}
f_2 \sim & 12^{1/4} b_i^{(2)} i e^x - 12^{1/4} a_i^{(1)} \frac{i \lambda_1 x}{2} e^x - \frac{i \lambda_1^2 x^2}{8} 12^{1/4} b^{(0)} e^x + 12^{1/4} b^{(0)} i \frac{X_i}{16} e^x (-2x^2 + 2x + 2 \log 2 - 1) \\
& + 12^{1/4} b^{(0)} i \frac{e^{X_{i-1} - X_i}}{G^2} e^{-x} + 12^{1/4} b^{(0)} i (\alpha_0 - \alpha_1 x + \alpha_2 x^2 - \alpha_3 x^3) e^x - b^{(0)} i \frac{X_i^2}{16} 12^{1/4} (1 + 2x) e^x \\
& + \frac{\lambda_2}{4} 12^{1/4} b^{(0)} (1 + 2x) e^x \quad \text{as } x \rightarrow -\infty. \quad (D12)
\end{aligned}$$

3. $O(G^3)$ terms in the inner expansion

At $O(G^3)$ we find

$$f_3 = a_i^{(3)} U_0 + a_i^{(1)} U_2 + b_i^{(2)} W_1 + b_i^{(0)} W_3,$$

where

$$\begin{aligned}
\frac{d^2 U_2}{dx^2} + V_0^4 (2U_2^* + 3U_2) - U_2 &= -\frac{\lambda_1^2 x}{2} V_0 - i \lambda_2 \frac{dV_0}{dx} - \frac{(x + X_i)^2}{4} \frac{dV_0}{dx} - 20V_1 V_0^3 \frac{dV_0}{dx}, \\
\frac{d^2 W_3}{dx^2} + V_0^4 (2W_3^* + 3W_3) - W_3 &= -\frac{\lambda_1^3 x^2 V_0}{8} + \lambda_1 V_1 - 2i \lambda_2 \lambda_1 \left(\frac{V_0}{4} + \frac{x}{2} \frac{dV_0}{dx} \right) + \lambda_3 V_0 \\
&\quad - \frac{(x + X_i)^2}{4} \lambda_1 \left(\frac{V_0}{4} + \frac{x}{2} \frac{dV_0}{dx} \right) - 20V_1 V_0^3 \lambda_1 \left(\frac{V_0}{4} + \frac{x}{2} \frac{dV_0}{dx} \right).
\end{aligned}$$

The solvability conditions are

$$\text{Im} \left[\frac{dU_2}{dx} V_0 - U_2 \frac{dV_0}{dx} \right]_{-R}^R = 0, \quad (D13)$$

$$\text{Re} \left[\frac{dU_2}{dx} \frac{dV_0}{dx} - U_2 \frac{d^2 V_0}{dx^2} \right]_{-R}^R = \frac{\sqrt{3} \pi (\lambda_1^2 - 1)}{8} + \left[\frac{d^2 V_1}{dx^2} \frac{dV_0}{dx} - \frac{dV_1}{dx} \frac{d^2 V_0}{dx^2} \right]_{-R}^R \quad (D14)$$

$$\text{Im} \left[\frac{dW_3}{dx} V_0 - W_3 \frac{dV_0}{dx} \right]_{-R}^R = 0, \quad (D15)$$

$$\text{Re} \left[\frac{dW_3}{dx} \frac{dV_0}{dx} - W_3 \frac{d^2 V_0}{dx^2} \right]_{-R}^R = \lambda_1 \int_{-R}^R \left(V_1 \frac{dV_0}{dx} - \left(\frac{x X_i}{2} + 20V_1 V_0^3 \right) \left(\frac{V_0}{4} + \frac{x}{2} \frac{dV_0}{dx} \right) \frac{dV_0}{dx} \right) dx, \quad (D16)$$

where we have taken advantage of the evenness of V_0 to simplify. The terms forced by λ_2 and λ_3 can be evaluated, so that we can write

$$\begin{aligned}
U_2 &= U_2^R - \frac{i \lambda_2 x}{2} V_0, \\
W_3 &= W_3^R - i \lambda_2 \lambda_1 \frac{x^2 V_0}{4} + \lambda_3 \left(\frac{V_0}{4} + \frac{x}{2} \frac{dV_0}{dx} \right),
\end{aligned}$$

where

$$\frac{d^2 U_2^R}{dx^2} + 5V_0^4 U_2^R - U_2^R = -\frac{\lambda_1^2 x}{2} V_0 - \frac{(x + X_i)^2}{4} \frac{dV_0}{dx} - 20V_1 V_0^3 \frac{dV_0}{dx}, \quad (D17)$$

$$\frac{d^2 W_3^R}{dx^2} + 5V_0^4 W_3^R - W_3^R = -\frac{\lambda_1^3 x^2 V_0}{8} + \lambda_1 V_1 - \frac{(x + X_i)^2}{4} \lambda_1 \left(\frac{V_0}{4} + \frac{x}{2} \frac{dV_0}{dx} \right) - 20V_1 V_0^3 \lambda_1 \left(\frac{V_0}{4} + \frac{x}{2} \frac{dV_0}{dx} \right) \quad (D18)$$

4. $O(G)$ terms in the outer expansion

At $O(G)$ in the outer we find

$$i\lambda_1 f_0 + \frac{d^2 f_1}{d\xi^2} - f_1 = 0,$$

with

$$f_0 = 12^{1/4} i b^{(0)} e^{\xi - X_{i+1}} + 12^{1/4} i b^{(0)} e^{-\xi + X_i}.$$

Matching requires

$$\begin{aligned} f_1 &\sim 12^{1/4} a_{i+1}^{(1)} e^{\xi - X_{i+1}} + 12^{1/4} b^{(0)} \left(\frac{\lambda_1 (\xi - X_{i+1})}{2} + \frac{\lambda_1}{4} \right) e^{\xi - X_{i+1}} \quad \text{as } \xi \rightarrow X_{i+1}, \\ f_1 &\sim -12^{1/4} a_i^{(1)} e^{-\xi + X_i} + 12^{1/4} b^{(0)} \left(-\frac{\lambda_1 (\xi - X_i)}{2} + \frac{\lambda_1}{4} \right) e^{-\xi + X_i} \quad \text{as } \xi \rightarrow X_i. \end{aligned}$$

Thus

$$\begin{aligned} f_1 &= 12^{1/4} \left(a_{i+1}^{(1)} + \frac{\lambda_1 b^{(0)} (\xi - X_{i+1})}{2} + \frac{\lambda_1 b^{(0)}}{4} \right) e^{\xi - X_{i+1}} \\ &\quad + 12^{1/4} \left(-a_i^{(1)} - \frac{\lambda_1 b^{(0)} (\xi - X_i)}{2} + \frac{\lambda_1 b^{(0)}}{4} \right) e^{-\xi + X_i}. \end{aligned}$$

In terms of $\xi = X_{i+1} + x$ this is

$$\begin{aligned} f_1 &= 12^{1/4} \left(a_{i+1}^{(1)} + \frac{\lambda_1 x}{2} b^{(0)} + \frac{\lambda_1}{4} b^{(0)} \right) e^x \\ &\quad + 12^{1/4} \left(-a_i^{(1)} - \frac{\lambda_1 (x + X_{i+1} - X_i)}{2} b^{(0)} + \frac{\lambda_1}{4} b^{(0)} \right) e^{-x - X_{i+1} + X_i}. \end{aligned}$$

giving the matching condition

$$f_3 G^2 \sim 12^{1/4} \left(-a_{i-1}^{(1)} - \frac{\lambda_1 (x + X_i - X_{i-1})}{2} b^{(0)} + \frac{\lambda_1}{4} b^{(0)} \right) e^{-x - X_i + X_{i-1}}, \quad (D19)$$

as $x \rightarrow -\infty$ on the inner solution. In terms of $\xi = X_i + x$ we have

$$\begin{aligned} f_1 &= 12^{1/4} \left(a_{i+1}^{(1)} + \frac{\lambda_1 (x + X_i - X_{i+1})}{2} b^{(0)} + \frac{\lambda_1}{4} b^{(0)} \right) e^{x + X_i - X_{i+1}} \\ &\quad + 12^{1/4} \left(-a_i^{(1)} - \frac{\lambda_1 x}{2} b^{(0)} + \frac{\lambda_1}{4} b^{(0)} \right) e^{-x}, \end{aligned}$$

giving the matching condition

$$f_3 G^2 \sim 12^{1/4} \left(a_{i+1}^{(1)} + \frac{\lambda_1 (x + X_i - X_{i+1})}{2} b^{(0)} + \frac{\lambda_1}{4} b^{(0)} \right) e^{x + X_i - X_{i+1}}, \quad (D20)$$

as $x \rightarrow \infty$ on the inner solution.

5. Solvability condition on f_3

The matching conditions (D19), (D20) give

$$\begin{aligned}
G^2 \left[\frac{df_3}{dx} V_0 - f_3 \frac{dV_0}{dx} \right]_{-R}^R &= 2\sqrt{3} \left(2a_{i+1}^{(1)} + \lambda_1(1 + R + X_i - X_{i+1})b^{(0)} \right) e^{X_i - X_{i+1}} \\
&\quad - 2\sqrt{3} \left(2a_{i-1}^{(1)} + \lambda_1(-1 - R + X_i - X_{i-1})b^{(0)} \right) e^{-X_i + X_{i-1}} \\
G^2 \left[\frac{df_3}{dx} \frac{dV_0}{dx} - f_3 \frac{d^2V_0}{dx^2} \right]_{-R}^R &= -2\sqrt{3} \left(2a_{i+1}^{(1)} + \lambda_1(1 + R + X_i - X_{i+1})b^{(0)} \right) e^{X_i - X_{i+1}} \\
&\quad - 2\sqrt{3} \left(2a_{i-1}^{(1)} + \lambda_1(-1 - R + X_i - X_{i-1})b^{(0)} \right) e^{-X_i + X_{i-1}}.
\end{aligned}$$

The solvability conditions (D13), (D14), (D15), (D16) then give

$$\begin{aligned}
&\frac{\sqrt{3}\pi a_i^{(1)}(\lambda_1^2 - 1)}{8} + a_i^{(1)} \left[\frac{d^2V_1}{dx^2} \frac{dV_0}{dx} - \frac{dV_1}{dx} \frac{d^2V_0}{dx^2} \right]_{-R}^R \\
&+ \lambda_1 b^{(0)} \int_{-R}^R \left(V_1 \frac{dV_0}{dx} - \left(\frac{xX_i}{2} + 20V_1V_0^3 \right) \left(\frac{V_0}{4} + \frac{x}{2} \frac{dV_0}{dx} \right) \frac{dV_0}{dx} \right) dx \\
&= -2\sqrt{3} \left(2a_{i+1}^{(1)} + \lambda_1(1 + R + X_i - X_{i+1})b^{(0)} \right) \frac{e^{X_i - X_{i+1}}}{G^2} \\
&\quad - 2\sqrt{3} \left(2a_{i-1}^{(1)} + \lambda_1(-1 - R + X_i - X_{i-1})b^{(0)} \right) \frac{e^{-X_i + X_{i-1}}}{G^2}. \quad (D21)
\end{aligned}$$

We show in §G that the terms proportional to R vanish as they should, and (D21) simplifies to

$$\begin{aligned}
&\frac{\pi a_i^{(1)}(\lambda_1^2 - 1)}{32} + (a_{i+1}^{(1)} - a_i^{(1)}) \frac{e^{X_i - X_{i+1}}}{G^2} + (a_{i-1}^{(1)} - a_i^{(1)}) \frac{e^{-X_i + X_{i-1}}}{G^2} \\
&= \frac{3\pi}{64} \lambda_1 b^{(0)} X_i - \frac{\lambda_1 b^{(0)}}{2} (X_i - X_{i+1}) \frac{e^{X_i - X_{i+1}}}{G^2} - \frac{\lambda_1 b^{(0)}}{2} (X_i - X_{i-1}) \frac{e^{-X_i + X_{i-1}}}{G^2}. \quad (D22)
\end{aligned}$$

Equation (D22) is equation (80) from the main text. When $b^{(0)}$ is non-zero it gives $a_i^{(1)}$ in terms of $b^{(0)}$, with no restriction on λ_1 . To determine λ_1 we need to go to one more order.

6. $O(G^4)$ terms in the inner expansion

At $O(G^4)$ in the inner expansion near hump i we find

$$f_4 = a_i^{(3)}U_1 + a_i^{(1)}U_3 + b_i^{(4)}W_0 + b_i^{(2)}W_2 + b_i^{(0)}W_4,$$

where

$$\begin{aligned}
&\frac{d^2U_3}{dx^2} + V_0^4(2U_3^* + 3U_3) - U_3 = -i\lambda_1 U_2^R - \lambda_1 \lambda_2 x V_0 - i\lambda_3 V_0' + \frac{i\lambda_1 x(x + X_i)^2}{8} V_0 + 2i\lambda_1 x V_1 V_0^4, \\
&\frac{d^2W_4}{dx^2} + V_0^4(2W_4^* + 3W_4) - W_4 = -i\lambda_1 \left(W_3^R - i\lambda_1 \lambda_2 \frac{x^2 V_0}{4} \right) - i\lambda_2 \left(-\frac{i\lambda_1^2 x^2 V_0}{8} + iV_1 + \lambda_2 \left(\frac{V_0}{4} + \frac{x}{2} \frac{dV_0}{dx} \right) \right) \\
&\quad - i\lambda_3 \lambda_1 \left(\frac{V_0}{4} + \frac{x}{2} \frac{dV_0}{dx} \right) + \lambda_4 V_0 - \frac{(x + X_i)^2}{4} \left(-\frac{i\lambda_1^2 x^2 V_0}{8} + iV_1 + \lambda_2 \left(\frac{V_0}{4} + \frac{x}{2} \frac{dV_0}{dx} \right) \right) \\
&\quad - 4V_1 V_0^3 \left(-\frac{i\lambda_1^2 x^2 V_0}{8} + iV_1 + 5\lambda_2 \left(\frac{V_0}{4} + \frac{x}{2} \frac{dV_0}{dx} \right) \right) - 2V_0^2(3V_1^2 + 2V_0 V_2)iV_0.
\end{aligned}$$

The relevant solvability conditions are

$$\text{Im} \left[\frac{dU_3}{dx} V_0 - U_3 \frac{dV_0}{dx} \right]_{-R}^R = \int_{-R}^R \left(-\lambda_1 U_2^R V_0 + \frac{\lambda_1}{4} x^2 X_i V_0^2 + 2\lambda_1 x V_1 V_0^5 \right) dx, \quad (\text{D23})$$

$$\begin{aligned} \text{Im} \left[\frac{dW_4}{dx} V_0 - W_4 \frac{dV_0}{dx} \right]_{-R}^R &= - \int_{-R}^R \left(\lambda_1 W_3^R V_0 + \left(\frac{(x + X_i)^2 V_0}{4} + 4V_1 V_0^4 \right) \left(V_1 - \frac{\lambda_1^2 x^2 V_0}{8} \right) \right. \\ &\quad \left. + 2V_0^4 (3V_1^2 + 2V_0 V_2) \right) dx. \end{aligned} \quad (\text{D24})$$

7. $O(G^2)$ terms in the outer expansion

At $O(G^2)$ in the outer

$$i\lambda_1 f_1 + i\lambda_2 f_0 + \frac{d^2 f_2}{d\xi^2} - f_2 = -\frac{\xi^2 f_0}{4}.$$

Matching with (D11), (D12) gives the solution as

$$\begin{aligned} f_2 &= 12^{1/4} b_i^{(2)} i e^{-\xi + X_i} - 12^{1/4} a_i^{(1)} \frac{i\lambda_1 (\xi - X_i)}{2} e^{-\xi + X_i} - b^{(0)} \frac{i\lambda_1^2 (\xi - X_i)^2}{8} 12^{1/4} e^{-\xi + X_i} \\ &\quad + 12^{1/4} i b^{(0)} \frac{X_i}{16} e^{-\xi + X_i} (2(\xi - X_i)^2 + 2(\xi - X_i) - 2 \log 2 + 1) + 12^{1/4} i b^{(0)} \frac{e^{X_i - X_{i+1}}}{G^2} e^{\xi - X_i} \\ &\quad + 12^{1/4} i b^{(0)} (\alpha_0 + \alpha_1 (\xi - X_i) + \alpha_2 (\xi - X_i)^2 + \alpha_3 (\xi - X_i)^3) e^{-\xi + X_i} - i \frac{X_i^2}{16} 12^{1/4} b^{(0)} (1 - 2(\xi - X_i)) e^{-\xi + X_i} \\ &\quad + \frac{\lambda_2}{4} 12^{1/4} b^{(0)} (1 - 2(\xi - X_i)) e^{-\xi + X_i} \\ &\quad + 12^{1/4} b_{i+1}^{(2)} i e^{\xi - X_{i+1}} - 12^{1/4} a_{i+1}^{(1)} \frac{i\lambda_1 (\xi - X_{i+1})}{2} e^{\xi - X_{i+1}} - \frac{i\lambda_1^2 (\xi - X_{i+1})^2}{8} 12^{1/4} b^{(0)} e^{\xi - X_{i+1}} \\ &\quad + 12^{1/4} b^{(0)} i \frac{X_{i+1}}{16} e^{\xi - X_{i+1}} (-2(\xi - X_{i+1})^2 + 2(\xi - X_{i+1}) + 2 \log 2 - 1) + 12^{1/4} b^{(0)} i \frac{e^{X_{i-1} - X_i}}{G^2} e^{-\xi + X_{i+1}} \\ &\quad + 12^{1/4} b^{(0)} i (\alpha_0 - \alpha_1 (\xi - X_{i+1}) + \alpha_2 (\xi - X_{i+1})^2 - \alpha_3 (\xi - X_{i+1})^3) e^{\xi - X_{i+1}} - b^{(0)} i \frac{X_{i+1}^2}{16} 12^{1/4} (1 + 2(\xi - X_{i+1})) e^{\xi - X_{i+1}} \\ &\quad + \frac{\lambda_2}{4} 12^{1/4} b^{(0)} (1 + 2(\xi - X_{i+1})) e^{\xi - X_{i+1}}. \end{aligned} \quad (\text{D25})$$

This then gives the matching conditions

$$\begin{aligned} G^2 f_4 &\sim 12^{1/4} b_{i-1}^{(2)} i e^{-x - X_i + X_{i-1}} - 12^{1/4} a_{i-1}^{(1)} \frac{i\lambda_1 (x + X_i - X_{i-1})}{2} e^{-x - X_i + X_{i-1}} \\ &\quad - b^{(0)} \frac{i\lambda_1^2 (x + X_i - X_{i-1})^2}{8} 12^{1/4} e^{-x - X_i + X_{i-1}} \\ &\quad + 12^{1/4} i b^{(0)} \frac{X_{i-1}}{16} e^{-x - X_i + X_{i-1}} (2(x + X_i - X_{i-1})^2 + 2(x + X_i - X_{i-1}) - 2 \log 2 + 1) \\ &\quad + 12^{1/4} i b^{(0)} (\alpha_0 + \alpha_1 (x + X_i - X_{i-1}) + \alpha_2 (x + X_i - X_{i-1})^2 + \alpha_3 (x + X_i - X_{i-1})^3) e^{-x - X_i + X_{i-1}} \\ &\quad - i \frac{X_{i-1}^2}{16} 12^{1/4} b^{(0)} (1 - 2(x + X_i - X_{i-1})) e^{-x - X_i + X_{i-1}} \\ &\quad + \frac{\lambda_2}{4} 12^{1/4} b^{(0)} (1 - 2(x + X_i - X_{i-1})) e^{-x - X_i + X_{i-1}} \quad \text{as } x \rightarrow -\infty \end{aligned} \quad (\text{D26})$$

$$\begin{aligned}
G^2 f_4 \sim & 12^{1/4} b_{i+1}^{(2)} i e^{x+X_i-X_{i+1}} - 12^{1/4} a_{i+1}^{(1)} \frac{i \lambda_1 (x + X_i - X_{i+1})}{2} e^{x+X_i-X_{i+1}} \\
& - \frac{i \lambda_1^2 (x + X_i - X_{i+1})^2}{8} 12^{1/4} b^{(0)} e^{x+X_i-X_{i+1}} \\
& + 12^{1/4} b^{(0)} i \frac{X_{i+1}}{16} e^{x+X_i-X_{i+1}} (-2(x + X_i - X_{i+1})^2 + 2(x + X_i - X_{i+1}) + 2 \log 2 - 1) \\
& + 12^{1/4} b^{(0)} i (\alpha_0 - \alpha_1(x + X_i - X_{i+1}) + \alpha_2(x + X_i - X_{i+1})^2 - \alpha_3(x + X_i - X_{i+1})^3) e^{x+X_i-X_{i+1}} \\
& - b^{(0)} i \frac{X_{i+1}^2}{16} 12^{1/4} (1 + 2(x + X_i - X_{i+1})) e^{x+X_i-X_{i+1}} \\
& + \frac{\lambda_2}{4} 12^{1/4} b^{(0)} (1 + 2(x + X_i - X_{i+1})) e^{x+X_i-X_{i+1}} \quad \text{as } x \rightarrow \infty. \quad (D27)
\end{aligned}$$

on the inner solution near hump i .

8. Final solvability condition

We have, from (D23), (D24)

$$\begin{aligned}
\text{Im} \left[\frac{df_4}{dx} V_0 - f_4 \frac{dV_0}{dx} \right]_{-R}^R &= a_i^{(1)} \int_{-R}^R \left(-\lambda_1 U_2^R V_0 + \frac{\lambda_1}{4} x^2 X_i V_0^2 + 2\lambda_1 x V_1 V_0^5 \right) dx \\
&- b^{(0)} \int_{-R}^R \left(\lambda_1 W_3^R V_0 + \left(\frac{(x + X_i)^2 V_0}{4} + 4V_1 V_0^4 \right) \left(V_1 - \frac{\lambda_1^2 x^2 V_0}{8} \right) + 2V_0^4 (3V_1^2 + 2V_0 V_2) \right) dx \\
&+ b_i^{(2)} \left(\frac{4\sqrt{3}}{G^2} e^{-X_{i+1}+X_i} + \frac{4\sqrt{3}}{G^2} e^{-X_i+X_{i-1}} \right) \quad (D28)
\end{aligned}$$

Evaluating the LHS by matching using (D26), (D27) gives

$$\begin{aligned}
\text{Im} \left[\frac{df_4}{dx} V_0 - f_4 \frac{dV_0}{dx} \right]_{-R}^R &= \frac{4\sqrt{3}}{G^2} e^{X_i-X_{i+1}} b_{i+1}^{(2)} - \frac{\sqrt{3}}{G^2} e^{X_i-X_{i+1}} \lambda_1 a_{i+1}^{(1)} (1 + 2R + 2X_i - 2X_{i+1}) \\
&- \frac{b^{(0)}}{32\sqrt{3}G^2} e^{X_i-X_{i+1}} (\pi^2 + 48\lambda_1^2 R + 48\lambda^2 R^2 + 16R^3 + 48(\lambda_1^2 + R)X_i^2 \\
&\quad + 16X_i^3 - 48(\lambda_1^2 + 2\lambda_1^2 R + \log 2)X_{i+1} + 48(1 + \lambda_1^2)X_{i+1}^2 - 16X_{i+1}^3 \\
&\quad + 48X_i(\lambda_1^2 + 2\lambda_1^2 R + R^2 - 2\lambda_1^2 X_{i+1})) \\
&+ \frac{4\sqrt{3}}{G^2} e^{X_{i-1}-X_i} b_{i-1}^{(2)} - \frac{\sqrt{3}}{G^2} e^{X_{i-1}-X_i} \lambda_1 a_{i-1}^{(1)} (-1 - 2R - 2X_{i-1} + 2X_i) \\
&- \frac{b^{(0)}}{32\sqrt{3}G^2} e^{X_{i-1}-X_i} (\pi^2 + 48\lambda_1^2 R + 48\lambda_1^2 R^2 + 16R^3 + 48(1 + \lambda_1^2)X_{i-1}^2 \\
&\quad + 16X_{i-1}^3 - 48(R^2 + \lambda_1^2(1 + 2R))X_i + 48(\lambda_1^2 + R)X_i^2 - 16X_i^3 \\
&\quad - 48X_{i-1}(\lambda_1^2(-1 - 2R) - \log 2 + 2\lambda_1^2 X_i)) .
\end{aligned}$$

We show in §H that all the terms in R cancel as they should, and (D28) simplifies to

$$\begin{aligned}
& \frac{b^{(0)}\lambda_1^2(\lambda_1^2 - 4)\pi^3}{512} + \frac{3\pi\lambda_1 X_i}{64}(b^{(0)}\lambda_1 X_i - 2a_i^{(1)}) \\
& + 4(b_{i+1}^{(2)} - b_i^{(2)})\frac{e^{X_i - X_{i+1}}}{G^2} + 4(b_{i-1}^{(2)} - b_i^{(2)})\frac{e^{X_{i-1} - X_i}}{G^2} \\
& + 2a_{i+1}^{(1)}(X_{i+1} - X_i)\lambda_1\frac{e^{X_i - X_{i+1}}}{G^2} + 2a_{i-1}^{(1)}(X_{i-1} - X_i)\lambda_1\frac{e^{X_{i-1} - X_i}}{G^2} \\
& - 3a_{i+1}^{(1)}\lambda_1\frac{e^{X_i - X_{i+1}}}{G^2} + 3a_{i-1}^{(1)}\lambda_1\frac{e^{X_{i-1} - X_i}}{G^2} \\
& + \frac{\lambda_1^2}{2}b^{(0)}\frac{e^{X_i - X_{i+1}}}{G^2}(-X_i^2 + 3X_{i+1} + 2X_i X_{i+1} - X_{i+1}^2) \\
& + \frac{\lambda_1^2}{2}b^{(0)}\frac{e^{X_{i-1} - X_i}}{G^2}(-X_i^2 - 3X_{i-1} + 2X_i X_{i-1} - X_{i-1}^2) = 0. \quad (\text{D29})
\end{aligned}$$

Equation (D29) is equation (81) from the main text. The sum over i is the equation which determines λ_1 .

Appendix E: Analysis of V_1

We have equation (27), which we restate for convenience

$$\frac{d^2 V_1}{dx^2} + 5V_0^4 V_1 - V_1 = -\frac{(x + X_i)^2 V_0}{4}. \quad (\text{E1})$$

The exponential growth of V_1 at infinity arises due to the term proportional to xV_0 on the RHS, which is not orthogonal to dV_0/dx . We divide V_1 into terms forced by the odd and even components on the RHS by setting

$$V_1 = V_o + V_e,$$

where

$$\frac{d^2 V_o}{dx^2} + 5V_0^4 V_o - V_o = -\frac{xX_i V_0}{2}, \quad (\text{E2})$$

$$\frac{d^2 V_e}{dx^2} + 5V_0^4 V_e - V_e = -\frac{(x^2 + X_i^2)V_0}{4}, \quad (\text{E3})$$

and $V_e \rightarrow 0$ as $x \rightarrow \pm\infty$. Note that V_e is even but this last boundary condition means that V_o is not odd but has an even component (which satisfies the homogeneous equation).

Since the homogeneous version of (E1) has linearly independent solutions

$$v_1 = \frac{\sinh(2\xi)}{\cosh^{3/2}(2\xi)}, \quad v_2 = \frac{\cosh(4\xi) - 3}{\cosh^{3/2}(2\xi)}, \quad (\text{E4})$$

the general solution of (E2) may be written as

$$V_o = \frac{X_i}{2} \frac{v_1(x)}{4} \int_a^x v_2(\bar{x}) \bar{x} V_0(\bar{x}) d\bar{x} - \frac{X_i}{2} \frac{v_2(x)}{4} \int_b^x v_1(\bar{x}) \bar{x} V_0(\bar{x}) d\bar{x},$$

for some constants a and b . Varying the constant a corresponds to translating the position of the inner region. To fix it we need to be more specific about how the X_i are defined. If we define X_i to be the position of the local maximum of the modulus of V , then we have $dV/d\xi = 0$ at $\xi = X_i$, so that in the inner

coordinate $dV/dx = 0$ at $x = 0$. This fixes $a = 0$. To determine b we use the matching conditions (D9), (D10), which give

$$V_o \sim 12^{1/4} \frac{e^{x+X_i-X_{i+1}}}{G^2} \quad \text{as } x \rightarrow \infty, \quad V_o \sim 12^{1/4} \frac{e^{-x+X_{i-1}-X_i}}{G^2} \quad \text{as } x \rightarrow -\infty.$$

We can set $b = -\infty$ if we add on the multiple of $v'_2(x)$ we expect there. This gives

$$\begin{aligned} V_o &= \frac{X_i}{2} \frac{v_1(x)}{4} \int_0^x v_2(\bar{x}) \bar{x} V_0(\bar{x}) d\bar{x} - \frac{X_i}{2} \frac{v_2(x)}{4} \int_{-\infty}^x v_1(\bar{x}) \bar{x} V_0(\bar{x}) d\bar{x} + 3^{1/4} \frac{e^{X_{i-1}-X_i}}{G^2} v_2(x) \\ &= 3^{1/4} \frac{X_i}{2} \frac{v_1(x)}{4} (\log(1 + e^{4x}) + x^2 - 2x - 2x \tanh 2x - \log 2) \\ &\quad + \frac{3^{1/4}}{4} \frac{X_i}{2} \frac{v_2(x)}{4} (2x \operatorname{sech} 2x - \sin^{-1} \operatorname{sech} 2x) + 3^{1/4} \frac{e^{X_{i-1}-X_i}}{G^2} v_2(x). \end{aligned} \quad (\text{E5})$$

Note the branch of \sin^{-1} is such that

$$\sin^{-1} \operatorname{sech} 2x = \begin{cases} \sin^{-1} \operatorname{sech} 2x & x < 0, \\ \pi - \sin^{-1} \operatorname{sech} 2x & x > 0. \end{cases}$$

The odd part of (E5) is

$$\begin{aligned} V_{\text{odd}} &= 3^{1/4} \frac{X_i}{2} \frac{v_1(x)}{4} (\log(1 + e^{4x}) + x^2 - 2x - 2x \tanh 2x - \log 2) \\ &\quad + \frac{3^{1/4}}{4} \frac{X_i}{2} \frac{v_2(x)}{4} \left(2x \operatorname{sech} 2x + \frac{\pi}{2} - \sin^{-1} \operatorname{sech} 2x \right) \end{aligned} \quad (\text{E6})$$

leaving an even multiple of v_2 ,

$$V_o^e = 3^{1/4} \left(-\frac{X_i \pi}{64} + \frac{e^{X_{i-1}-X_i}}{G^2} \right) v_2(x) = \frac{3^{1/4}}{2} \left(\frac{e^{X_i-X_{i+1}}}{G^2} + \frac{e^{X_{i-1}-X_i}}{G^2} \right) v_2(x).$$

As $x \rightarrow -\infty$,

$$V_o \sim 3^{1/4} \frac{X_i}{16} \sqrt{2} e^x (-2x^2 + 2x + 2 \log 2 - 1) + 3^{1/4} \frac{e^{X_{i-1}-X_i}}{G^2} \sqrt{2} e^{-x}, \quad (\text{E7})$$

while as $x \rightarrow \infty$,

$$V_o \sim 3^{1/4} \frac{X_i}{16} \sqrt{2} e^{-x} (2x^2 + 2x - 2 \log 2 + 1) + 3^{1/4} \sqrt{2} \frac{e^{X_i-X_{i+1}}}{G^2} e^x, \quad (\text{E8})$$

where we have used (31) to simplify. Let us now turn to (E3). The solution may be written

$$V_e = \hat{V}_1 - \frac{X_i^2}{4} \left(\frac{V_0}{4} + \frac{x}{2} \frac{dV_0}{dx} \right),$$

where

$$\hat{V}_1(x) = v_1(x) \int_0^x \frac{v_2(\bar{x}) \bar{x}^2 V_0(\bar{x}) d\bar{x}}{16} + v_2(x) \int_{\bar{x}}^{\infty} \frac{v_1(\bar{x}) \bar{x}^2 V_0(\bar{x}) d\bar{x}}{16},$$

is the perturbation to the single hump solution (i.e. without the change of origin). As $x \rightarrow \infty$,

$$\hat{V}_1 \sim 12^{1/4} (\alpha_0 + \alpha_1 x + \alpha_2 x^2 + \alpha_3 x^3) e^{-x},$$

with

$$\alpha_0 = \frac{1}{32} \left(1 - \frac{\pi^2}{12} \right), \quad \alpha_1 = \frac{1}{16}, \quad \alpha_2 = \frac{1}{16}, \quad \alpha_3 = \frac{1}{24}. \quad (\text{E9})$$

Since \hat{V}_1 is even, as $x \rightarrow -\infty$,

$$\hat{V}_1 \sim 12^{1/4}(\alpha_0 - \alpha_1 x + \alpha_2 x^2 - \alpha_3 x^3)e^x.$$

Thus

$$V_e \sim 12^{1/4}(\alpha_0 + \alpha_1 x + \alpha_2 x^2 + \alpha_3 x^3)e^{-x} - \frac{X_i^2}{16} 3^{1/4} \sqrt{2} (1 - 2x) e^{-x} \quad \text{as } x \rightarrow \infty, \quad (\text{E10})$$

$$V_e \sim 12^{1/4}(\alpha_0 - \alpha_1 x + \alpha_2 x^2 - \alpha_3 x^3)e^x - \frac{X_i^2}{16} 3^{1/4} \sqrt{2} (1 + 2x) e^x \quad \text{as } x \rightarrow -\infty. \quad (\text{E11})$$

Together (E7), (E8), (E10), and (E11) give (D9) and (D10).

PGK: here there is a citation missing.

Appendix F: Analysis of V_2

If we proceed to $O(G^4)$ in the local analysis of §IV A, §IV C we find the equation for V_2 is

$$\frac{d^2 V_2}{dx^2} + 5V_0^4 V_2 - V_2 = -\frac{(x + X_i)^2 V_1}{4} - 10V_0^3 V_1^2.$$

Multiplying by V_0 and integrating gives

$$\begin{aligned} -\int_{-R}^R \frac{(x + X_i)^2 V_1 V_0}{4} + 10V_0^4 V_1^2 dx &= \int_{-R}^R V_0 \left(\frac{d^2 V_2}{dx^2} + 5V_0^4 V_2 - V_2 \right) dx \\ &= \int_{-R}^R \left(V_2 \frac{d^2 V_0}{dx^2} + 5V_0^5 V_2 - V_0 V_2 \right) dx + \left[V_0 \frac{dV_2}{dx} - V_2 \frac{dV_0}{dx} \right]_{-R}^R \\ &= \int_{-R}^R 4V_0^5 V_2 dx + \left[V_0 \frac{dV_2}{dx} - V_2 \frac{dV_0}{dx} \right]_{-R}^R \end{aligned}$$

Thus

$$\int_{-R}^R 4V_0^5 V_2 + 10V_0^4 V_1^2 + \frac{(x + X_i)^2 V_1 V_0}{4} dx = - \left[V_0 \frac{dV_2}{dx} - V_2 \frac{dV_0}{dx} \right]_{-R}^R. \quad (\text{F1})$$

To evaluate the right-hand side we need to go to one more term in the outer region between humps than we did in §IV B. Equating coefficients of G^2 in the region between humps gives

$$\frac{d^2 V_1}{d\xi^2} - V_1 = -\frac{\xi^2}{4} V_0 = -\frac{12^{1/4} \xi^2}{4} (e^{-\xi + X_i} + e^{\xi - X_{i+1}}). \quad (\text{F2})$$

Thus

$$V_1 = 12^{1/4} \left(C_1 - \frac{\xi}{16} + \frac{\xi^2}{16} - \frac{\xi^3}{24} \right) e^{\xi - X_{i+1}} + 12^{1/4} \left(C_2 + \frac{\xi}{16} + \frac{\xi^2}{16} + \frac{\xi^3}{24} \right) e^{-\xi + X_i}. \quad (\text{F3})$$

The coefficients C_1 and C_2 are determined by matching with the subdominant exponentials in the inner solution V_1 . As $x \rightarrow -\infty$ in the inner solution, from (E7), (E11),

$$\begin{aligned} V_1 &\sim 3^{1/4} \frac{X_i}{16} \sqrt{2} e^x (-2x^2 + 2x + 2 \log 2 - 1) + 3^{1/4} \frac{e^{X_{i-1} - X_i}}{G^2} \sqrt{2} e^{-x} \\ &\quad + 12^{1/4} (\alpha_0 - \alpha_1 x + \alpha_2 x^2 - \alpha_3 x^3) e^x - \frac{X_i^2}{16} 3^{1/4} \sqrt{2} (1 + 2x) e^x. \end{aligned}$$

With $x = \xi - X_{i+1}$ (and $i \rightarrow i + 1$) this is

$$V_1 \sim 3^{1/4} \frac{X_{i+1}}{16} \sqrt{2} e^{\xi - X_{i+1}} (-2(\xi - X_{i+1})^2 + 2(\xi - X_{i+1}) + 2 \log 2 - 1) + 3^{1/4} \frac{e^{X_i - X_{i+1}}}{G^2} \sqrt{2} e^{-(\xi - X_{i+1})} \\ + 12^{1/4} (\alpha_0 - \alpha_1(\xi - X_{i+1}) + \alpha_2(\xi - X_{i+1})^2 - \alpha_3(\xi - X_{i+1})^3) e^{\xi - X_{i+1}} - \frac{X_{i+1}^2}{16} 3^{1/4} \sqrt{2} (1 + 2(\xi - X_{i+1})) e^{\xi - X_{i+1}}.$$

Removing the terms which match with V_0 in the outer leaves

$$V_1 \sim 12^{1/4} e^{\xi - X_{i+1}} \left(\frac{X_{i+1}}{16} (-2(\xi - X_{i+1})^2 + 2(\xi - X_{i+1}) + 2 \log 2 - 1) \right. \\ \left. + (\alpha_0 - \alpha_1(\xi - X_{i+1}) + \alpha_2(\xi - X_{i+1})^2 - \alpha_3(\xi - X_{i+1})^3) - \frac{X_{i+1}^2}{16} (1 + 2(\xi - X_{i+1})) \right) \\ \sim 12^{1/4} e^{\xi - X_{i+1}} \left(\frac{1}{32} \left(1 - \frac{\pi^2}{12} \right) - \frac{\xi}{16} + \frac{\xi^2}{16} - \frac{\xi^3}{24} - \frac{X_{i+1}^2}{8} + \frac{X_{i+1}^3}{24} + \frac{X_{i+1} \log 2}{8} \right).$$

Thus

$$C_1 = \frac{1}{32} \left(1 - \frac{\pi^2}{12} \right) - \frac{X_{i+1}^2}{8} + \frac{X_{i+1}^3}{24} + \frac{X_{i+1} \log 2}{8}.$$

As $x \rightarrow \infty$ in the inner solution, from (E8), (E10),

$$V_1 \sim 3^{1/4} \frac{X_i}{16} \sqrt{2} e^{-x} (2x^2 + 2x - 2 \log 2 + 1) + 3^{1/4} \sqrt{2} \frac{e^{X_i - X_{i+1}}}{G^2} e^x \\ + 12^{1/4} (\alpha_0 + \alpha_1 x + \alpha_2 x^2 + \alpha_3 x^3) e^{-x} - \frac{X_i^2}{16} 3^{1/4} \sqrt{2} (1 - 2x) e^{-x}.$$

With $x = \xi - X_i$ this is

$$V_1 \sim 3^{1/4} \frac{X_i}{16} \sqrt{2} e^{-(\xi - X_i)} (2(\xi - X_i)^2 + 2(\xi - X_i) - 2 \log 2 + 1) + 3^{1/4} \sqrt{2} \frac{e^{X_i - X_{i+1}}}{G^2} e^{(\xi - X_i)} \\ + 12^{1/4} (\alpha_0 + \alpha_1(\xi - X_i) + \alpha_2(\xi - X_i)^2 + \alpha_3(\xi - X_i)^3) e^{-(\xi - X_i)} \\ - \frac{X_i^2}{16} 3^{1/4} \sqrt{2} (1 - 2(\xi - X_i)) e^{-(\xi - X_i)}.$$

Removing the terms which match with V_0 in the outer leaves

$$V_1 \sim 12^{1/4} e^{-(\xi - X_i)} \left(\frac{X_i}{16} (2(\xi - X_i)^2 + 2(\xi - X_i) - 2 \log 2 + 1) \right. \\ \left. + (\alpha_0 + \alpha_1(\xi - X_i) + \alpha_2(\xi - X_i)^2 + \alpha_3(\xi - X_i)^3) - \frac{X_i^2}{16} (1 - 2(\xi - X_i)) \right) \\ \sim 12^{1/4} e^{-\xi + X_i} \left(\frac{1}{32} \left(1 - \frac{\pi^2}{12} \right) + \frac{\xi}{16} + \frac{\xi^2}{16} + \frac{\xi^3}{24} - \frac{X_i^2}{8} - \frac{X_i^3}{24} - \frac{X_i \log 2}{8} \right).$$

Thus

$$C_2 = \frac{1}{32} \left(1 - \frac{\pi^2}{12} \right) - \frac{X_i^2}{8} - \frac{X_i^3}{24} - \frac{X_i \log 2}{8}.$$

Thus the outer solution for V_1 when $X_i < \xi < X_{i+1}$ is

$$V_1 = 12^{1/4} e^{-\xi + X_i} \left(\frac{1}{32} \left(1 - \frac{\pi^2}{12} \right) + \frac{\xi}{16} + \frac{\xi^2}{16} + \frac{\xi^3}{24} - \frac{X_i^2}{8} - \frac{X_i^3}{24} - \frac{X_i \log 2}{8} \right) \\ + 12^{1/4} e^{\xi - X_{i+1}} \left(\frac{1}{32} \left(1 - \frac{\pi^2}{12} \right) - \frac{\xi}{16} + \frac{\xi^2}{16} - \frac{\xi^3}{24} - \frac{X_{i+1}^2}{8} + \frac{X_{i+1}^3}{24} + \frac{X_{i+1} \log 2}{8} \right). \quad (\text{F4})$$

Thus the matching condition on V_2 is

$$\begin{aligned}
G^2 V_2 &\sim 12^{1/4} e^{x+X_i-X_{i+1}} \left(\frac{1}{32} \left(1 - \frac{\pi^2}{12} \right) - \frac{x+X_i}{16} + \frac{(x+X_i)^2}{16} - \frac{(x+X_i)^3}{24} - \frac{X_{i+1}^2}{8} + \frac{X_{i+1}^3}{24} + \frac{X_{i+1} \log 2}{8} \right) \\
&\sim 12^{1/4} e^{x+X_i-X_{i+1}} \left(\frac{1}{32} \left(1 - \frac{\pi^2}{12} \right) + \frac{x(-1+2X_i-2X_i^2)}{16} + \frac{x^2(1-2X_i)}{16} - \frac{x^3}{24} \right. \\
&\quad \left. - \frac{X_i}{16} + \frac{X_i^2}{16} - \frac{X_i^3}{24} - \frac{X_{i+1}^2}{8} + \frac{X_{i+1}^3}{24} + \frac{X_{i+1} \log 2}{8} \right),
\end{aligned}$$

as $x \rightarrow \infty$, and

$$\begin{aligned}
G^2 V_2 &\sim 12^{1/4} e^{-(x+X_i)+X_{i-1}} \left(\frac{1}{32} \left(1 - \frac{\pi^2}{12} \right) + \frac{(x+X_i)}{16} + \frac{(x+X_i)^2}{16} + \frac{(x+X_i)^3}{24} - \frac{X_{i-1}^2}{8} - \frac{X_{i-1}^3}{24} - \frac{X_{i-1} \log 2}{8} \right) \\
&\sim 12^{1/4} e^{-x-X_i+X_{i-1}} \left(\frac{1}{32} \left(1 - \frac{\pi^2}{12} \right) + \frac{x(1+2X_i+2X_i^2)}{16} + \frac{x^2(1+2X_i)}{16} + \frac{x^3}{24} \right. \\
&\quad \left. + \frac{X_i}{16} + \frac{X_i^2}{16} + \frac{X_i^3}{24} - \frac{X_{i-1}^2}{8} - \frac{X_{i-1}^3}{24} - \frac{X_{i-1} \log 2}{8} \right),
\end{aligned}$$

as $x \rightarrow -\infty$. Thus, finally,

$$\begin{aligned}
&\left[V_0 \frac{dV_2}{dx} - V_2 \frac{dV_0}{dx} \right]_{-R}^R \\
&= \frac{\sqrt{3}}{96} e^{X_i-X_{i+1}} \left(-\pi^2 - 16R^3 - 48X_i R^2 - 48X_i^2 R - 16X_i^3 - 48X_{i+1}^2 + 16X_{i+1}^3 + 48 \log 2 X_{i+1} \right) \\
&+ \frac{\sqrt{3}}{96} e^{-X_i+X_{i-1}} \left(-\pi^2 - 16R^3 + 48X_i R^2 - 48X_i^2 R + 16X_i^3 - 48X_{i-1}^2 - 16X_{i-1}^3 - 48 \log 2 X_{i-1} \right). \quad (\text{F5})
\end{aligned}$$

Appendix G: Derivation of (D22)

The solvability condition (D21) involves the integral

$$\begin{aligned}
\lim_{R \rightarrow \infty} \int_{-R}^R \left(V_1 \frac{dV_0}{dx} - \left(\frac{xX_i}{2} + 20V_1 V_0^3 \right) \left(\frac{V_0}{4} + \frac{x}{2} \frac{dV_0}{dx} \right) \frac{dV_0}{dx} \right) dx \\
= -\frac{\sqrt{3}\pi^3 X_i}{256} + \lim_{R \rightarrow \infty} \int_{-R}^R V_{\text{odd}} \left(\frac{dV_0}{dx} - 20V_0^3 \left(\frac{V_0}{4} + \frac{x}{2} \frac{dV_0}{dx} \right) \frac{dV_0}{dx} \right) dx
\end{aligned}$$

where we have used the fact that

$$\int_{-\infty}^{\infty} \frac{x}{2} \left(\frac{V_0}{4} + \frac{x}{2} \frac{dV_0}{dx} \right) \frac{dV_0}{dx} dx = \frac{\sqrt{3}\pi^3}{256},$$

and that only the odd part of V_1 contributes to the integral. Using (E6) we find numerically that

$$\int_{-\infty}^{\infty} 20V_{\text{odd}} V_0^3 \left(\frac{V_0}{4} + \frac{x}{2} \frac{dV_0}{dx} \right) \frac{dV_0}{dx} dx \approx -0.0731175 X_i.$$

Thus we are left with evaluating

$$\int_{-R}^R V_{\text{odd}} \frac{dV_0}{dx} dx.$$

Now

$$\int_{-R}^x v_2(\bar{x}) V_0'(\bar{x}) d\bar{x} = -3^{1/4} (\log \cosh 2x + \operatorname{sech}^2 2x).$$

Thus, integrating by parts,

$$\begin{aligned} \lim_{R \rightarrow \infty} \int_{-R}^R v_2(\bar{x}) V_0'(\bar{x}) 3^{1/4} \frac{X_i}{32} \left(2\bar{x} \operatorname{sech} 2\bar{x} + \frac{\pi}{2} - \sin^{-1} \operatorname{sech} 2\bar{x} \right) d\bar{x} \\ = \sqrt{3} \lim_{R \rightarrow \infty} \left[-(\log \cosh 2x + \operatorname{sech}^2 2x) \frac{X_i}{32} \left(2x \operatorname{sech} 2x + \frac{\pi}{2} - \sin^{-1} \operatorname{sech} 2x \right) \right]_{-R}^R \\ + \frac{\sqrt{3} X_i}{32} \int_{-\infty}^{\infty} (\log \cosh 2\bar{x} + \operatorname{sech}^2 2\bar{x}) (-4\bar{x} \operatorname{sech} 2\bar{x} \tanh 2\bar{x}) d\bar{x} \\ = \sqrt{3} (2R - \log 2) \frac{X_i \pi}{32} - 0.31625 X_i, \end{aligned}$$

where we have used the fact that

$$\frac{\sqrt{3}}{32} \int_{-\infty}^{\infty} (\log \cosh 2\bar{x} + \operatorname{sech}^2 2\bar{x}) (-4\bar{x} \operatorname{sech} 2\bar{x} \tanh 2\bar{x}) d\bar{x} \approx -0.31625.$$

Since, numerically,

$$\int_{-\infty}^{\infty} \frac{3^{1/4}}{8} V_0'(x) v_1(x) (\log(1 + e^{4x}) + x^2 - 2x - 2x \tanh 2x - \log 2) dx \approx -0.109394,$$

we have

$$\lim_{R \rightarrow \infty} \int_{-R}^R V_{\text{odd}} \frac{dV_0}{dx} dx = \sqrt{3} (2R - \log 2) \frac{X_i \pi}{32} - 0.425644 X_i. \quad (\text{G1})$$

Thus, finally,

$$\begin{aligned} \lim_{R \rightarrow \infty} \int_{-R}^R \left(V_1 \frac{dV_0}{dx} - \left(\frac{x X_i}{2} + 20 V_1 V_0^3 \right) \left(\frac{V_0}{4} + \frac{x}{2} \frac{dV_0}{dx} \right) \frac{dV_0}{dx} \right) dx \\ = -\frac{\sqrt{3} \pi^3 X_i}{256} + 0.0731175 X_i + \sqrt{3} (2R - \log 2) \frac{X_i \pi}{32} - 0.425644 X_i \\ = \frac{\sqrt{3} R \pi X_i}{16} - 0.680174 X_i. \end{aligned} \quad (\text{G2})$$

Using (G2) and (65) in (D21) gives

$$\begin{aligned} \frac{\sqrt{3} \pi a_i^{(1)} (\lambda_1^2 - 1)}{8} + a_i^{(1)} \left(-\frac{4\sqrt{3}}{G^2} e^{-X_{i+1} + X_i} - \frac{4\sqrt{3}}{G^2} e^{-X_i + X_{i-1}} \right) + \lambda_1 b^{(0)} \left(\frac{\sqrt{3} R \pi X_i}{16} - 0.680174 X_i \right) \\ = -2\sqrt{3} \left(2a_{i+1}^{(1)} + \lambda_1 (1 + R + X_i - X_{i+1}) b^{(0)} \right) \frac{e^{X_i - X_{i+1}}}{G^2} \\ - 2\sqrt{3} \left(2a_{i-1}^{(1)} + \lambda_1 (-1 - R + X_i - X_{i-1}) b^{(0)} \right) \frac{e^{-X_i + X_{i-1}}}{G^2}. \end{aligned}$$

Using (31) the terms proportional to R cancel as they should, leaving

$$\begin{aligned} \frac{\sqrt{3} \pi a_i^{(1)} (\lambda_1^2 - 1)}{8} + 4\sqrt{3} (a_{i+1}^{(1)} - a_i^{(1)}) \frac{e^{X_i - X_{i+1}}}{G^2} + 4\sqrt{3} (a_{i-1}^{(1)} - a_i^{(1)}) \frac{e^{-X_i + X_{i-1}}}{G^2} \\ = 1.02026 \lambda_1 b^{(0)} X_i - 2\sqrt{3} \lambda_1 b^{(0)} \left((X_i - X_{i+1}) \frac{e^{X_i - X_{i+1}}}{G^2} + (X_i - X_{i-1}) \frac{e^{-X_i + X_{i-1}}}{G^2} \right). \end{aligned}$$

Dividing by $4\sqrt{3}$ gives

$$\begin{aligned} & \frac{\pi a_i^{(1)}(\lambda_1^2 - 1)}{32} + (a_{i+1}^{(1)} - a_i^{(1)}) \frac{e^{X_i - X_{i+1}}}{G^2} + (a_{i-1}^{(1)} - a_i^{(1)}) \frac{e^{-X_i + X_{i-1}}}{G^2} \\ &= 0.147262 \lambda_1 b^{(0)} X_i - \frac{\lambda_1 b^{(0)}}{2} \left((X_i - X_{i+1}) \frac{e^{X_i - X_{i+1}}}{G^2} + (X_i - X_{i-1}) \frac{e^{-X_i + X_{i-1}}}{G^2} \right). \end{aligned} \quad (\text{G3})$$

We can check our analysis, and identify the constant 0.147262, by considering the exact eigenfunction corresponding to $\lambda = 2G$. For this eigenfunction

$$f = iV_s + G \left(\frac{V_s}{2} + \xi \frac{dV_s}{d\xi} - \frac{iG\xi V_s}{2} \right)$$

so that with $\xi = x + X_i$,

$$f = iV_0 + G \left(\frac{V_0}{2} + (x + X_i) \frac{dV_0}{d\xi} \right) + iG^2 \left(V_1 - \frac{(x + X_i)V_0}{2} \right) + G^3 \left(\frac{V_1}{2} + \xi \frac{dV_1}{d\xi} \right) + \dots$$

Comparing to our expansion, with $b^{(0)} = 1$, and $\lambda_1 = 2$,

$$f = iV_0 + G \left(a_i^{(1)} \frac{dV_0}{dx} + \frac{V_0}{2} + x \frac{dV_0}{dx} \right) + iG^2 \left(-a_i^{(1)} x V_0 + b_i^{(2)} V_0 - \frac{x^2 V_0}{2} + V_1 \right) + G^3 (\dots)$$

we have

$$a_i^{(1)} = X_i, \quad b_i^{(2)} = -\frac{X_i^2}{2}.$$

Substituting this into (G3) gives

$$\begin{aligned} & \frac{3\pi X_i}{32} + (X_{i+1} - X_i) \frac{e^{X_i - X_{i+1}}}{G^2} + (X_{i-1} - X_i) \frac{e^{-X_i + X_{i-1}}}{G^2} \\ &= 2 \times 0.147262 X_i - \left((X_i - X_{i+1}) \frac{e^{X_i - X_{i+1}}}{G^2} + (X_i - X_{i-1}) \frac{e^{-X_i + X_{i-1}}}{G^2} \right). \end{aligned} \quad (\text{G4})$$

This identifies the constant as

$$0.147262 = \frac{3\pi}{64}, \quad (\text{G5})$$

so that (G3) becomes (D22).

Appendix H: Derivation of (D29)

Let us evaluate the integrals on the right-hand side of (D28), namely

$$I_1 = \lim_{R \rightarrow \infty} \int_{-R}^R \left(-\lambda_1 U_2^R V_0 + \frac{\lambda_1}{4} x^2 X_i V_0^2 + 2\lambda_1 x V_1 V_0^5 \right) dx \quad (\text{H1})$$

and

$$I_2 = - \lim_{R \rightarrow \infty} \int_{-R}^R \lambda_1 W_3^R V_0 + \left(\frac{(x + X_i)^2 V_0}{4} + 4V_1 V_0^4 \right) \left(V_1 - \frac{\lambda_1^2 x^2 V_0}{8} \right) + 2V_0^4 (3V_1^2 + 2V_0 V_2) dx. \quad (\text{H2})$$

For (H1) we require the odd part of V_1 . Using (E6) gives, numerically

$$\int_{-\infty}^{\infty} \left(\frac{\lambda_1}{4} x^2 X_i V_0^2 + 2\lambda_1 x V_1 V_0^5 \right) dx \approx 0.373466\lambda_1 X_i. \quad (\text{H3})$$

From (F1) we have

$$\int_{-R}^R 4V_0^5 V_2 + 10V_0^4 V_1^2 + \frac{(x + X_i)^2 V_1 V_0}{4} dx = - \left[V_0 \frac{dV_2}{dx} - V_2 \frac{dV_0}{dx} \right]_{-R}^R. \quad (\text{H4})$$

so that (H2) is

$$I_2 = \left[V_0 \frac{dV_2}{dx} - V_2 \frac{dV_0}{dx} \right]_{-R}^R - \int_{-R}^R \lambda_1 W_3^R V_0 + \left(\frac{(x + X_i)^2 V_0}{4} + 4V_1 V_0^4 \right) \left(-\frac{\lambda_1^2 x^2 V_0}{8} \right) dx \quad (\text{H5})$$

Also

$$\int_{-\infty}^{\infty} \frac{(x + X_i)^2 V_0}{4} \left(-\frac{\lambda_1^2 x^2 V_0}{8} \right) dx = -\lambda_1^2 \frac{\sqrt{3} \pi^3 (5\pi^2 + 16X_i^2)}{16384}, \quad (\text{H6})$$

$$\int_{-\infty}^{\infty} 4V_1 V_0^4 \left(-\frac{\lambda_1^2 x^2 V_0}{8} \right) dx = -\frac{\lambda_1^2}{2} \int_{-\infty}^{\infty} x^2 V_{\text{even}} V_0^5 dx, \quad (\text{H7})$$

where

$$V_{\text{even}} = \frac{3^{1/4}}{2} \left(\frac{e^{X_i - X_{i+1}}}{G^2} + \frac{e^{X_{i-1} - X_i}}{G^2} \right) v_2(x) + \hat{V}_1(x) - \frac{X_i^2}{4} \left(\frac{V_0}{4} + \frac{x}{2} \frac{dV_0}{dx} \right). \quad (\text{H8})$$

Since

$$\begin{aligned} \int_{-\infty}^{\infty} v_2(x) x^2 V_0(x)^5 dx &= \frac{3^{1/4}(24 - \pi^2)}{24}, \\ \int_{-\infty}^{\infty} \hat{V}_1(x) x^2 V_0(x)^5 dx &\approx 0.0227007, \\ \int_{-\infty}^{\infty} \left(\frac{V_0}{4} + \frac{x}{2} \frac{dV_0}{dx} \right) x^2 V_0(x)^5 dx &= 0, \end{aligned}$$

$$-\frac{\lambda_1^2}{2} \int_{-\infty}^{\infty} x^2 V_{\text{even}} V_0^5 dx = -\lambda_1^2 \left(\frac{\sqrt{3}(24 - \pi^2)}{96} \left(\frac{e^{X_i - X_{i+1}}}{G^2} + \frac{e^{X_{i-1} - X_i}}{G^2} \right) + 0.0113504 \right). \quad (\text{H9})$$

Collecting all this together gives

$$I_1 = -\lambda_1 \lim_{R \rightarrow \infty} \int_{-R}^R U_2^R V_0 dx + 0.373466\lambda_1 X_i, \quad (\text{H10})$$

$$\begin{aligned} I_2 &= -\lambda_1 \int_{-R}^R W_3^R V_0 dx + \left[V_0 \frac{dV_2}{dx} - V_2 \frac{dV_0}{dx} \right]_{-R}^R + \lambda_1^2 \frac{\sqrt{3} \pi^3 (5\pi^2 + 16X_i^2)}{16384} \\ &\quad + \lambda_1^2 \left(\frac{\sqrt{3}(24 - \pi^2)}{96} \left(\frac{e^{X_i - X_{i+1}}}{G^2} + \frac{e^{X_{i-1} - X_i}}{G^2} \right) + 0.0113504 \right). \end{aligned} \quad (\text{H11})$$

The term in square brackets involving V_0 and V_2 is evaluated in §F and given by (F5). We are left with the integrals involving U_2^R and W_3^R .

1. Analysis of U_2^R and W_3^R

Differentiating (27) gives

$$\frac{d^3 V_1}{dx^3} + 5V_0^4 \frac{dV_1}{dx} - \frac{dV_1}{dx} = -20V_0^3 V_1 \frac{dV_0}{dx} - \frac{(x + X_i)V_0}{2} - \frac{(x + X_i)^2}{4} \frac{dV_0}{dx}.$$

Thus, recalling (D17), (D18) we may write

$$U_2^R = \frac{dV_1}{dx} + U, \quad (H12)$$

$$W_3^R = \lambda_1 \left(\frac{V_1}{4} + \frac{x}{2} \frac{dV_1}{dx} \right) + W, \quad (H13)$$

where

$$\begin{aligned} \frac{d^2 U}{dx^2} + 5V_0^4 U - U &= \frac{(1 - \lambda_1^2)}{2} x V_0 + \frac{X_i}{2} V_0, \\ \frac{d^2 W}{dx^2} + 5V_0^4 W - W &= \frac{\lambda_1(2x^2 + 3xX_i + X_i^2)}{4} V_0 - \frac{\lambda_1^3 x^2}{8} V_0. \end{aligned}$$

Integrating by parts

$$\int_{-R}^R \frac{dV_1}{dx} V_0 dx = [V_1 V_0]_{-R}^R - \int_{-R}^R V_1 \frac{dV_0}{dx} dx = [V_1 V_0]_{-R}^R - \int_{-R}^R V_{\text{odd}} \frac{dV_0}{dx} dx, \quad (H14)$$

where we evaluated the final integral already in (G1). Note that

$$[V_1 V_0]_{-R}^R = 2\sqrt{3} \frac{e^{X_i - X_{i+1}}}{G^2} - 2\sqrt{3} \frac{e^{-X_i + X_{i-1}}}{G^2} = -\frac{\sqrt{3} \pi X_i}{16}. \quad (H15)$$

Also

$$\int_{-R}^R \left(\frac{V_1}{4} + \frac{x}{2} \frac{dV_1}{dx} \right) V_0 dx = \int_{-R}^R \left(\frac{V_{\text{even}}}{4} + \frac{x}{2} \frac{dV_{\text{even}}}{dx} \right) V_0 dx,$$

where V_{even} is given by (H8). Since

$$\begin{aligned} \lim_{R \rightarrow \infty} \int_{-R}^R \left(\frac{v_2}{4} + \frac{x}{2} \frac{dv_2}{dx} \right) V_0 dx &= 3^{1/4} \left(\frac{1}{2} - \frac{\pi^2}{48} + R^2 + R \right), \\ \int_{-\infty}^{\infty} \left(\frac{\hat{V}_1}{4} + \frac{x}{2} \frac{d\hat{V}_1}{dx} \right) V_0 dx &\approx 0.173106, \\ \int_{-\infty}^{\infty} V_0 \left(\frac{1}{4} + \frac{x}{2} \frac{d}{dx} \right)^2 V_0 dx &= -\frac{\sqrt{3} \pi^3}{256}, \end{aligned}$$

we find

$$\begin{aligned} \lim_{R \rightarrow \infty} \int_{-R}^R \left(\frac{V_1}{4} + \frac{x}{2} \frac{dV_1}{dx} \right) V_0 dx &= \frac{\sqrt{3}}{2} \left(\frac{e^{X_i - X_{i+1}}}{G^2} + \frac{e^{X_{i-1} - X_i}}{G^2} \right) \left(\frac{1}{2} - \frac{\pi^2}{48} + R^2 + R \right) \\ &\quad + 0.173106 + \frac{\sqrt{3} \pi^3}{1024} X_i^2. \end{aligned} \quad (H16)$$

This leaves us just with the integrals involving U and W . To determine U and W we will need to match with the solution in between the humps, which means we have to reintroduce the constant multipliers. The actual term in the integral (D28) is

$$I_3 = \lim_{R \rightarrow \infty} \int_{-R}^R a_i^{(1)} U + b^{(0)} W dx. \quad (H17)$$

The general solution to

$$\frac{d^2 f}{dx^2} + 5V_0^4 f - f = g,$$

is

$$f = -\frac{v_1(x)}{4} \int_a^x v_2(\bar{x})g(\bar{x}) d\bar{x} + \frac{v_2(x)}{4} \int_b^x v_1(\bar{x})g(\bar{x}) d\bar{x},$$

where v_1 and v_2 are the homogeneous solutions given by (E4). With $f = U$, we have

$$g = g_U = \frac{(1 - \lambda_1^2)}{2} x V_0 + \frac{X_i}{2} V_0,$$

while with $f = W$, we have

$$g = g_W = \frac{\lambda_1(2x^2 + 3xX_i + X_i^2)}{4} V_0 - \frac{\lambda_1^3 x^2}{8} V_0.$$

Note that

$$\begin{aligned} \int_a^x V_0(\bar{x})v_1(\bar{x}) d\bar{x} &= -\frac{V_0(x)^2}{2 \times 3^{1/4}}, \\ \int_b^x V_0(\bar{x})v_2(\bar{x}) d\bar{x} &= 2 \times 3^{1/4}(x - \tanh 2x). \end{aligned}$$

Then, integrating by parts,

$$\begin{aligned} \lim_{R \rightarrow \infty} \int_{-R}^R f V_0 dx &= \frac{1}{4 \times 3^{1/4}} \lim_{R \rightarrow \infty} \int_{-R}^R V_0(x) V_0'(x) \int_a^x v_2(\bar{x})g(\bar{x}) d\bar{x} dx \\ &\quad - \frac{1}{4 \times 3^{1/4}} \lim_{R \rightarrow \infty} \int_{-R}^R V_0(x) v_2(x) \int_b^x V_0'(\bar{x})g(\bar{x}) d\bar{x} dx \\ &= \frac{1}{4 \times 3^{1/4}} \lim_{R \rightarrow \infty} \left[\frac{V_0(x)^2}{2} \int_a^x v_2(\bar{x})g(\bar{x}) d\bar{x} \right]_{-R}^R - \frac{1}{4 \times 3^{1/4}} \lim_{R \rightarrow \infty} \int_{-R}^R \frac{V_0(x)^2}{2} v_2(x)g(x) dx \\ &\quad - \frac{1}{2} \lim_{R \rightarrow \infty} \left[(x - \tanh 2x) \int_b^x V_0'(\bar{x})g(\bar{x}) d\bar{x} \right]_{-R}^R + \frac{1}{2} \lim_{R \rightarrow \infty} \int_{-R}^R (x - \tanh 2x) V_0'(x)g(x) dx \\ &= -\frac{1}{4 \times 3^{1/4}} \int_{-\infty}^{\infty} \frac{V_0(x)^2}{2} v_2(x)g(x) dx - \frac{1}{2} (R-1) \int_b^{\infty} V_0'(\bar{x})g(\bar{x}) d\bar{x} \\ &\quad - \frac{1}{2} (R-1) \int_b^{-\infty} V_0'(\bar{x})g(\bar{x}) d\bar{x} + \frac{1}{2} \int_{-\infty}^{\infty} (x - \tanh 2x) V_0'(x)g(x) dx. \end{aligned}$$

Evaluating the full range integrals we find

$$\begin{aligned} \int_{-\infty}^{\infty} V_0(x)^2 v_2(x) g_U(x) dx &= 0, \\ \int_{-\infty}^{\infty} (x - \tanh 2x) V_0'(x) g_U(x) dx &= 0, \\ \int_{-\infty}^{\infty} V_0(x)^2 v_2(x) g_W(x) dx &= \frac{\lambda_1(4 - \lambda_1^2)}{8} \frac{3^{3/4} \pi}{2}, \\ \int_{-\infty}^{\infty} (x - \tanh 2x) V_0'(x) g_W(x) dx &= \frac{\lambda_1(4 - \lambda_1^2)}{8} \frac{\sqrt{3} \pi (4 - \pi^2)}{32}. \end{aligned}$$

Thus

$$\lim_{R \rightarrow \infty} \int_{-R}^R UV_0 = -\frac{1}{2}(R-1) \int_b^\infty V_0'(\bar{x}) g_U(\bar{x}) d\bar{x} - \frac{1}{2}(R-1) \int_b^{-\infty} V_0'(\bar{x}) g_U(\bar{x}) d\bar{x}, \quad (\text{H18})$$

$$\begin{aligned} \lim_{R \rightarrow \infty} \int_{-R}^R WV_0 &= -\frac{1}{2}(R-1) \int_b^\infty V_0'(\bar{x}) g_W(\bar{x}) d\bar{x} \\ &\quad - \frac{1}{2}(R-1) \int_b^{-\infty} V_0'(\bar{x}) g_W(\bar{x}) d\bar{x} - \frac{\sqrt{3} \pi^3 \lambda_1 (4 - \lambda_1^2)}{512}. \end{aligned} \quad (\text{H19})$$

To evaluate the remainging integrals we need to determine b using the matching conditions (D19), (D20) on f_3 , which give

$$\begin{aligned} (a_i^{(1)} U_2 + b^{(0)} W_3) G^2 &\sim 12^{1/4} \left(-a_{i-1}^{(1)} - \frac{\lambda_1(x + X_i - X_{i-1})}{2} b^{(0)} + \frac{\lambda_1}{4} b^{(0)} \right) e^{-x - X_i + X_{i-1}} \quad \text{as } x \rightarrow -\infty, \\ (a_i^{(1)} U_2 + b^{(0)} W_3) G^2 &\sim 12^{1/4} \left(a_{i+1}^{(1)} + \frac{\lambda_1(x + X_i - X_{i+1})}{2} b^{(0)} + \frac{\lambda_1}{4} b^{(0)} \right) e^{x + X_i - X_{i+1}} \quad \text{as } x \rightarrow \infty. \end{aligned}$$

Using (D10), (D9), (H12), (H13), gives the matching conditions

$$\begin{aligned} a_i^{(1)} U + b^{(0)} W &\sim 12^{1/4} \left(a_i^{(1)} - a_{i-1}^{(1)} - \frac{\lambda_1(X_i - X_{i-1})}{2} b^{(0)} \right) \frac{e^{-x - X_i + X_{i-1}}}{G^2} \quad \text{as } x \rightarrow -\infty, \\ a_i^{(1)} U + b^{(0)} W &\sim 12^{1/4} \left(-a_i^{(1)} + a_{i+1}^{(1)} + \frac{\lambda_1(X_i - X_{i+1})}{2} b^{(0)} \right) \frac{e^{x + X_i - X_{i+1}}}{G^2} \quad \text{as } x \rightarrow \infty. \end{aligned}$$

We can satisfy the conditions at $-\infty$ by setting $b = -\infty$ in both U and W and adding an appropriate multiple of v_2 corresponding to the matching condition. Since

$$v_2 \sim \sqrt{2} e^{-x} \text{ as } x \rightarrow -\infty,$$

this multiple is

$$3^{1/4} \left(a_i^{(1)} - a_{i-1}^{(1)} - \frac{\lambda_1(X_i - X_{i-1})}{2} b^{(0)} \right) \frac{e^{-X_i + X_{i-1}}}{G^2} v_2(x). \quad (\text{H20})$$

As a check, at infinity then

$$\begin{aligned} a_i^{(1)} U + b^{(0)} W &\sim 3^{1/4} \left(a_i^{(1)} - a_{i-1}^{(1)} - \frac{\lambda_1(X_i - X_{i-1})}{2} b^{(0)} \right) \frac{e^{-X_i + X_{i-1}}}{G^2} v_2(x) \\ &\quad + \frac{v_2}{4} \int_{-\infty}^\infty v_1(\bar{x}) \left(a_i^{(1)} g_U + b^{(0)} g_W \right) d\bar{x} \\ &= 3^{1/4} \left(a_i^{(1)} - a_{i-1}^{(1)} - \frac{\lambda_1(X_i - X_{i-1})}{2} b^{(0)} \right) \frac{e^{-X_i + X_{i-1}}}{G^2} v_2(x) \\ &\quad - \frac{v_2}{4 \times 3^{1/4}} \left(a_i^{(1)} \frac{(1 - \lambda_1^2)}{2} + b^{(0)} \frac{\lambda_1 3 X_i}{4} \right) \int_{-\infty}^\infty V_0'(\bar{x}) \bar{x} V_0(\bar{x}) d\bar{x} \\ &= 12^{1/4} \left(a_i^{(1)} - a_{i-1}^{(1)} - \frac{\lambda_1(X_i - X_{i-1})}{2} b^{(0)} \right) \frac{e^{-X_i + X_{i-1}}}{G^2} e^x \\ &\quad + 12^{1/4} \pi \left(a_i^{(1)} \frac{(1 - \lambda_1^2)}{32} + b^{(0)} \frac{\lambda_1 3 X_i}{64} \right) e^x \\ &= 12^{1/4} \left(a_{i+1}^{(1)} - a_i^{(1)} + \frac{\lambda_1(X_i - X_{i+1})}{2} b^{(0)} \right) \frac{e^{x + X_i - X_{i+1}}}{G^2} \end{aligned}$$

as required, using (D22) (which also provides proof of (G5)). With $b = -\infty$ we have two further integrals to evaluate. We have

$$\begin{aligned} -\frac{1}{2}(R-1) \int_{-\infty}^{\infty} V_0'(a_i^{(1)} g_U + b^{(0)} g_W) dx &= -\frac{1}{2}(R-1) \left(a_i^{(1)} \frac{(1-\lambda_1^2)}{2} + b^{(0)} \frac{3\lambda_1 X_i}{4} \right) \int_{-\infty}^{\infty} V_0' x V_0 dx \\ &= \frac{1}{2}(R-1) \left(a_i^{(1)} \frac{(1-\lambda_1^2)}{2} + b^{(0)} \frac{3\lambda_1 X_i}{4} \right) \frac{\sqrt{3}\pi}{4} \end{aligned} \quad (\text{H21})$$

and we also need the integral of the extra term (H20),

$$\begin{aligned} 3^{1/4} \left(a_i^{(1)} - a_{i-1}^{(1)} - \frac{\lambda_1(X_i - X_{i-1})}{2} b^{(0)} \right) \frac{e^{-X_i+X_{i-1}}}{G^2} \int_{-R}^R v_2 V_0 dx \\ = 4\sqrt{3} \left(a_i^{(1)} - a_{i-1}^{(1)} - \frac{\lambda_1(X_i - X_{i-1})}{2} b^{(0)} \right) \frac{e^{-X_i+X_{i-1}}}{G^2} (R-1). \end{aligned} \quad (\text{H22})$$

Collecting together the results of this section we have, using (H12), (H15), and (G1),

$$\lim_{R \rightarrow \infty} \int_{-R}^R U_2^R V_0 dx = -\frac{\sqrt{3} R X_i \pi}{16} + 0.203422 X_i + \lim_{R \rightarrow \infty} \int_{-R}^R U V_0 dx \quad (\text{H23})$$

since

$$-\sqrt{3} \frac{X_i \pi}{16} + \frac{\sqrt{3} \pi \log 2}{32} + 0.425644 \approx 0.203422.$$

Using (H13), (H16),

$$\begin{aligned} \lim_{R \rightarrow \infty} \int_{-R}^R W_3^R V_0 dx &= \frac{\sqrt{3} \lambda_1}{2} \left(\frac{e^{X_i-X_{i+1}}}{G^2} + \frac{e^{X_{i-1}-X_i}}{G^2} \right) \left(\frac{1}{2} - \frac{\pi^2}{48} + R^2 + R \right) \\ &\quad + 0.173106 \lambda_1 + \frac{\sqrt{3} \pi^3 \lambda_1}{1024} X_i^2 + \lim_{R \rightarrow \infty} \int_{-R}^R W V_0 dx. \end{aligned} \quad (\text{H24})$$

Using (H18), (H19), (H21), (H22),

$$\begin{aligned} \int_{-R}^R (a_i^{(1)} U + b^{(0)} W) V_0 dx &= -b^{(0)} \lambda_1 (4 - \lambda_1^2) \frac{\sqrt{3} \pi^3}{512} \\ &\quad + (R-1) \left(a_i^{(1)} \frac{(1-\lambda_1^2)}{16} + b^{(0)} \frac{3\lambda_1 X_i}{32} \right) \sqrt{3} \pi \\ &\quad + 4\sqrt{3} \left(a_i^{(1)} - a_{i-1}^{(1)} - \frac{\lambda_1(X_i - X_{i-1})}{2} b^{(0)} \right) \frac{e^{-X_i+X_{i-1}}}{G^2} (R-1) \\ &= -b^{(0)} \lambda_1 (4 - \lambda_1^2) \frac{\sqrt{3} \pi^3}{512} \\ &\quad + \sqrt{3} (R-1) \left(\lambda_1 b^{(0)} (X_i - X_{i+1}) \frac{e^{X_i-X_{i+1}}}{G^2} - \lambda_1 b^{(0)} (X_i - X_{i-1}) \frac{e^{-X_i+X_{i-1}}}{G^2} \right) \\ &\quad + \sqrt{3} (R-1) \left(2(a_{i+1}^{(1)} - a_i^{(1)}) \frac{e^{X_i-X_{i+1}}}{G^2} - 2(a_{i-1}^{(1)} - a_i^{(1)}) \frac{e^{-X_i+X_{i-1}}}{G^2} \right) \end{aligned} \quad (\text{H25})$$

using (D22).

2. Putting it all together

Using (H10), (H11), (F5), (H23), (H24) and (H25) in (D28) gives, after some simplification,

$$\begin{aligned}
\text{Im} \left[\frac{df_4}{dx} V_0 - f_4 \frac{dV_0}{dx} \right]_{-R}^R &= 0.170044 a_i^{(1)} \lambda_1 X_i + \frac{\sqrt{3} a_i^{(1)} R \lambda_1 X_i \pi}{16} + b^{(0)} \lambda_1^2 (4 - \lambda_1^2) \frac{\sqrt{3} \pi^3}{512} \\
&\quad - \sqrt{3} (R-1) \lambda_1^2 \left(b^{(0)} (X_i - X_{i+1}) \frac{e^{X_i - X_{i+1}}}{G^2} - b^{(0)} (X_i - X_{i-1}) \frac{e^{-X_i + X_{i-1}}}{G^2} \right) \\
&\quad - 2\sqrt{3} (R-1) \lambda_1 \left((a_{i+1}^{(1)} - a_i^{(1)}) \frac{e^{X_i - X_{i+1}}}{G^2} - (a_{i-1}^{(1)} - a_i^{(1)}) \frac{e^{-X_i + X_{i-1}}}{G^2} \right) \\
&\quad - b^{(0)} \lambda_1^2 \frac{\sqrt{3}}{2} \left(\frac{e^{X_i - X_{i+1}}}{G^2} + \frac{e^{X_{i-1} - X_i}}{G^2} \right) (R^2 + R) \\
&\quad + b^{(0)} \frac{\sqrt{3}}{96} e^{X_i - X_{i+1}} (-\pi^2 - 16R^3 - 48X_i R^2 - 48X_i^2 R - 16X_i^3 - 48X_{i+1}^2 + 16X_{i+1}^3 + 48 \log 2 X_{i+1}) \\
&\quad + b^{(0)} \frac{\sqrt{3}}{96} e^{-X_i + X_{i-1}} (-\pi^2 - 16R^3 + 48X_i R^2 - 48X_i^2 R + 16X_i^3 - 48X_{i-1}^2 - 16X_{i-1}^3 - 48 \log 2 X_{i-1}) \\
&\quad + b_i^{(2)} \left(\frac{4\sqrt{3}}{G^2} e^{-X_{i+1} + X_i} + \frac{4\sqrt{3}}{G^2} e^{-X_i + X_{i-1}} \right)
\end{aligned}$$

where we have set

$$0.173106 - 0.0113504 = \frac{5\sqrt{3} \pi^5}{16384}.$$

Thus the final solvability condition is

$$\begin{aligned}
& \frac{4\sqrt{3}}{G^2} e^{X_i - X_{i+1}} b_{i+1}^{(2)} - \frac{\sqrt{3}}{G^2} e^{X_i - X_{i+1}} \lambda_1 a_{i+1}^{(1)} (1 + 2R + 2X_i - 2X_{i+1}) \\
& - \frac{b^{(0)}}{32\sqrt{3}G^2} e^{X_i - X_{i+1}} (\pi^2 + 48\lambda_1^2 R + 48\lambda_1^2 R^2 + 16R^3 + 48(\lambda_1^2 + R)X_i^2 + 16X_i^3 \\
& \quad - 48(\lambda_1^2 + 2\lambda_1^2 R + \log 2)X_{i+1} + 48(1 + \lambda_1^2)X_{i+1}^2 \\
& \quad - 16X_{i+1}^3 + 48X_i(\lambda_1^2 + 2\lambda_1^2 R + R^2 - 2\lambda_1^2 X_{i+1})) \\
& + \frac{4\sqrt{3}}{G^2} e^{X_{i-1} - X_i} b_{i-1}^{(2)} - \frac{\sqrt{3}}{G^2} e^{X_{i-1} - X_i} \lambda_1 a_{i-1}^{(1)} (-1 - 2R - 2X_{i-1} + 2X_i) \\
& - \frac{b^{(0)}}{32\sqrt{3}G^2} e^{X_{i-1} - X_i} (\pi^2 + 48\lambda_1^2 R + 48\lambda_1^2 R^2 + 16R^3 + 48(1 + \lambda_1^2)X_{i-1}^2 \\
& \quad + 16X_{i-1}^3 - 48(R^2 + \lambda_1^2(1 + 2R))X_i + 48(\lambda_1^2 + R)X_i^2 \\
& \quad - 16X_i^3 - 48X_{i-1}(\lambda_1^2(-1 - 2R) - \log 2 + 2\lambda_1^2 X_i)) \\
& = 0.170044 a_i^{(1)} \lambda_1 X_i + \frac{\sqrt{3} a_i^{(1)} R \lambda_1 X_i \pi}{16} + b^{(0)} \lambda_1^2 (4 - \lambda_1^2) \frac{\sqrt{3} \pi^3}{512} \\
& - \sqrt{3} (R - 1) \lambda_1^2 \left(b^{(0)} (X_i - X_{i+1}) \frac{e^{X_i - X_{i+1}}}{G^2} - b^{(0)} (X_i - X_{i-1}) \frac{e^{-X_i + X_{i-1}}}{G^2} \right) \\
& - 2\sqrt{3} (R - 1) \lambda_1 \left((a_{i+1}^{(1)} - a_i^{(1)}) \frac{e^{X_i - X_{i+1}}}{G^2} - (a_{i-1}^{(1)} - a_i^{(1)}) \frac{e^{-X_i + X_{i-1}}}{G^2} \right) \\
& \quad - b^{(0)} \lambda_1^2 \frac{\sqrt{3}}{2} \left(\frac{e^{X_i - X_{i+1}}}{G^2} + \frac{e^{X_{i-1} - X_i}}{G^2} \right) (R^2 + R) \\
& + b^{(0)} \frac{\sqrt{3}}{96} e^{X_i - X_{i+1}} (-\pi^2 - 16R^3 - 48X_i R^2 - 48X_i^2 R - 16X_i^3 \\
& \quad - 48X_{i+1}^2 + 16X_{i+1}^3 + 48 \log 2 X_{i+1}) \\
& + b^{(0)} \frac{\sqrt{3}}{96} e^{-X_i + X_{i-1}} (-\pi^2 - 16R^3 + 48X_i R^2 - 48X_i^2 R + 16X_i^3 \\
& \quad - 48X_{i-1}^2 - 16X_{i-1}^3 - 48 \log 2 X_{i-1}) \\
& \quad + b_i^{(2)} \left(\frac{4\sqrt{3}}{G^2} e^{-X_{i+1} + X_i} + \frac{4\sqrt{3}}{G^2} e^{-X_i + X_{i-1}} \right).
\end{aligned}$$

The terms proportional to R^3 are

$$- \frac{b^{(0)}}{32\sqrt{3}} \frac{e^{X_i - X_{i+1}}}{G^2} 16R^3 - \frac{b^{(0)}}{32\sqrt{3}} \frac{e^{X_{i-1} - X_i}}{G^2} 16R^3 = - \frac{b^{(0)}\sqrt{3}}{96} \frac{e^{X_i - X_{i+1}}}{G^2} 16R^3 - \frac{b^{(0)}\sqrt{3}}{96} \frac{e^{X_{i-1} - X_i}}{G^2} 16R^3$$

These cancel as they should. The terms proportional to R^2 are

$$\begin{aligned}
& - \frac{b^{(0)}}{32\sqrt{3}} \frac{e^{X_i - X_{i+1}}}{G^2} (48\lambda_1^2 R^2 + 48X_i R^2) - \frac{b^{(0)}}{32\sqrt{3}} \frac{e^{X_{i-1} - X_i}}{G^2} (48\lambda_1^2 R^2 - 48X_i R^2) \\
& = -b^{(0)} \frac{\sqrt{3}\lambda_1^2}{2} \left(\frac{e^{X_i - X_{i+1}}}{G^2} + \frac{e^{X_{i-1} - X_i}}{G^2} \right) R^2 \\
& \quad + \frac{b^{(0)}\sqrt{3}}{96} \frac{e^{X_i - X_{i+1}}}{G^2} (-48X_i R^2) + \frac{b^{(0)}\sqrt{3}}{96} \frac{e^{X_{i-1} - X_i}}{G^2} (48X_i R^2)
\end{aligned}$$

These cancel as they should. The terms proportional to R are

$$\begin{aligned}
& -\frac{\sqrt{3}}{G^2} e^{X_i - X_{i+1}} \lambda_1 a_{i+1}^{(1)} 2R - \frac{b^{(0)}}{32\sqrt{3}} \frac{e^{X_i - X_{i+1}}}{G^2} (48\lambda_1^2 R + 48X_i^2 R - 96\lambda_1^2 X_{i+1} R + 96X_i \lambda_1^2 R) \\
& - \frac{\sqrt{3}}{G^2} e^{X_{i-1} - X_i} \lambda_1 a_{i-1}^{(1)} (-2R) - \frac{b^{(0)}}{32\sqrt{3}} \frac{e^{X_{i-1} - X_i}}{G^2} (48\lambda_1^2 R - 96\lambda_1^2 X_i R + 48X_i^2 R + 96X_{i-1} \lambda_1^2 R) \\
& = \lambda_1 a_i^{(1)} \frac{2\sqrt{3} R \pi X_i}{32} - b^{(0)} \frac{\sqrt{3} \lambda_1^2}{2} \left(\frac{e^{X_i - X_{i+1}}}{G^2} + \frac{e^{X_{i-1} - X_i}}{G^2} \right) R \\
& - \sqrt{3} R \lambda_1^2 b^{(0)} \left((X_i - X_{i+1}) \frac{e^{X_i - X_{i+1}}}{G^2} - (X_i - X_{i-1}) \frac{e^{-X_i + X_{i-1}}}{G^2} \right) \\
& - 2\sqrt{3} R \lambda_1 \left((a_{i+1}^{(1)} - a_i^{(1)}) \frac{e^{X_i - X_{i+1}}}{G^2} - (a_{i-1}^{(1)} - a_i^{(1)}) \frac{e^{-X_i + X_{i-1}}}{G^2} \right) \\
& + \frac{b^{(0)} \sqrt{3}}{96} \frac{e^{X_i - X_{i+1}}}{G^2} (-48X_i^2 R) + \frac{b^{(0)} \sqrt{3}}{96} \frac{e^{X_{i-1} - X_i}}{G^2} (-48X_i^2 R)
\end{aligned}$$

These cancel as they should. Thus, finally,

$$\begin{aligned}
& \frac{4\sqrt{3}}{G^2} e^{X_i - X_{i+1}} b_{i+1}^{(2)} - \frac{\sqrt{3}}{G^2} e^{X_i - X_{i+1}} \lambda_1 a_{i+1}^{(1)} (1 + 2X_i - 2X_{i+1}) \\
& - \frac{b^{(0)}}{32\sqrt{3}G^2} e^{X_i - X_{i+1}} (\pi^2 + 48\lambda_1^2 X_i^2 + 16X_i^3 - 48(\lambda_1^2 + \log 2)X_{i+1} + 48(1 + \lambda_1^2)X_{i+1}^2 \\
& \quad - 16X_{i+1}^3 + 48X_i(\lambda_1^2 - 2\lambda_1^2 X_{i+1})) \\
& + \frac{4\sqrt{3}}{G^2} e^{X_{i-1} - X_i} b_{i-1}^{(2)} - \frac{\sqrt{3}}{G^2} e^{X_{i-1} - X_i} \lambda_1 a_{i-1}^{(1)} (-1 - 2X_{i-1} + 2X_i) \\
& - \frac{b^{(0)}}{32\sqrt{3}G^2} e^{X_{i-1} - X_i} (\pi^2 + 48(1 + \lambda_1^2)X_{i-1}^2 + 16X_{i-1}^3 - 48\lambda_1^2 X_i + 48\lambda_1^2 X_i^2 \\
& \quad - 16X_i^3 - 48X_{i-1}(-\lambda_1^2 - \log 2 + 2\lambda_1^2 X_i)) \\
& = 0.170044 a_i^{(1)} \lambda_1 X_i + b^{(0)} \lambda_1^2 (4 - \lambda_1^2) \frac{\sqrt{3} \pi^3}{512} \\
& + \sqrt{3} \lambda_1^2 \left(b^{(0)} (X_i - X_{i+1}) \frac{e^{X_i - X_{i+1}}}{G^2} - b^{(0)} (X_i - X_{i-1}) \frac{e^{-X_i + X_{i-1}}}{G^2} \right) \\
& + 2\sqrt{3} \lambda_1 \left((a_{i+1}^{(1)} - a_i^{(1)}) \frac{e^{X_i - X_{i+1}}}{G^2} - (a_{i-1}^{(1)} - a_i^{(1)}) \frac{e^{-X_i + X_{i-1}}}{G^2} \right) \\
& + b^{(0)} \frac{\sqrt{3}}{96} e^{X_i - X_{i+1}} (-\pi^2 - 16X_i^3 - 48X_{i+1}^2 + 16X_{i+1}^3 + 48 \log 2 X_{i+1}) \\
& + b^{(0)} \frac{\sqrt{3}}{96} e^{-X_i + X_{i-1}} (-\pi^2 + 16X_i^3 - 48X_{i-1}^2 - 16X_{i-1}^3 - 48 \log 2 X_{i-1}) \\
& + b_i^{(2)} \left(\frac{4\sqrt{3}}{G^2} e^{-X_{i+1} + X_i} + \frac{4\sqrt{3}}{G^2} e^{-X_i + X_{i-1}} \right).
\end{aligned}$$

Simplifying gives

$$\begin{aligned}
& -0.170044a_i^{(1)}\lambda_1 X_i + b^{(0)}\lambda_1^2(\lambda_1^2 - 4)\frac{\sqrt{3}\pi^3}{512} \\
& + 4\sqrt{3}(b_{i+1}^{(2)} - b_i^{(2)})\frac{e^{X_i - X_{i+1}}}{G^2} + 4\sqrt{3}(b_{i-1}^{(2)} - b_i^{(2)})\frac{e^{X_{i-1} - X_i}}{G^2} \\
& + 2\sqrt{3}a_{i+1}^{(1)}(X_{i+1} - X_i)\lambda_1\frac{e^{X_i - X_{i+1}}}{G^2} + 2\sqrt{3}a_{i-1}^{(1)}(X_{i-1} - X_i)\lambda_1\frac{e^{X_{i-1} - X_i}}{G^2} \\
& + \sqrt{3}(2a_i^{(1)} - 3a_{i+1}^{(1)})\lambda_1\frac{e^{X_i - X_{i+1}}}{G^2} + \sqrt{3}(-2a_i^{(1)} + 3a_{i-1}^{(1)})\lambda_1\frac{e^{X_{i-1} - X_i}}{G^2} \\
& + \frac{\sqrt{3}}{2}b^{(0)}\frac{e^{X_i - X_{i+1}}}{G^2}(-3\lambda_1^2 X_i - \lambda_1^2 X_i^2 + 3\lambda_1^2 X_{i+1} + 2\lambda_1^2 X_i X_{i+1} - \lambda_1^2 X_{i+1}^2) \\
& + \frac{\sqrt{3}}{2}b^{(0)}\frac{e^{X_{i-1} - X_i}}{G^2}(3\lambda_1^2 X_i - \lambda_1^2 X_i^2 - 3\lambda_1^2 X_{i-1} + 2\lambda_1^2 X_i X_{i-1} - \lambda_1^2 X_{i-1}^2) = 0.
\end{aligned}$$

We can check our analysis and identify the constant 0.170044 using the exact eigenvalue $\lambda_1 = 2$, for which

$$b^{(0)} = 1, \quad a_i^{(1)} = X_i, \quad b_i^{(2)} = -\frac{X_i^2}{2}.$$

Substituting this in and simplifying using (31) gives

$$-0.170044 \times 2X_i^2 + \sqrt{3}X_i^2 \frac{\pi}{16} = 0,$$

so that

$$0.170044 = \frac{\sqrt{3}\pi}{32}.$$

Thus, using (31) again to simplify, the final solvability condition is

$$\begin{aligned}
& \frac{b^{(0)}\lambda_1^2(\lambda_1^2 - 4)\pi^3}{512} + \frac{3\pi\lambda_1 X_i}{64}(b^{(0)}\lambda_1 X_i - 2a_i^{(1)}) \\
& + 4(b_{i+1}^{(2)} - b_i^{(2)})\frac{e^{X_i - X_{i+1}}}{G^2} + 4(b_{i-1}^{(2)} - b_i^{(2)})\frac{e^{X_{i-1} - X_i}}{G^2} \\
& + 2a_{i+1}^{(1)}(X_{i+1} - X_i)\lambda_1\frac{e^{X_i - X_{i+1}}}{G^2} + 2a_{i-1}^{(1)}(X_{i-1} - X_i)\lambda_1\frac{e^{X_{i-1} - X_i}}{G^2} \\
& - 3a_{i+1}^{(1)}\lambda_1\frac{e^{X_i - X_{i+1}}}{G^2} + 3a_{i-1}^{(1)}\lambda_1\frac{e^{X_{i-1} - X_i}}{G^2} \\
& + \frac{\lambda_1^2}{2}b^{(0)}\frac{e^{X_i - X_{i+1}}}{G^2}(-X_i^2 + 3X_{i+1} + 2X_i X_{i+1} - X_{i+1}^2) \\
& + \frac{\lambda_1^2}{2}b^{(0)}\frac{e^{X_{i-1} - X_i}}{G^2}(-X_i^2 - 3X_{i-1} + 2X_i X_{i-1} - X_{i-1}^2) = 0. \quad (\text{H26})
\end{aligned}$$

This is (D29).